

Illinois State Water Survey Division

SURFACE WATER SECTION

AT THE

UNIVERSITY OF ILLINOIS



SWS Contract Report 394

INTERACTIVE BASINWIDE MODEL FOR INSTREAM FLOW AND AQUATIC HABITAT ASSESSMENT

by

Krishan P. Singh, Principal Scientist

Sally McConkey Broeren, Assistant Professional Scientist

Robin B. King, Assistant Supportive Scientist

Prepared for

Division of Water Resources

Illinois Department of Transportation

Champaign, Illinois

August 1986



Illinois Department of Energy and Natural Resources

ABSTRACT

Quantification of sufficient or minimum flows needed to sustain the aquatic habitat is necessary for satisfactory resolution of water use conflicts and planning of water allocation strategies. The Instream Flow Group (IFG) of the U.S. Fish and Wildlife Service has developed a methodology to gage the quantity of suitable habitat in a stream. Application of this methodology has been limited because conventional flow models are inadequate to simulate the detailed hydraulic information needed. Currently, evaluation of aquatic habitats requires extensive field work for each reach studied. There is no methodology for extending results to other reaches with dissimilar drainage areas.

A basin flow model was developed which provides the hydraulic information needed to evaluate the aquatic habitat of all streams within a hydrologically homogeneous basin. The model uses hydraulic geometry relations to compute average flow parameter values for unmeasured streams. The variability of reach average conditions with respect to basinwide average conditions for similar drainage area streams was investigated and adjustment factors were developed defining the range of possible parameter values. Information on the local variations of depth and velocity through riffles and pools is needed to evaluate aquatic habitats. This information is obtained from probability distribution models developed from field data collected on the Sangamon and South Fork Sangamon River Basins. Stream habitat suitability calculations using the basin flow model with the IFG methodology are illustrated.

Singh, Krishan P., Broeren, Sally McConkey, and King, Robin B.

INTERACTIVE BASINWIDE MODEL FOR INSTREAM FLOW AND AQUATIC HABITAT ASSESSMENT--Project Completion Report to the Division of Water Resources, Illinois Department of Transportation, August 1986, Champaign, Illinois, 101 p.

KEYWORDS--instream flow/ aquatic habitats/ stream fisheries/ channel morphology/ physical models/ simulation/ habitat suitability/ incremental methodology

CONTENTS

| | PAGE |
|--|------|
| Introduction | 1 |
| Objectives and Scope..... | 2 |
| Acknowledgments..... | 5 |
| Background Information and Related Research..... | 6 |
| IFG Incremental Methodology..... | 6 |
| IFG Hydraulic Modeling..... | 8 |
| Stream Network Relations..... | 11 |
| Hydrologic and Geomorphologic Basin Characteristics..... | 12 |
| Hydrologic Divisions of the Sangamon River Basin..... | 12 |
| Geology..... | 15 |
| Station Hydraulic Geometry Relations..... | 20 |
| Data..... | 21 |
| Station Hydraulic Geometry..... | 24 |
| Regression Analyses..... | 44 |
| Approximations for High Flows Not Measured at Wading Sections..... | 45 |
| Basin Hydraulic Geometry Relations..... | 49 |
| Field Study..... | 51 |
| Selection of Study Reaches..... | 51 |
| Field Procedures..... | 59 |
| Analysis of Field Data..... | 62 |
| Riffles and Pools..... | 64 |
| Depth Distribution..... | 66 |
| Velocity Distribution..... | 71 |
| Joint Distribution of Depth and Velocity..... | 73 |
| Comparison of Field Data and Results of Hydraulic Geometry Equations..... | 78 |
| Development of the Flow Model for Basinwide Assessment of Weighted Usable Area..... | 82 |
| Example Calculation..... | 84 |
| Basin WUA Relations..... | 89 |
| Comparison of Computational Techniques for WUA..... | 89 |
| Summary..... | 95 |
| Recommendations for Future Research..... | 97 |
| References..... | 99 |

TABLES

| | Page |
|---|------|
| 1. Basin Regression Coefficients for Discharge..... | 14 |
| 2. Gaging Stations..... | 22 |
| 3. Sangamon Basin Station Hydraulic Geometry Equations..... | 46 |
| 4. South Fork Sangamon Basin Station Hydraulic Geometry Equations... | 47 |
| 5. Salt Creek Basin Station Hydraulic Geometry Equations..... | 48 |
| 6. Basin Hydraulic Geometry Equations..... | 52 |
| 7. Simple Correlation Coefficients for W, D, and V with A_d and F.... | 53 |
| 8. Study Reaches..... | 60 |
| 9. Discharge and Average Values of W, D, V, and A Measured at Study Reaches..... | 63 |
| 10. Joint Frequency of Occurrence in Percent with Depth Probability and Normalized Velocity..... | 75 |
| 11. Selected Values of the Inverse Normal (0,1) Probability Distribution Function..... | 86 |
| 12. Average WUA/1000 ft Stream Length for Bluegill Adults..... | 90 |
| 13. Joint Preference Values from Alternative Computational Techniques , Sangamon Basin..... | 94 |

FIGURES

| | Page |
|--|------|
| 1. Sangamon River stream network, USGS gaging stations, and study reaches..... | 4 |
| 2. Q_{90} versus A_d for Sangamon, South Fork Sangamon, and Salt Creek Basins..... | 16 |
| 3. Physiographic divisions and glacial advances in Illinois..... | 18 |
| 4. Stream entrenchment in the Sangamon River, South Fork Sangamon River, and Salt Creek..... | 19 |
| 5. Station hydraulic geometry, Goose Creek near DeLand..... | 25 |
| 6. Station hydraulic geometry, Friends Creek at Argenta..... | 26 |
| 7. Station hydraulic geometry, Sangamon River at Fisher..... | 27 |
| 8. Station hydraulic geometry, Sangamon River at Mahomet..... | 28 |
| 9. Station hydraulic geometry, Sangamon River at Monticello..... | 29 |
| 10. Station hydraulic geometry, Sangamon River near Niantic..... | 30 |
| 11. Station hydraulic geometry, Sangamon River at Riverton..... | 31 |
| 12. Station hydraulic geometry, South Fork Sangamon near Nokomis..... | 32 |
| 13. Station hydraulic geometry, Brush Creek near Divernon..... | 33 |
| 14. Station hydraulic geometry, Horse Creek at Pawnee..... | 34 |
| 15. Station hydraulic geometry, Spring Creek at Springfield..... | 35 |
| 16. Station hydraulic geometry, Flat Branch near Taylorville..... | 36 |
| 17. Station hydraulic geometry, South Fork Sangamon at Kincaid..... | 37 |
| 18. Station hydraulic geometry, South Fork Sangamon near Rochester..... | 38 |
| 19. Station hydraulic geometry, Kickapoo Creek near Heyworth..... | 39 |
| 20. Station hydraulic geometry, Kickapoo Creek at Waynesville..... | 40 |
| 21. Station hydraulic geometry, Kickapoo Creek near Lincoln..... | 41 |
| 22. Station hydraulic geometry, Salt Creek near Rowell..... | 42 |
| 23. Station hydraulic geometry, Salt Creek near Greenvew..... | 43 |
| 24. Sangamon Basin hydraulic geometry relations..... | 54 |

| | |
|--|----|
| 25. South Fork Sangamon Basin hydraulic geometry relations..... | 55 |
| 26. Salt Creek Basin hydraulic geometry relations..... | 56 |
| 27. Sangamon River Basin stream channelization..... | 58 |
| 28. Schematic sketch of transect locations and divisions of channel cross section..... | 61 |
| 29. Study-reach riffle spacing versus W_{20} | 65 |
| 30. Standard deviation of depth, S_d , versus drainage area, A_d | 68 |
| 31. Non-dimensional depth distribution..... | 70 |
| 32. Standard deviation of velocity, S_v , versus reach average velocity, V | 72 |
| 33. Coefficient of variation of velocity, CV , versus reach average velocity, V | 72 |
| 34. Non-dimensional velocity distribution with $CV_v = 0.6$ | 77 |
| 35. Hydraulic geometry correction factors for W , D , and V versus flow duration..... | 80 |
| 36. WUA versus flow duration for Bluegill in the Sangamon Basin..... | 91 |
| 37. WUA versus flow duration for Catfish in the Sangamon Basin..... | 92 |

INTERACTIVE BASINWIDE MODEL FOR INSTREAM FLOW
AND AQUATIC HABITAT ASSESSMENT

by Krishan P. Singh, Sally Broeren, and Robin King

INTRODUCTION

Streams and rivers are an important source of water supply for public, industrial, and agricultural use. They also serve navigation, waste assimilation, and recreational purposes and are an integral part of the habitat structure for fish and wildlife (Illinois State Water Plan Task Force, 1984). As communities and industries expand so does the demand for water withdrawals and streamflow regulation as well as the quantity of effluents discharged into streams and rivers. Increased pressure to optimize agricultural productivity has also generated an interest in water withdrawals for irrigation. Water regulation and withdrawals alter the streamflow regimen and may severely and irreversibly impair stream environments if a sufficient quantity of water is not retained within streams and rivers to support fish and wildlife and to maintain stream ecology and water quality. Management of water resources requires a balancing of competing demands for off-stream uses and instream flow needs. Instream flow needs must be quantified for a satisfactory resolution of water use conflicts. Prediction of aquatic habitat needs and stream ecological response to flow modification is necessary for planning optimal water allocation strategies with minimal adverse impacts on stream environments.

Instream flow needs may be investigated by relating the amount of suitable aquatic habitat to the quantity of flow. Comparisons of the quantity of suitable habitat provided at various flow levels can be used to assess the impact of flow regulation and water withdrawals on the stream environment. The Instream Flow Group (IFG) of the U.S. Fish and Wildlife Service has been actively involved in developing analytic tools to evaluate the quantity and quality of stream habitats. Since 1979 the IFG has been refining a methodology which relates habitat suitability to measurable streamflow parameters such as velocity and depth as well as substrate, cover, and temperature. The IFG methodology is a state-of-the-art tool relating aquatic habitat suitability to instream flow.

Depth and velocity variations through riffles and pools create the diversity of habitat conditions needed by various riverine life forms. Evaluation of the quantity of suitable habitat in a stream requires information on these local variations in depth and velocity. Currently this hydraulic information is collected by direct field measurement of flow parameters in a stream reach. Depths and velocities for unmeasured discharges are simulated using hydraulic models calibrated with the field data. However, available hydraulic models are frequently inaccurate and unreliable. Furthermore they are site-specific, and habitat assessment can be made only for the study reaches and measured discharges. The IFG methodology presents no procedure for basinwide application of the results from the study reaches.

This study is concerned primarily with development of a methodology which provides the needed hydraulic information in the form of a basin flow model for habitat evaluation on a basinwide level. The basin flow model consists of relationships which define channel geometry and flow patterns of streams in a hydrologically homogeneous basin. The morphologic similarity of streams within such a basin provides the basis for generalizing relationships linking flow parameter (width, depth, velocity) values and the relative distributions of local depths and velocities in streams throughout a basin. Previously there has been no reliable means available for extrapolating observed local variations in depth and velocity in one reach to other unmeasured stream reaches.

Implementation of water use policies protecting stream environments will require broad-based assessment of instream flow needs. The basin flow model will greatly facilitate basinwide evaluation of instream flow needs, using the most advanced habitat assessment techniques.

Objectives and Scope

Broad-based evaluation of instream aquatic habitat flow needs using the IFG methodology requires determination of both basin hydrology and flow characteristics of individual streams throughout the basin. Currently available flow models have several disadvantages: they can model only a limited range of flows; they require extensive field measurements; their basic assumptions are not applicable to modeling localized flow conditions;

and they lack a methodology for extending results to other streams. The focus of this project is the investigation and development of generalized relationships which define the needed hydraulic information in terms of readily available descriptive stream parameters, such as drainage area and flow duration, for streams throughout the basin over a broad range of flows. Such relationships can be used to model expected values of flow parameters for any given stream conditions.

The Sangamon River Basin in Illinois was selected for this pilot study. The Sangamon River at its outlet to the Illinois River has a drainage area of 5452 square miles. There are five reservoirs in the system. Numerous long- and short-term USGS gaging stations have been in operation in the basin, and ample discharge measurement data and daily flow records are available.

Flow duration information was developed from daily streamflow records at each gaging station. Three hydrologically homogeneous basins were identified: the Sangamon (main stem upstream of Riverton), the South Fork Sangamon, and the Salt Creek. Glaciation, soil types, and other geomorphologic attributes were investigated, as well as the history of artificial channel modifications. Figure 1 shows the Sangamon River Basin stream network and the locations of selected gaging stations. Data from flow measurements near these stations were used in developing hydraulic geometry equations for each of the three basins. These equations relate average values of width, depth, and velocity in a stream to drainage area and flow duration. The principles of hydraulic geometry are applicable only to natural streams. Therefore, only data from field measurements in natural streams were used in the analyses.

Nine stream reaches representing a range of drainage areas were selected for field measurement of depths and velocities: five along the main stem of the Sangamon and four along the South Fork Sangamon. Two adjacent pool and riffle sequences were identified to define each reach. Velocities, depths, and widths were measured at two different discharges for each reach. The reaches studied are also shown in Figure 1. The field data were analyzed to derive relationships for the variation of depths and velocities about mean values throughout a reach.

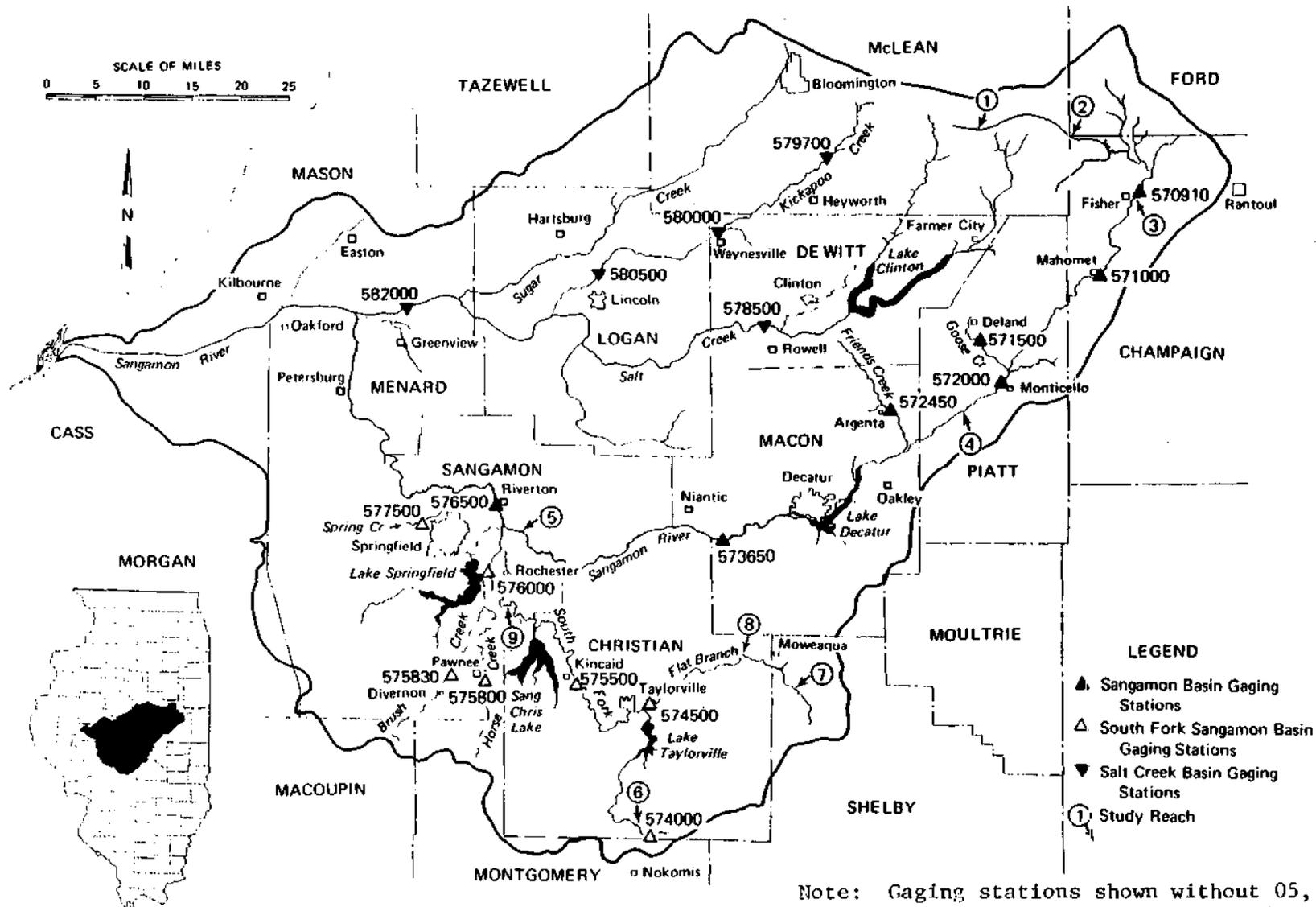


Figure 1. Sangamon River stream network, USGS gaging Stations and study reaches

Specifically the following objectives were accomplished:

- 1) Hydrologically and geomorphologically similar basins within the Sangamon River Basin were identified.
- 2) On the basis of hydraulic geometry concepts, basin relations were developed to define average stream geometry and flow parameter values for streams throughout each basin.
- 3) Field measurements were made to determine depths and velocities occurring throughout typical riffle-pool sequences in a variety of streams in a basin.
- 4) Relations defining expected depth and velocity distributions through riffle-pool sequences over a range of flows were developed from the field data.
- 5) A methodology was developed to extend the relationships to the entire stream network through the medium of hydraulic geometry.
- 6) The hydraulic geometry basin equations and relations defining depth and velocity distributions for the basin were integrated and computerized. The resulting basin flow model was calibrated for each basin.
- 7) The basin flow model was combined with the IFG incremental methodology, creating a basinwide flow and aquatic habitat model.
- 8) The basinwide flow and aquatic habitat model was computerized and used to calculate the Weighted Usable Area (WUA) for two basins and as a function of flow duration and drainage area. The WUA functions for the basin were illustrated graphically.

Acknowledgments

The study was jointly supported by the Division of Water Resources of the Illinois Department of Transportation and the State Water Survey Division of the Illinois Department of Energy and Natural Resources. Gary Clark of the Division of Water Resources served in a liaison capacity during the course of this study. The field work was financed in part by the U.S. Department of Interior through the Water Resources Center, University of Illinois. The help of the staff of the U.S. Geological Survey, Urbana office, in providing flow measurement information for the years of record at various stations in the Sangamon Basin is deeply appreciated.

Joseph Odencrantz, graduate research assistant, helped in field work and computerization of data. Paul Mueller, John Baliga, and Michael Pubentz, students at the University of Illinois, helped in data storage and processing. Becky Howard and Kathleen Brown typed the camera-ready copy. Linda Riggin and John Brother prepared the graphics.

BACKGROUND INFORMATION AND RELATED RESEARCH

Numerous case studies have been conducted to assess the environmental impact of completed or proposed alterations of streamflow characteristics and to evaluate instream flow needs of selected stream reaches. The most widely recognized means of investigating instream flow needs is to relate the quantity of suitable habitat to discharge using the incremental methodology developed by the IFG. The incremental methodology is compatible for use with optimization models for water resources allocations and can be applied to the design and operation of water projects for water supply, power generation, flood protection, and economic efficiency (Loar and Sale, 1981; Milhous and Grenney, 1980).

IFG Incremental Methodology

The most significant flow parameters related to aquatic habitat suitability are depth and velocity. Variations in depth and velocity throughout a stream reach create a continuum of conditions essential to meet the diverse needs of a variety of fish species at different life stages and of other riverine life forming the food chain. The IFG incremental methodology (Stalnaker, 1979) relates these critical streamflow parameters to the quantity of suitable habitat. The basis of the IFG approach is a tabulation of fish species habitat preference functions for depth and velocity as well as substrate, temperature, and cover. All preference functions vary between 0.0 and 1.0, based on the preference of a given species (at its different life stages) for various depths, velocities, substrate, etc. A source file of preference functions for more than 500 warm and cold water fish species is maintained by the IFG (Loar and Sale, 1981). Typical life stages are adult (A), juvenile (J), fry (F), and spawning (S).

The aquatic habitat of a stream reach is analyzed on an incremental basis. A stream reach is conceptually segmented into an array of individual cells by partitions transverse and parallel to the flow. Each cell is defined by its flow surface area, characteristic depth and velocity, substrate, etc., for each measured (or simulated) discharge. The habitat suitability for each cell, as defined by these parameters, is independently evaluated using the preference functions for the given fish species and life stages. By segmenting a stream reach into a number of cells, the local variations in habitat suitability created by differing flow conditions, such as in riffles and pools, can be accounted for.

The suitable habitat is quantified by computing the Weighted Usable Area, WUA:

$$WUA = \sum_{i=1}^N S(d_i) \cdot S(v_i) \cdot \dots \cdot a_i \quad (1)$$

in which $S(d_i)$ and $S(v_i)$, ..., are the preference indexes for depth, d_i , velocity, v_i , ... characteristic of a portion of the stream having a flow surface area a_i . a_i is the total surface area of the study reach. This procedure approximates the total water surface area in a simulated reach as an equivalent area of preferred habitat for a given flow condition. The values of WUA computed for different discharges may be compared to assess the relative quantity of suitable habitat expected under various flow scenarios.

There is some controversy about calculating WUA as a sum of weighted products of preference indexes. Alternatives have been proposed by Singh and Ramamurthy (1981). These are represented by the following expressions:

$$WUA = \sum_{i=1}^N \sqrt{S(d_i) \cdot S(v_i) \cdot \dots \cdot a_i} \quad (2)$$

and

$$WUA = \sum_{i=1}^N \min [S(d_i), S(v_i), \dots] \cdot a_i \quad (3)$$

Equation 2 uses the geometric mean of the preferences and equation 3 the minimum of the set of preferences for area a_i . Generally, equation 2

will yield a higher value of WUA than equation 3 and, in turn, equation 3 yields a higher value than equation 1.

A stream habitat study yields the habitat response functions (WUA versus discharge relations) for various fish species and their life stages. Once the relation between the quantity of habitat and discharge is defined for a stream, the impact of altering the streamflow regime can be assessed. Critical low flow limits for sustenance of the stream fishery can be evaluated.

The local variations in depth and velocity throughout the stream reach must be known to evaluate the WUA for each discharge. Currently, the stream hydraulics is determined by measuring the flow velocities and depths in a representative stream reach across about 6 to 10 transects for 2 or more discharges. In order to evaluate WUA at other discharges, a relationship between discharge and local values of velocity and depth must be established. At present the collected field data are used to calibrate a hydraulic model supported by the IFG.

IFG Hydraulic Modeling

The hydraulic modeling of study reaches is a critical aspect of an instream flow needs study. Reliable flow modeling is essential for extrapolation of results beyond the discharges physically measured. Currently there are two basic approaches to flow modeling for habitat evaluation, each of which is available as a computer algorithm supported by the IFG. One approach is based on Manning's equation and performs a modified step-backwater calculation. This is commonly referred to as the water surface profile (WSP) program or IFG-2. The second modeling approach (IFG-4) relies on developing log-log linear relationships between stage and discharge at each transect and between individual cell discharge and associated average velocity (Milhous et al., 1984).

The IFG-2 model (water surface profile) is typically used with the IFG habitat analysis. For each reach studied, field measurements of depth and velocity are needed as well as level surveying to determine the water surface profile for a measured discharge. Conventional water surface profile models such as IFG-2 and HEC-2 have often been found to be inaccurate under low flow conditions (Miller and Wenzel, 1984). This is because these models are based on assumptions which preclude extrapolation to low

and medium flow hydraulic simulations. During low discharges, flow alternates between pool and riffle conditions. Flow conditions change rapidly through successive riffle-pool sequences, and the underlying assumption of gradually varied flow, which can be approximated by subdividing the reach into sections of uniform flow, does not apply. Furthermore, Manning's n values vary with discharge in a stream, and the IFG-2 flow model, which uses constant n values, cannot reliably predict flow parameters for a wide range of discharges. This is particularly true for low flows when the value of n is changing rapidly.

Velocity distributions across a transect (e.g., the average column velocities) are determined by applying Manning's equation to each sub-area of a transect. The n values for each sub-section of the transect cross-sectional flow area are adjusted to force an agreement between model velocities and field data. These sub-transect values are used for all simulations. This methodology for deriving the velocity distributions is not generally accepted (Bovee and Milhous, 1978). Partitioning a stream into segments with piece-wise application of Manning's equation has not been thoroughly studied. A single field test of this methodology (Elser, 1976) showed that 24% of velocity predictions had errors of 20% or greater and another 23% of velocity predictions had errors of 10 to 20%. Manning's equation, which is the basis of IFG-2, is an empirically derived relation for cross-sectional average parameter values, applicable to uniform flow conditions, which by definition have constant depth and velocity. Manipulations to simulate local velocities and depths often result in unrealistic values of roughness factors, testifying to the inapplicability of this model.

Investigators using the IFG-2 hydraulic model report that even with manipulations of n values and water surface slopes the model often cannot reproduce depth and velocity values measured at low flow. Studies have also shown that the model, calibrated from different flow measurements and used to simulate the same discharge, predicts depths and velocities which vary greatly. The range of applicable discharges is very limited and in practice the model must be calibrated for various discharge ranges. Most importantly, WUA predictions using different hydraulic model calibrations

may have vast numerical differences, and a continuous WUA discharge relation cannot be defined -- only qualitative assessments may be made in the end.

The IFG-4 model requires measurement of three flows in each reach studied to calibrate rating curves (stage-discharge and velocity-discharge for incremental areas). Determination of the velocity distribution across a transect, represented by average water column velocities, is an essential part of the hydraulic data input to the habitat model. The individual water column velocities are mathematically modeled by fitting a log-log linear regression curve between the measured column velocities and the incremental discharge through each subsection of the transect. A relationship between transect average velocity and discharge is generally accepted, but the relationship is frequently curvilinear, particularly at low flow. There is no physical basis for applying a similar relationship to individual column velocities and incremental discharges. The model developers (Bovee and Milhous, 1978; Milhous et al., 1984) provide no verification of the model by comparison to independent field data under a range of flow conditions. There is no basis for estimating potential errors in velocity calculations.

Reach-specific calibrated models such as IFG-2 and IFG-4 cannot be used to reliably predict flow conditions in other unmeasured streams in a basin. Typically, two or three representative reaches in a basin are selected for detailed hydraulic modeling. The results of the model for the study reaches may be extended to other reaches with similar drainage areas using the principles of hydraulic geometry. Hydraulic geometry relations provide a link between average flow conditions (e.g., velocity, depth, and width) and drainage area. However, relative differences in pool and riffle depths vary with drainage area, and the analysis described provides no empirical or theoretical basis for interpolating the local variations in depths and velocities between streams of different orders.

Practical applications and consideration of engineering principles indicate that the IFG hydraulic models are inadequate for a broad-based evaluation of stream networks. Extensive field work is required to gather the hydraulic data to calibrate the model for each reach studied. Even with careful calibration, model simulations for other discharges may be grossly inaccurate as the models are based on inappropriate assumptions and

empirical relations. Finally, there is no reliable means of transferring the findings from a study reach to other stream reaches throughout the basin. Thus there is no basinwide application.

Stream Network Relations

Numerous researchers have observed that stream networks show a consistent, interdependent pattern of formation. The consistency in the nature of stream channel formation is evidenced in recurring stream geometry patterns such as pool-riffle sequences. The pool-riffle sequence forms in a fairly predictable pattern, repeating on the average every 5 to 7 times the stream width; and the width increases with drainage area (Leopold and Wolman, 1957; Harvey, 1975; Nunnally and Keller, 1979). The average pool depth will also increase with increasing drainage area. In an extensive review of river patterns in Russia, Rzhanitsyn (1960) reported that the maximum pool depth to width ratio and riffle depth to width ratio maintain similar relationships when plotted against drainage area for a given discharge frequency such as average annual discharge.

Leopold and Maddock (1953) first stated the concept of hydraulic geometry by relating width (W), depth (D), and velocity (V) to discharge (Q) at a particular stream cross section (e.g., gaging station):

$$\begin{aligned} W &= aQ^b \\ D &= cQ^f \\ V &= kQ^m \end{aligned} \tag{4}$$

in which $b + f + m = 1.0$ and $a \cdot c \cdot k = 1.0$, and D is the average depth of flow and equals $Q/(W \cdot V)$. Similar power functions express the trend of increasing W, D, and V with drainage area for a constant frequency of discharge. Hydraulic geometry relations illustrate an orderly, consistent progression of change in a stream system.

Relations linking flow parameters throughout the basin may be constructed as functions of drainage area and flow duration. Stall and Fok (1968), expanding on the original concepts of hydraulic geometry, defined basin relations for hydraulic parameters in the form:

$$\ln(\text{parameter}) = a + bF + c(\ln A_d) \tag{5}$$

in which a , b , and c are regression coefficients for a basin, F is the decimal flow duration, and A_d is the drainage area. These general relations were confirmed for Illinois streams and for selected basins in the United States (Stall and Yang, 1970). The form of the relationship remains constant for different basins regardless of the physiographic setting.

The regular progressive change in stream geometry and flow characteristics in a basin with increasing drainage area (when compared at similar frequency flows) provides the basis for generalizing W , D , and V relations. The distributions of depths and velocities through pools and riffles in different reaches may likewise be linked by relating their distribution parameters (such as the standard deviation) to drainage area and flow duration.

HYDROLOGIC AND GEOMORPHOLOGIC BASIN CHARACTERISTICS

The Sangamon River Basin in Illinois is tributary to the Illinois River. The Sangamon River at its confluence with the Illinois River has a drainage area of 5452 square miles and is ranked as a 7th-order stream according to the Horton-Strahler system (Stall and Fok, 1968). The structure of the drainage network is dendritic. There are three main branches in the stream network: the Sangamon (main stem above Riverton) and the South Fork Sangamon, each of which is a 5th-order stream; and Salt Creek, which is a 6th-order stream. The Sangamon is a 6th-order stream downstream of its confluence with the South Fork Sangamon. The respective drainage areas of the Sangamon, South Fork Sangamon, and Salt Creek are 1445, 883, and 1856 sq mi. Due to hydrologic and geomorphologic differences in the watersheds of these three streams, the Sangamon River Basin may be divided into three hydrologically homogeneous basins: the Sangamon (mainstem), South Fork Sangamon, and Salt Creek.

Hydrologic Divisions of the Sangamon River Basin

Singh (1971) divided the Sangamon River Basin (excluding the Havana lowlands) into three relatively hydrologically homogeneous basins: Sangamon (above Riverton), South Fork Sangamon, and Salt Creek. Singh and Stall (1973) show similar sub-basins for regionalizing the 7-day 10-year

low flows. Recent streamgauge network analyses also support division of the entire basin into three hydrologically homogeneous basins.

Daily flow data from 22 USGS gaging stations on the Sangamon, South Fork Sangamon, and Salt Creek were analyzed to evaluate relations between discharge and drainage area. The relationship was generalized for a basin:

$$\log Q_j = a_j + b_j (\log A_d) \quad (6)$$

where A_d = drainage area

Q_j = discharge at flow duration j

a_j and b_j = regression coefficients for flow duration j

The regression coefficients a_j and b_j vary with flow duration. The b_j or the slope of the $\log Q$ versus $\log A_d$ line is practically constant for a given flow duration for the three basins. However, higher correlations are achieved if a_j is evaluated independently for each of the three basins. The regression coefficients for several flow durations are listed in Table 1 for each basin. Equation 6 may be expressed as

$$\log C_{i,j} = a_{i,j} + b_j (\log A_d) \quad (7)$$

The subscript i ($i = 1, 2, \text{ or } 3$) denotes the Sangamon, South Fork Sangamon, or Salt Creek basin. The regression analysis was performed using two dummy variables, D_1 and D_2 , given by

$$\begin{aligned} a_{2,j} &= a_{1,j} + D_1 \\ a_{3,j} &= a_{1,j} + D_2 \end{aligned} \quad (8)$$

The reliability of these relations is indicated by the high correlation coefficients, r , and low standard errors of estimate, S , which are also included in Table 1.

The basin equations developed for discharges corresponding to various flow durations for the Sangamon, South Fork Sangamon, and Salt Creek were used in this study. Flow measurement data from which hydraulic geometry relations were developed were collected at long-term gaging stations, temporary gaging stations, water quality sites, and partial-record low-flow stations maintained by the U.S. Geological Survey. A sufficient record of daily flow data to construct flow duration curves is not collected at all

Table 1. Basin Regression Coefficients for Discharge
 $\log(\text{VAR}) = a_{i,j} + b_j (\log A_d) \quad (i=1,2,3)$

| VAR(j) | Regression coefficients | | | Regression statistics | | Sample size | | |
|--------|-------------------------|----------------------------|-------------------|-----------------------|-----------|-------------|-----------|-------|
| | <u>Sangamon</u> | <u>South Fork Sangamon</u> | <u>Salt Creek</u> | $a_{i,j}$ | $a_{2,j}$ | | $a_{3,j}$ | b_j |
| Q(99) | -5.1183 | -5.5025 | -4.4167 | 1.9488 | 0.924 | 0.3172 | 12 | |
| Q(95) | -3.6001 | -4.0998 | -3.1499 | 1.5833 | 0.967 | 0.1864 | 13 | |
| Q(90) | -2.8257 | -3.1131 | -2.4983 | 1.3909 | 0.975 | 0.1351 | 13 | |
| Q(80) | -2.2448 | -2.3825 | -2.0045 | 1.2864 | 0.984 | 0.0974 | 13 | |
| Q(70) | -1.7144 | -1.8431 | -1.5770 | 1.2070 | 0.991 | 0.0736 | 14 | |
| Q(60) | -1.1887 | -1.3260 | -1.1065 | 1.1220 | 0.995 | 0.0540 | 14 | |
| Q(50) | -0.7843 | -0.9254 | -0.7571 | 1.0640 | 0.996 | 0.0434 | 14 | |
| Q(40) | -0.5583 | -0.6833 | -0.5453 | 1.0507 | 0.997 | 0.0357 | 14 | |
| Q(30) | -0.3554 | -0.4473 | -0.3559 | 1.0433 | 0.998 | 0.0296 | 14 | |
| Q(20) | -0.0880 | -0.1742 | -0.1181 | 1.0222 | 0.998 | 0.0304 | 14 | |
| Q(10) | 0.1903 | 0.1581 | 0.1424 | 1.0175 | 0.996 | 0.0409 | 14 | |
| Q(5) | 0.4516 | 0.4686 | 0.3926 | 0.9991 | 0.996 | 0.0429 | 14 | |
| Q(1) | 1.0833 | 1.1219 | 1.0392 | 0.8964 | 0.996 | 0.0373 | 14 | |

Note: r = correlation coefficient
 S_e = standard error

of these stations. Therefore, the basin flow duration equations were used to develop flow duration curves at all these stations. The basin discharge equations provide a consistent method of computing discharges for a given flow duration at all stations within a hydrologically homogeneous region.

Low flow periods are critical for the stream ecological environment, and differences between the low flows of the three basins are significant for habitat studies. The trend in low flow variation between the basins is clearly illustrated in a plot of the Q_{90} discharge (a discharge equaled or exceeded 90% of the time) obtained from the basin flow duration equations for successive drainage areas (Figure 2). Salt Creek maintains the highest discharge, while the South Fork maintains the lowest. The Sangamon supports a flow rate between the other two.

The geology of a region greatly influences the low flow hydrology of the drainage system. For basins having similar climatic conditions, differences in low flow hydrology are largely explained by differences in geology (given similar urbanization and artificial human modifications). Geologic structure, soil types, and maturity of the drainage system influence the runoff patterns, the structure of the drainage network, and the proportion of precipitation which goes directly to surface water, subsurface soil water, and ground water. Low flows are greatly influenced by these factors.

The geologic structure of the underlying strata, the drift thickness, and the degree of stream entrenchment define the ground water-surface water interaction. The amount of baseflow to a stream is directly affected by the availability of ground water. Soil permeability is an important factor in runoff characteristics. Soils with low infiltration rates produce relatively high peak surface runoff and low subsurface and ground water accretions from a rainfall event. Precipitation falling on highly permeable soils will have lower peak surface runoff as more water travels as subsurface flow or percolates to the ground-water aquifer. This contributes to higher sustained baseflows.

Geology

The Sangamon River Basin lies in a region that has undergone extensive glaciation in recent geologic time. Even though the entire watershed is covered with glacial deposits, the origin and character of

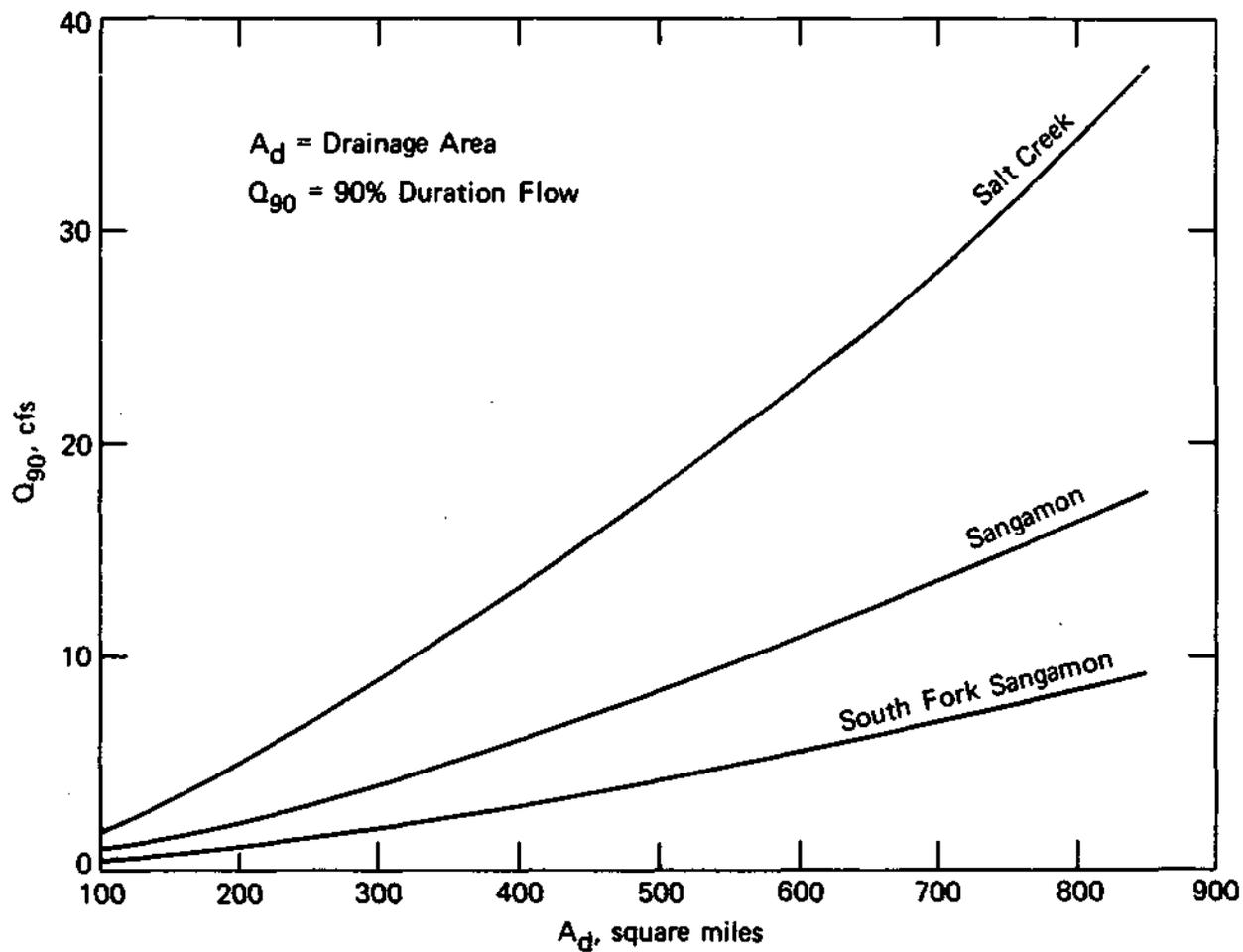


Figure 2. Q_{90} versus A , for Sangamon, South Fork Sangamon, and Salt Creek Basins

these deposits exhibit significant differences. The most recent glacial advance, the Wisconsinan, covered approximately 40% of the entire Sangamon River Basin. This area includes the upper part of the Salt Creek and Sangamon Basins as shown in Figure 3. In contrast, the South Fork Basin is covered by the older Illinoian glacial deposits. Leighton et al. (1948) have divided the Sangamon watershed into two physiographic regions related to differences in glacial history. These regions are the Bloomington Ridged Plain, which is Wisconsinan in age, and the older Springfield Plain, which is Illinoian in age. These plains are delineated in Figure 3. The relevant features of these plains as described by Singh and Stall (1971) are given below:

Bloomington Ridged Plain: Glacial deposits relatively thick; low, broad morainic ridges with intervening stretches of relatively flat or gently undulating moraine; drainage development generally in the initial stage; relatively deep entrenchment of drainage.

Springfield Plain: Level portion of Illinoian drift sheet; shallow entrenchment of drainage; fewer moraines in the southwestern portion; thinning of drift toward the southern and southwestern boundary.

Drift thickness varies widely throughout the region. The Salt Creek and Sangamon Basins have relatively high drift thickness, varying from 50 to 350 ft with an average of 300 ft, characteristic of the Bloomington Ridged Plain. The South Fork region drift thickness varies from 0 ft to 200 ft with an average of approximately 50 ft, characteristic of the Springfield Plain.

Stream entrenchment may be illustrated in a plot of stream bed elevation and corresponding average basin divide elevation versus distance along the main stream starting from its projection to the upstream basin boundary. The variation in stream entrenchment between the three basins is shown in Figure 4. The elevations of the stream bed and average basin divide were obtained from USGS 7-1/2-minute quadrangle topographic maps. The elevation of the basin divide was determined by computing the average of the highest elevations of the basin perpendicular to the stream course at various locations.

Over 90% of the soils in the Sangamon River Basin belong to the Mollisol soil order. The remaining watershed area belongs to the Alfisol order, but this occurs exclusively in the Sangamon River valley and the

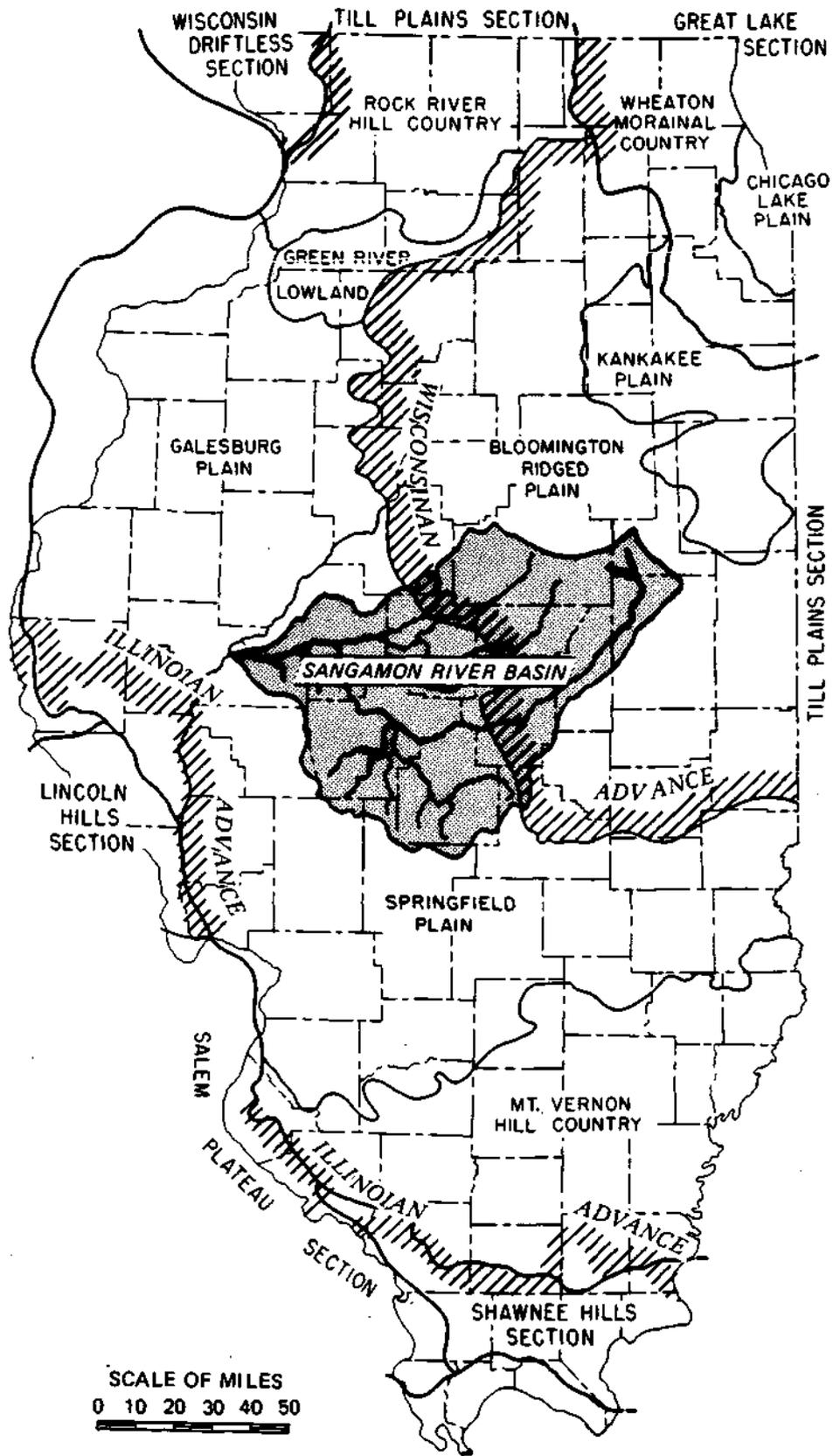


Figure 3. Physiographic divisions and glacial advances in Illinois

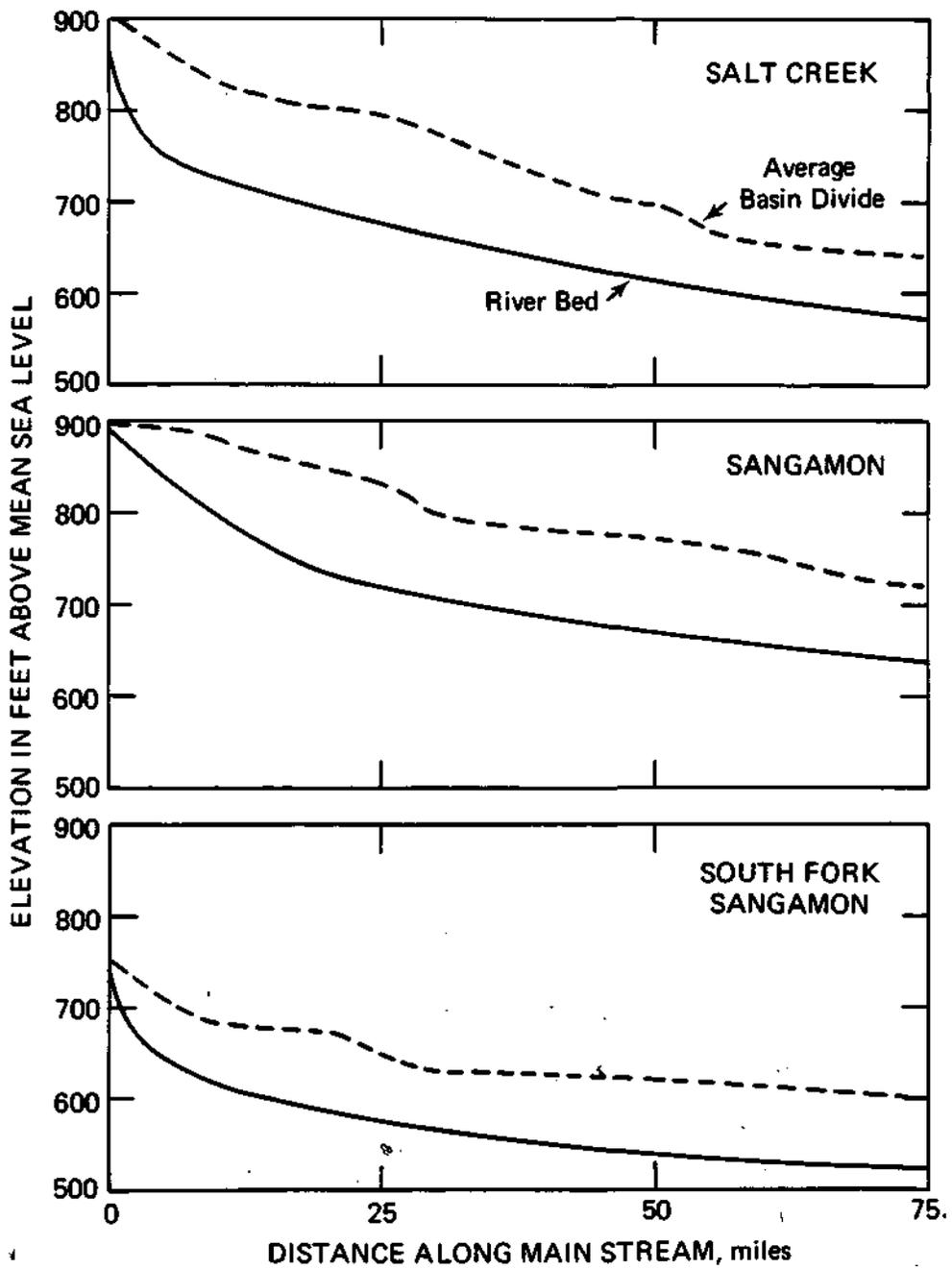


Figure 4. Stream entrenchment in the Sangamon River, South Fork Sangamon River, and Salt Creek

upland area of Salt Creek. Mollisols are dark-colored soils which formed under grass by the decomposition of underground vegetation remains. They can vary widely in texture, permeability, degree of subsoil developed, and many other properties. Alfisols are usually light-colored and formed under forest cover (Fehrenbacher et al., 1984).

Over 60% of the soils in the Bloomington Ridged Plain are either Drummer silty clay loam or Flanagan silt loam. Although poor in natural drainage, these soils are moderate in permeability and have high water availability.

Soils of the Springfield Plain in the South Fork Basin consist largely of Tama silty clay loam, Harrison silty clay loam, and Clinton silty clay loam. In general, the permeability is slow to moderately slow throughout the basin due to the relatively high amount of clay present in all the predominant soil types.

Observed variations in low flows in the three basins may be traced to the glacial history of the region. Much of the Salt Creek and Sangamon Basins have soils with relatively higher permeability, higher drift thickness, and more deeply entrenched streams. These conditions contribute to higher baseflows. The South Fork Sangamon Basin has soils which are less permeable (providing less water retention for slow release into streams), lesser drift thickness, and shallower entrenchment of streams, thus reducing subsurface and ground-water accretion to the streams. These conditions contribute to lower baseflows.

STATION HYDRAULIC GEOMETRY RELATIONS

The fundamental building blocks of the basin hydraulic geometry relations are the station equations. These equations relate the flow parameters width (W), depth (D), and velocity (V), to discharge measured at a cross section near the station. When plotted on log-log paper, W , D , and V increase in a consistent manner with increasing discharge at a station.

The station relationships for the log-transformed variables may be evaluated by regression analysis. The variables are expressed as polynomial functions of $\log Q$. Alternative formulations with different order polynomials may then be compared on the basis of regression parameters qualifying the goodness of fit. Polynomial regression analysis has the

advantage of providing a compact mathematical expression instead of a graphical relation, and repeatability given the same data and criteria. The value and reliability of the regression equations are dependent on the data used to compute them. Typically data from streamflow measurements made by USGS personnel near streamgaging stations are used to develop the relations. The available data from the streamgaging stations were carefully screened before they were used in developing the station relations and ultimately the basin hydraulic geometry relations.

Data

The U.S. Geological Survey conducts an extensive program of streamflow measurements. As part of that continuing program, between 10 to 20 detailed current meter flow measurements are made every year at each active gaging station. Through this effort there is available a mass of data on streamflow and associated velocities, depths, and geometry of flow section. For each measurement, velocities and depths are sampled at a stream cross section, the top width (W) is measured, and gage height is recorded. The flow cross-sectional area (A), the average velocity (V), and discharge (Q) are computed. The average depth (D), defined as the hydraulic depth, may be computed from $D = A/W$ (Chow, 1959). Low to medium flows are typically measured by wading along a stream cross section. High flows with depths exceeding approximately 3 feet are usually measured from a bridge near the gage installation, from a cable car if available, or from a boat. The flow measurement data are not published but are available at USGS district offices.

Data collected near 28 streamgaging or water quality stations on the Sangamon main stem and South Fork Sangamon Rivers and Salt Creek were obtained from the USGS district office in Urbana, Illinois. Data from 9 stations and some data points from other stations were not included in developing the final equations. Hydraulic geometry relations were developed from data obtained near 19 stations; the stations, drainage areas, and years of record used are listed in Table 2.

Data used in developing parameter rating curves must be obtained at cross sections representative of the natural channel (Leopold and Maddock, 1953). Stream reaches which are dredged or leveed, or where flows are

Table 2. Gaging Stations

| <u>USGS No.</u> | <u>Stream name</u> | <u>Station</u> | <u>Drainage area (mi²)</u> | <u>Period of record</u> | <u>Number of data points</u> |
|----------------------------------|--------------------|----------------|---|-----------------------------|----------------------------------|
| Sangamon River | | | | | |
| 05571500 | Goose Creek | Deland | 47.3 | 6/51 to 4/59 | 55 |
| 05572450 | Friends Creek | Argenta | 111.0 | 9/66 to 10/82 | 134 |
| 05570910 | Sangamon | Fisher | 240.0 | 8/78 to 9/82 | 31 |
| 05571000 | Sangamon | Mahomet | 362.0 | 3/48 to 9/78 | 246 |
| 05572000 | Sangamon | Monticello | 550.0 | 3/41 to 11/68 | 177 |
| 05573650 | Sangamon | Niantic | 1054.0 | 12/77 to 8/83 | 23 |
| 05576500 | Sangamon | Riverton | 2618.0 | 11/34 to 12/56 | 69 |
| South Fork Sangamon River | | | | | |
| 05574000 | So. Fork Sang. | Nokomis | 10.8 | 1/51 to 10/75 | 155 |
| 05575830 | Brush Creek | Divernon | 32.4 | 9/73 to 10/82 | 74 |
| 05575800 | Horse Creek | Pawnee | 52.2 | 4/66 to 11/82 | 113 |
| 05577500 | Spring Creek | Springfield | 107.0 | 6/58 to 10/82 | 158 |
| 05574500 | Flat Branch | Taylorville | 279.0 | 7/49 to 9/82 | 203 |
| 05575500 | So. Fork Sang. | Kincaid | 562.0 | 10/33 to 8/60 | 88 |
| 05576000 | So. Fork Sang. | Rochester | 867.0 | 4/66 to 10/82 | 80 |
| Salt Creek | | | | | |
| 05579700 | Kickapoo Creek | Heyworth | 71.8 | 12/48 to 8/64 | 28 |
| 05580000 | Kickapoo Creek | Waynesville | 227.0 | 3/48 to 9/82 | 260 |
| 05580500 | Kickapoo Creek | Lincoln | 306.0 | 10/44 to 10/71 | 195 |
| 05578500 | Salt Creek | Rowell | 335.0 | 9/42 to 11/82 | 223 |
| 05582000 | Salt Creek | Greenview | 1800.0 | 9/42 to 10/82 | 199 |

regulated or influenced by a dam or backwater, are typically not representative of the stream system hydraulics. The relationship between depth or velocity with discharge at a section constricted by bridge piers or abutments will differ from that found at a natural section.

Detailed gaging station descriptions and histories were gathered from the USGS for each of the stations initially reviewed. Information provided in the descriptions led to the elimination of 8 stations from the study: Gage 05583000 at Oakford is located in a dredged and leveed reach; Gage 05573540 at Highway 48 near Decatur was not used as all flows may be affected by gate operation of the Lake Decatur Dam; Gage 05572500 at Oakley is affected by backwater from the Lake Decatur Dam; all low and medium flows measured at the temporary gage near Petersburg are made directly upstream of a dam; at Gage 05572100 on Wildcat Creek, flows are measured at a culvert; and Gage 05582500 at Crane Creek near Easton, Gage 05579700 at Sugar Creek near Bloomington, and Gage 05579500 at Lake Fork near Cornland are located in dredged channels. Data from a ninth station, Gage 05581500 at Sugar Creek near Hartsburg, also were not included in development of the basin equations because plots of W , D , and V versus discharge exhibited markedly different relationships from other station plots.

Gage 05582000 on Salt Creek near Greenview is located in a reach in which some artificial channel modifications may have been performed. Apparently, levees have been constructed in the vicinity of the gage. However, the USGS station description does not indicate that the active channel has been modified, and there are no other gaging station data available for large drainage area streams in the Salt Creek Basin. Thus the Greenview station was included in the development of station hydraulic geometry relations.

The gaging station descriptions typically document activities which may have modified the hydraulic conditions or stream morphology at the gage such as dam or bridge construction in the reach during the period of record, relocation of the gaging installation, or flow diversion at high stages. For each station only flow measurement data representative of a homogeneous hydraulic regime were included.

The hydraulic consistency and accuracy of the flow data were checked by examining the stage discharge relationship for the period of record and also by verifying that the physical law, $Q = V.D.W$, was satisfied by the

recorded information. Gage height versus discharge was plotted on log-log scale from the available data. In a few cases multiple rating curves were evident. Only data forming a single curve were retained. This elimination process reduced data scatter in the flow parameter versus discharge plots to some extent. Measurements were omitted if V.A was not within 5% of the reported discharge. Usually from 1 to 5% of the measurements were omitted from the final data set because of these considerations.

The original field notes for each measurement were reviewed to identify it as a wading measurement (information collected by field personnel traversing the stream on foot or by boat) or bridge measurement (measurement made by lowering equipment into the stream from a bridge). There are no cable car installations in the Sangamon Basin. The approximate location of the measured section relative to the gage was noted if reported.

Station Hydraulic Geometry

Station hydraulic geometry plots were developed from the final data sets. There are three log-log plots for each station: W, D, and V versus Q. The plots for each station appear in Figures 5 through 23. Data collected at a wading section are plotted with a 0 symbol, and data obtained at a bridge section are plotted with a + symbol. The vertical dashed line labeled "cut off" in each graph is plotted at a discharge equal to 1.5 times the 10% flow duration discharge. The relationships developed in this project were limited to flows at or below this limit. Flows less than this limit may be expected to be contained within the channel banks. One exception is at the gage located near Fisher, where flows exceeding approximately 200 cfs are diverted through a culvert; here 200 cfs was used as the "cut off." The "cut off" is not shown on the plots for the Heyworth gage on Kickapoo Creek, as the highest discharge measured was less than the 10% flow duration discharge.

Several general observations are clearly evident from the plots. There is a discontinuity between the wading data and the bridge data in nearly every station graph. This discontinuity does not correspond to the bankfull event. The slope of the data from wading sections is different from that of the bridge data, suggesting that the relationship between flow parameters and discharge is different at wading sections and bridge

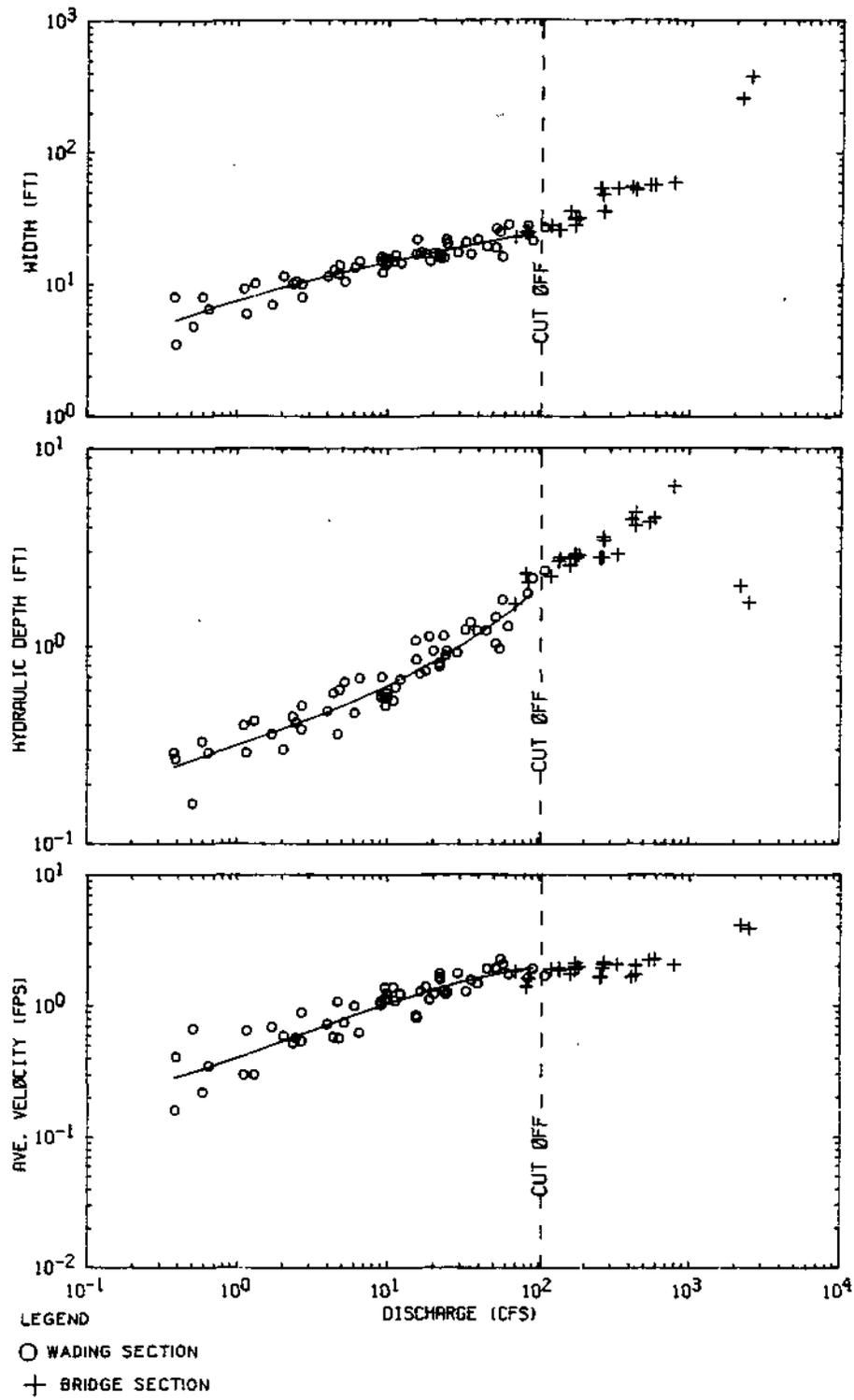


Figure 5. Station hydraulic geometry, Goose Creek near Deland

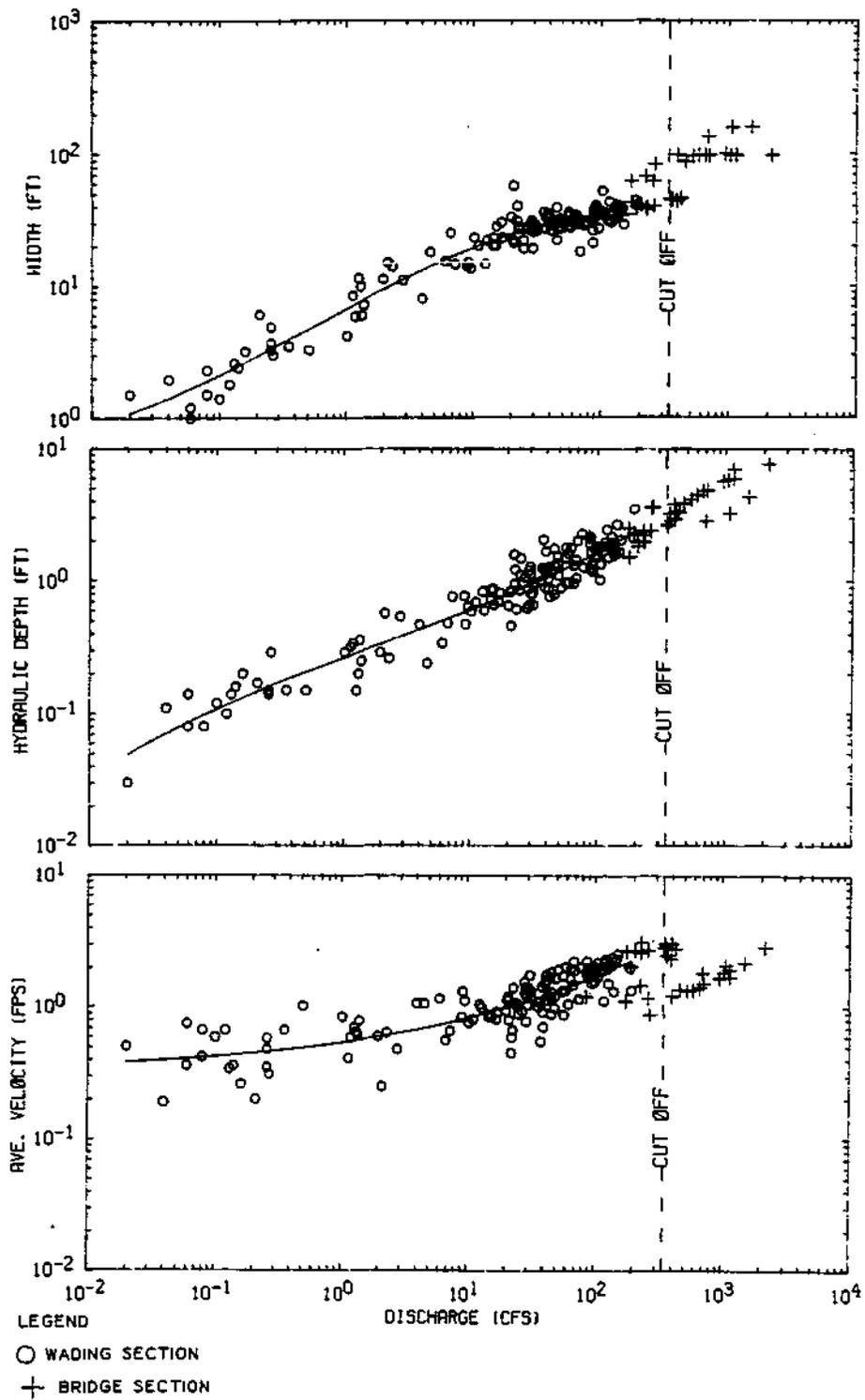


Figure 6. Station hydraulic geometry, Friends Creek at Argenta

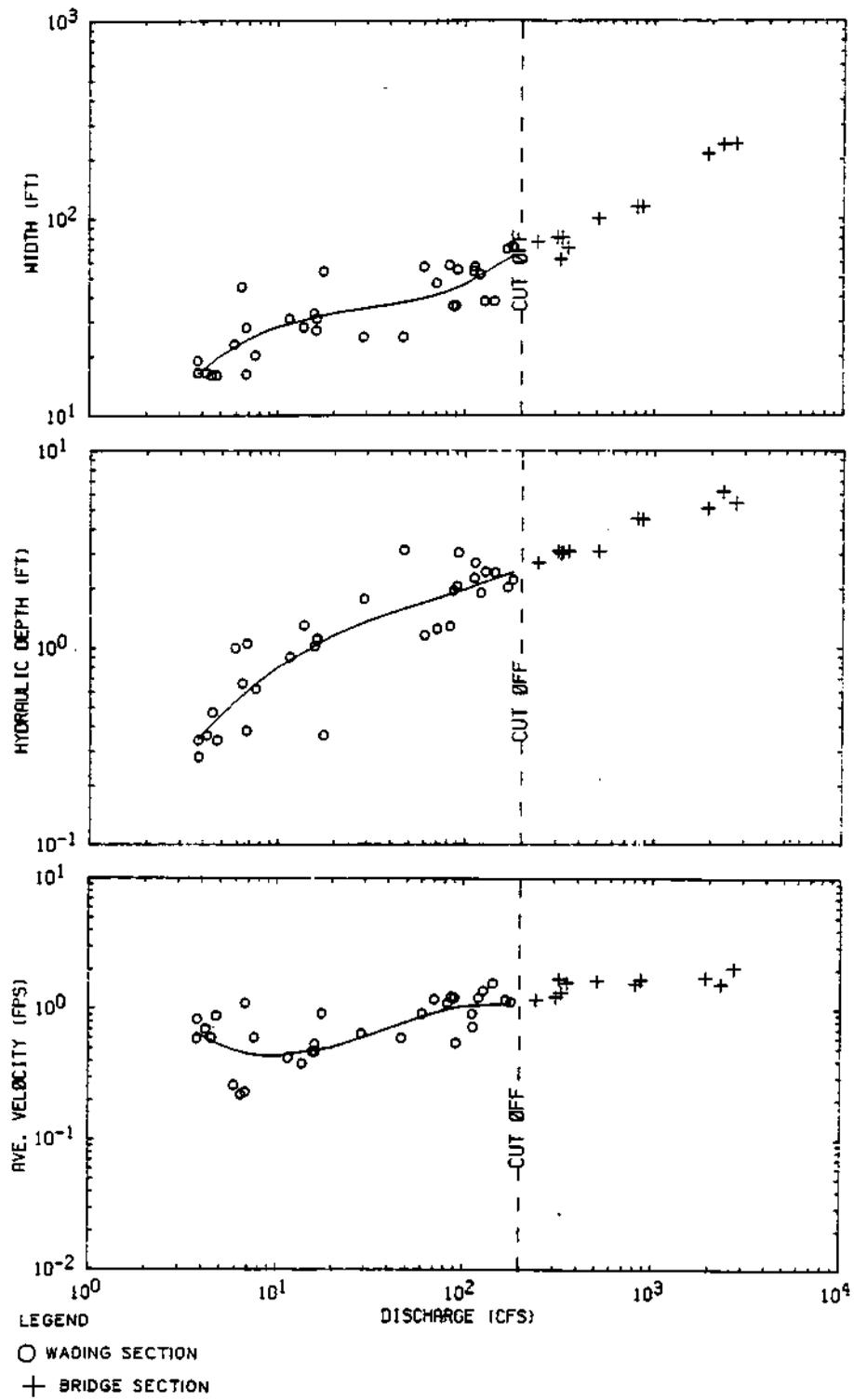


Figure 7. Station hydraulic geometry, Sangamon River at Fisher

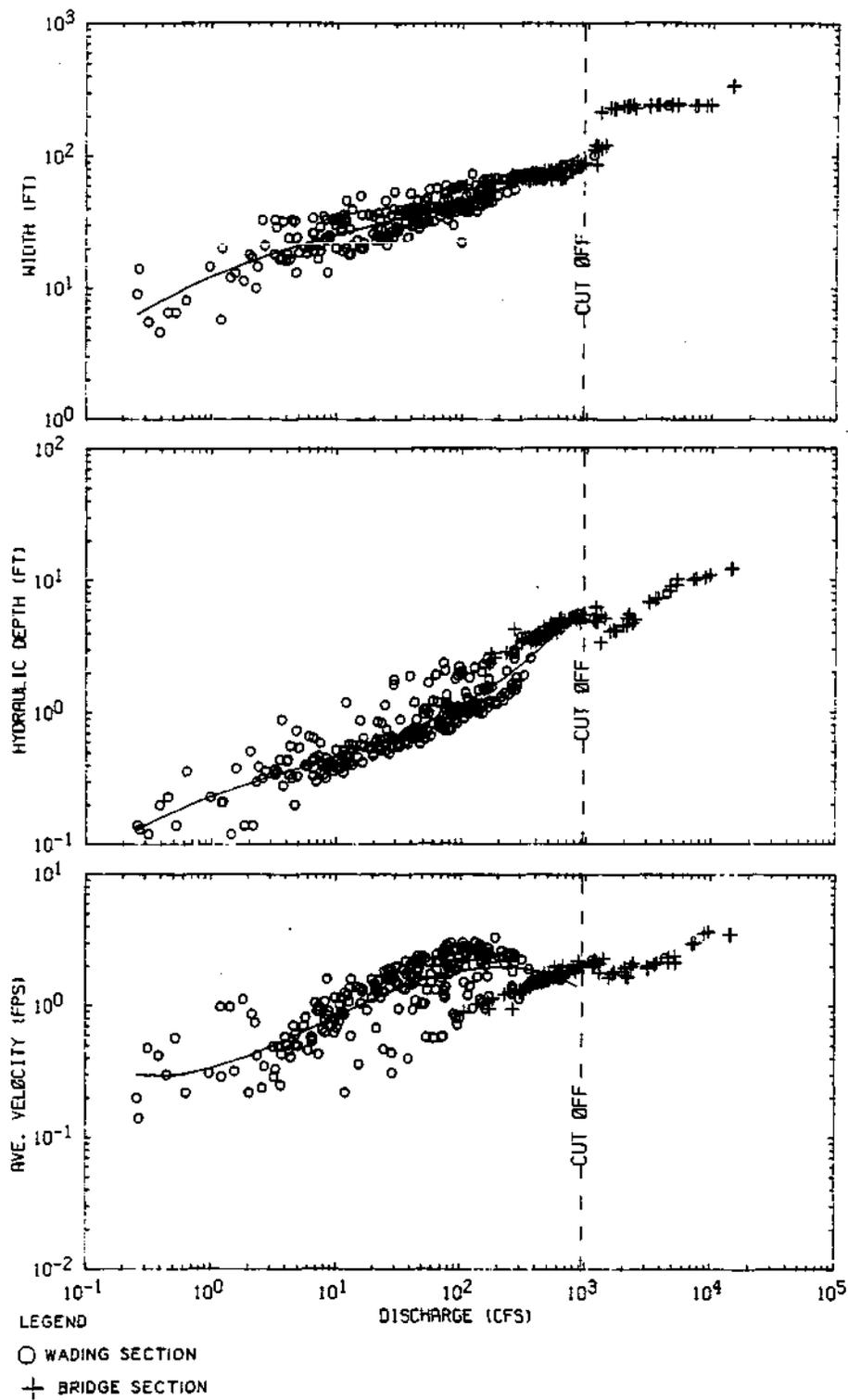


Figure 8. Station hydraulic geometry, Sangamon River at Mahomet

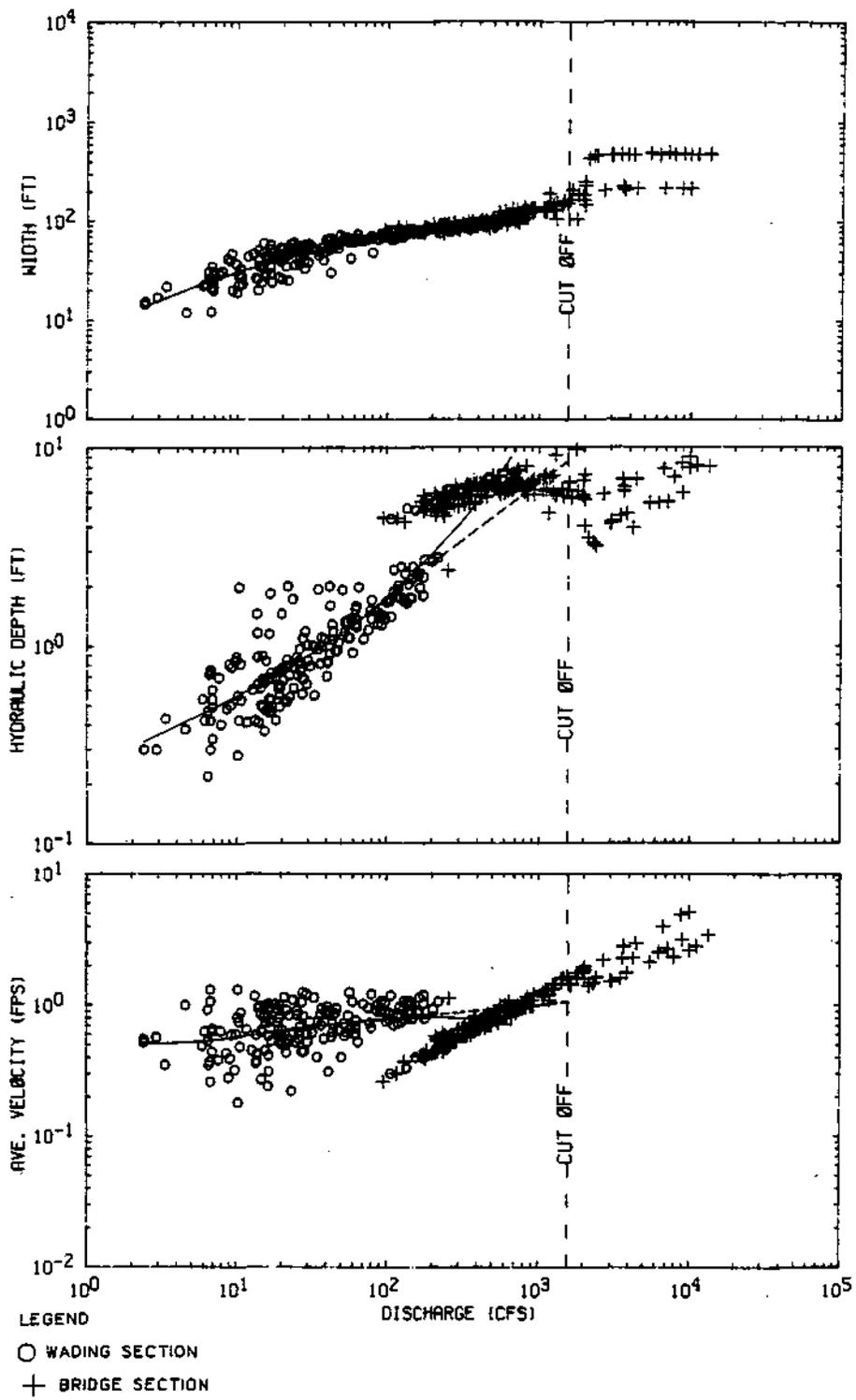


Figure 9. Station hydraulic geometry, Sangamon River at Monticellp

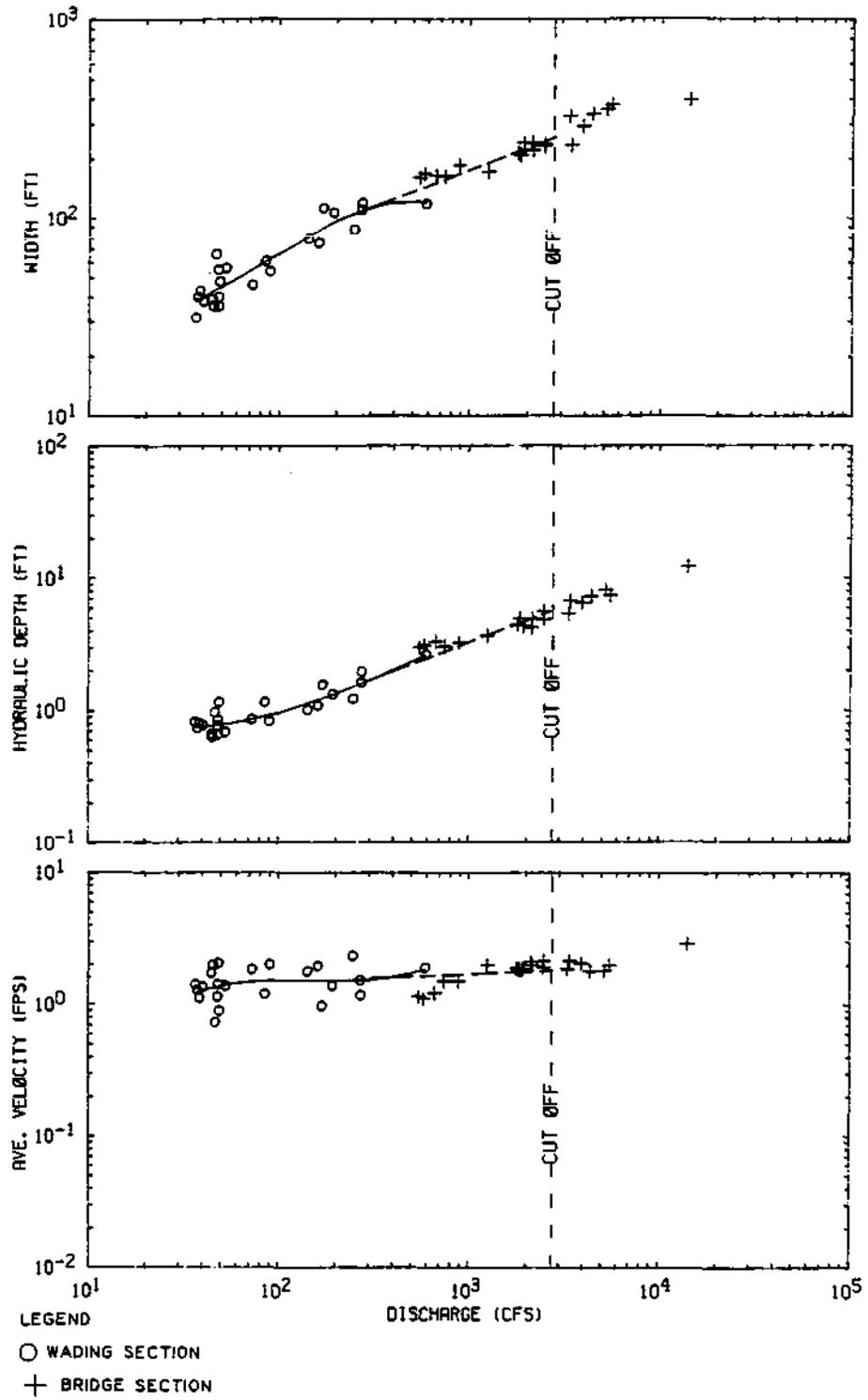


Figure 10. Station hydraulic geometry, Sangamon River near Niantic

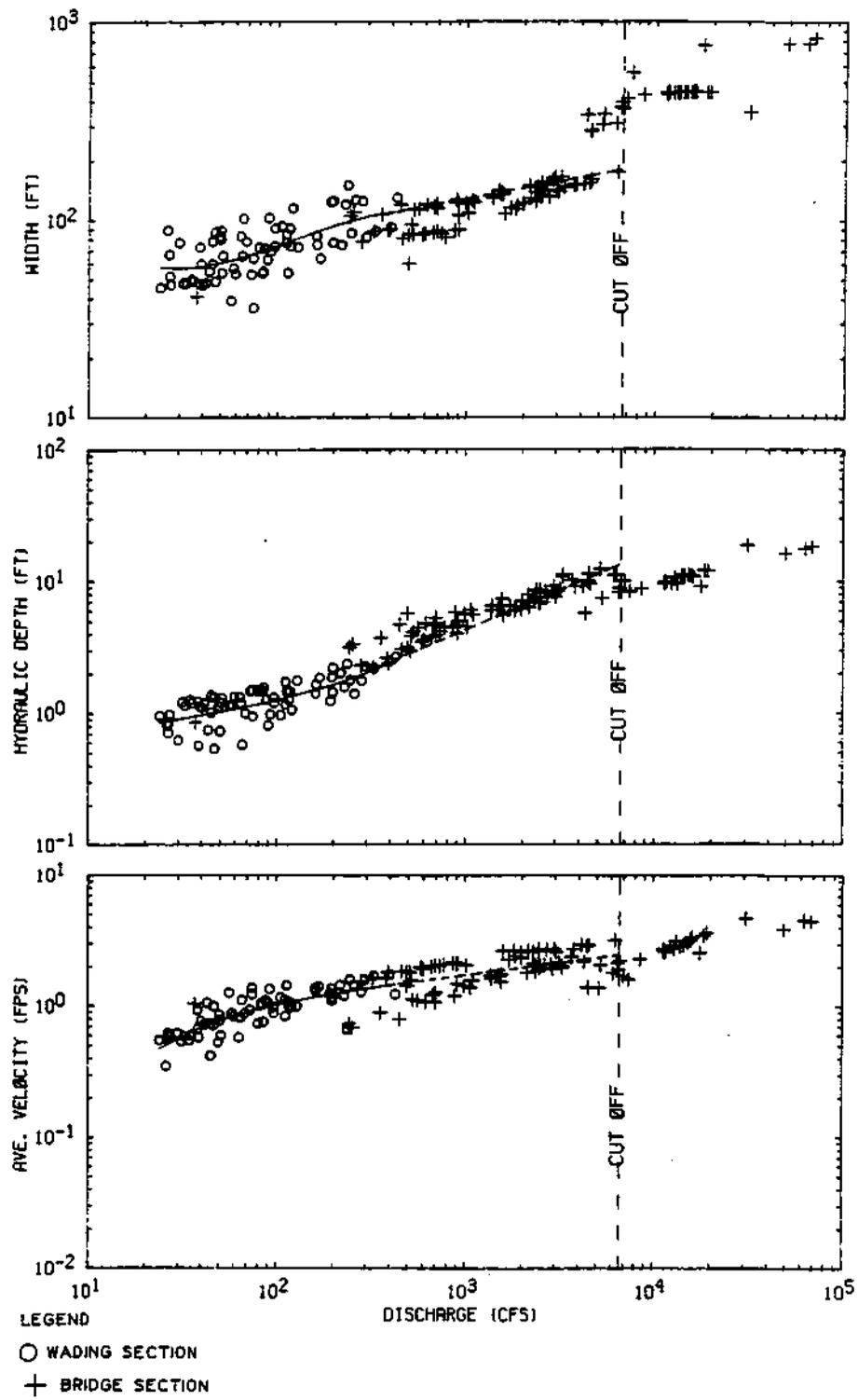


Figure 11. Station hydraulic geometry, Sangamon River at Riverton

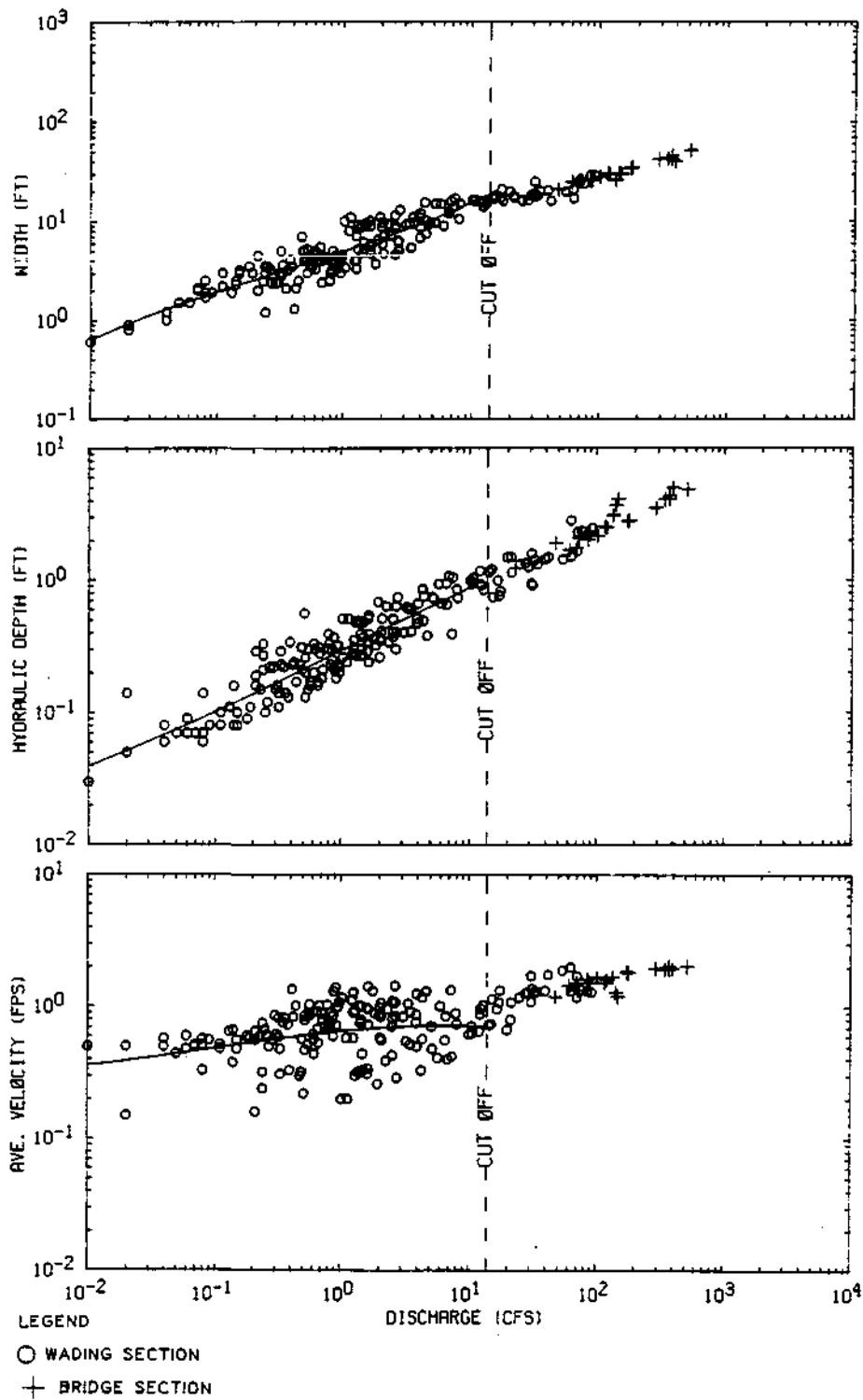


Figure 12. Station hydraulic geometry, South Fork Sangamon near Nokomis

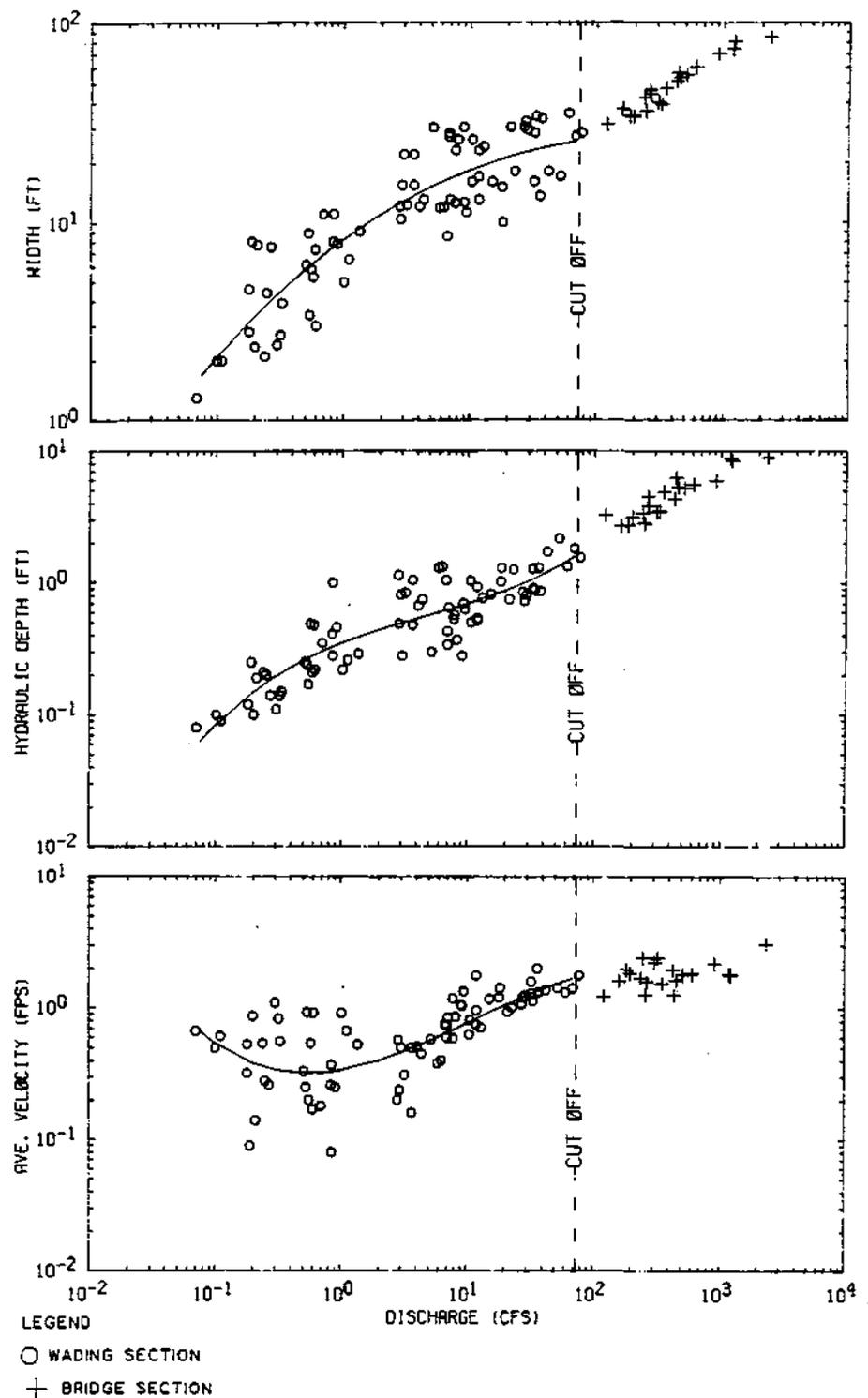


Figure 13. Station hydraulic geometry, Brush Creek near Divernon

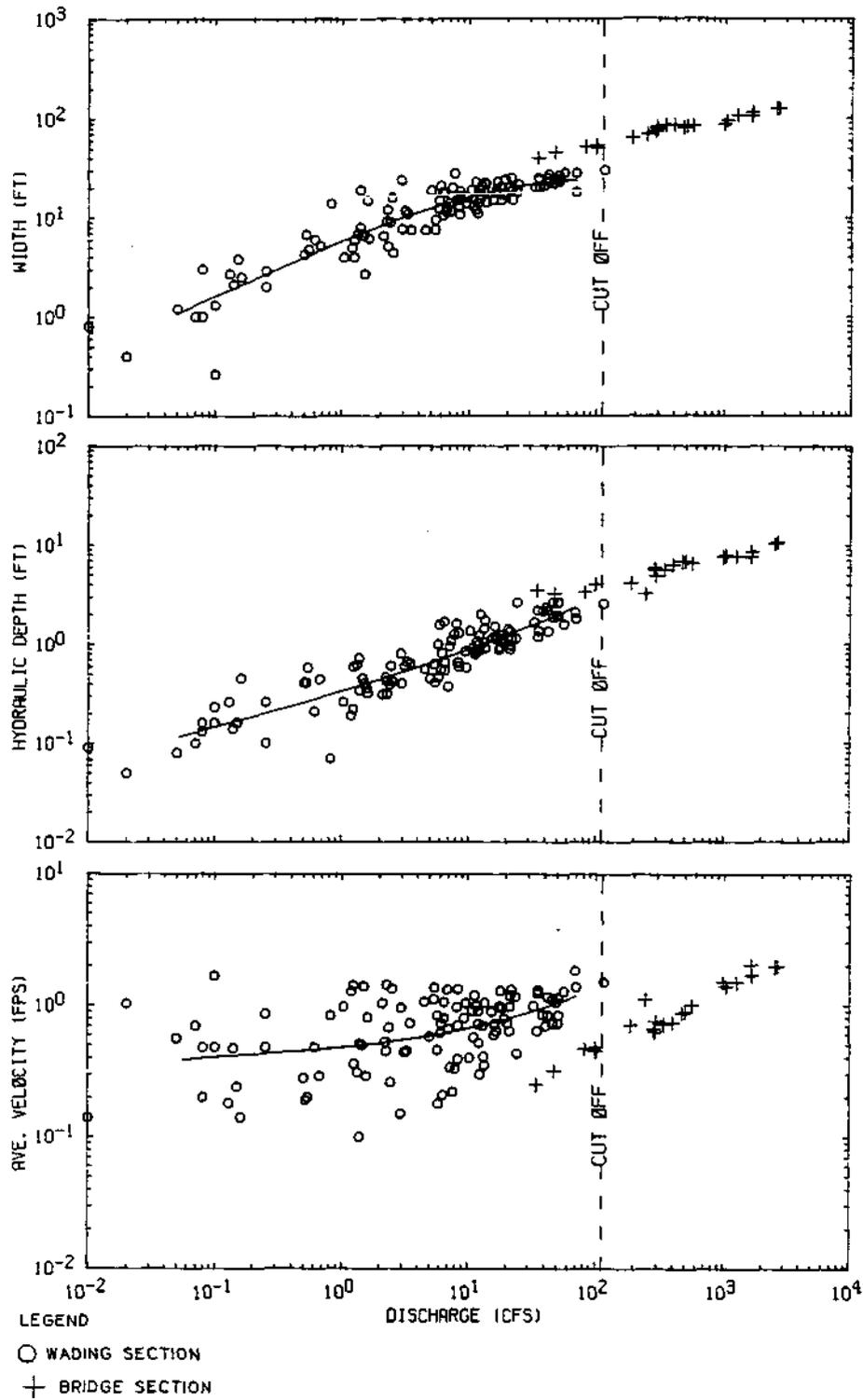


Figure 14. Station hydraulic geometry, Horse Creek at Pawnee

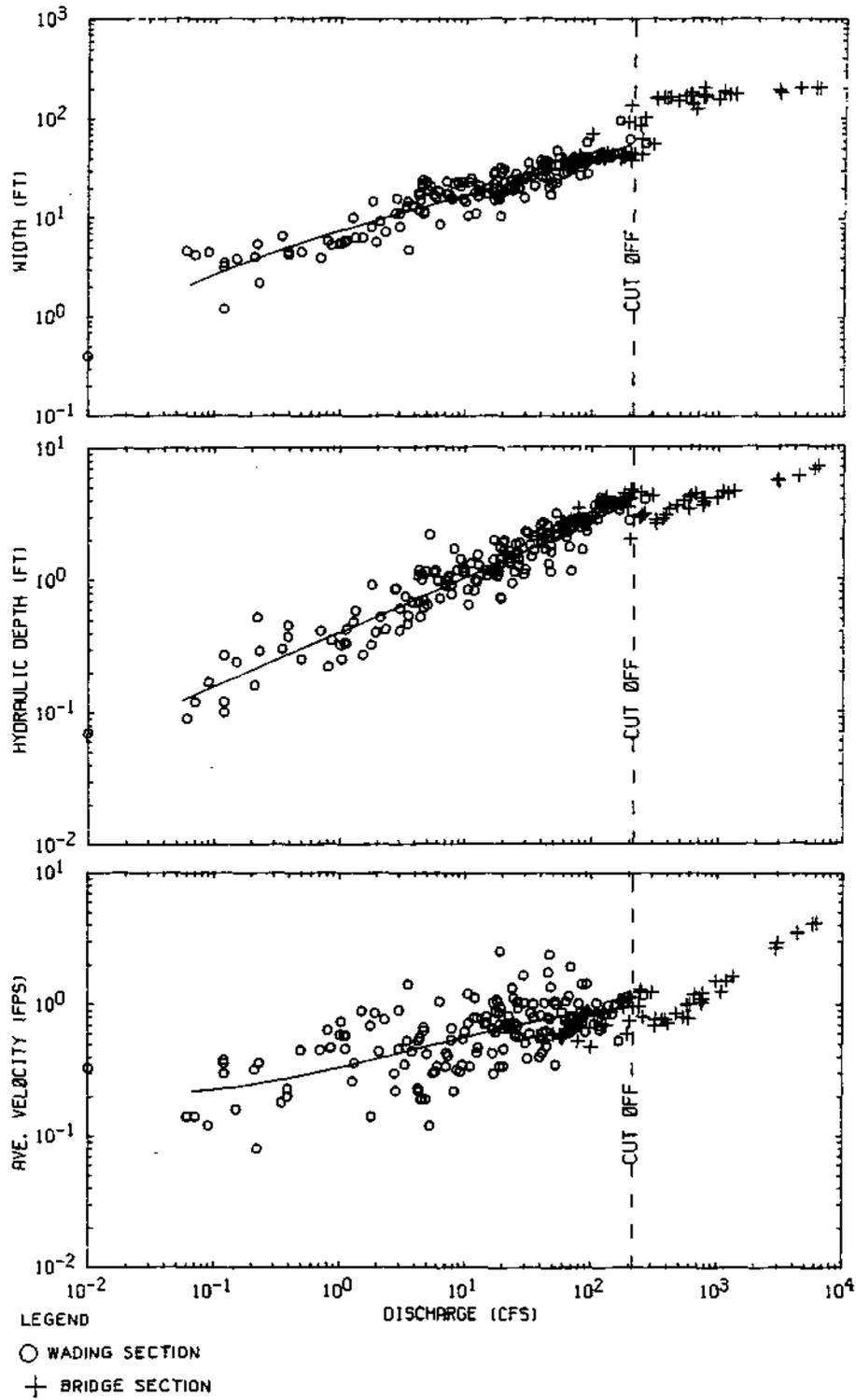


Figure 15. Station hydraulic geometry, Spring Creek at Springfield

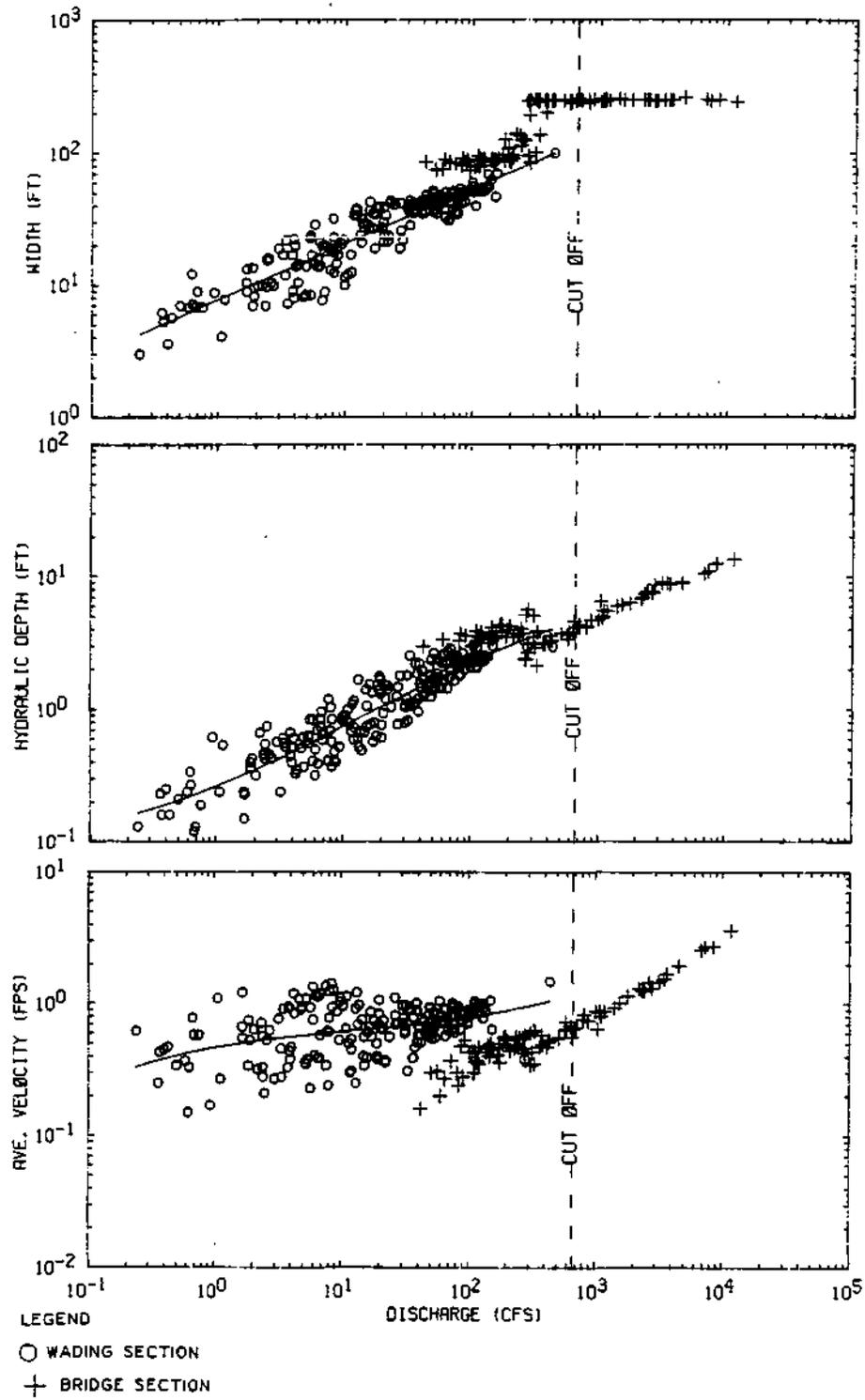


Figure 16. Station hydraulic geometry, Flat Branch near Taylorville

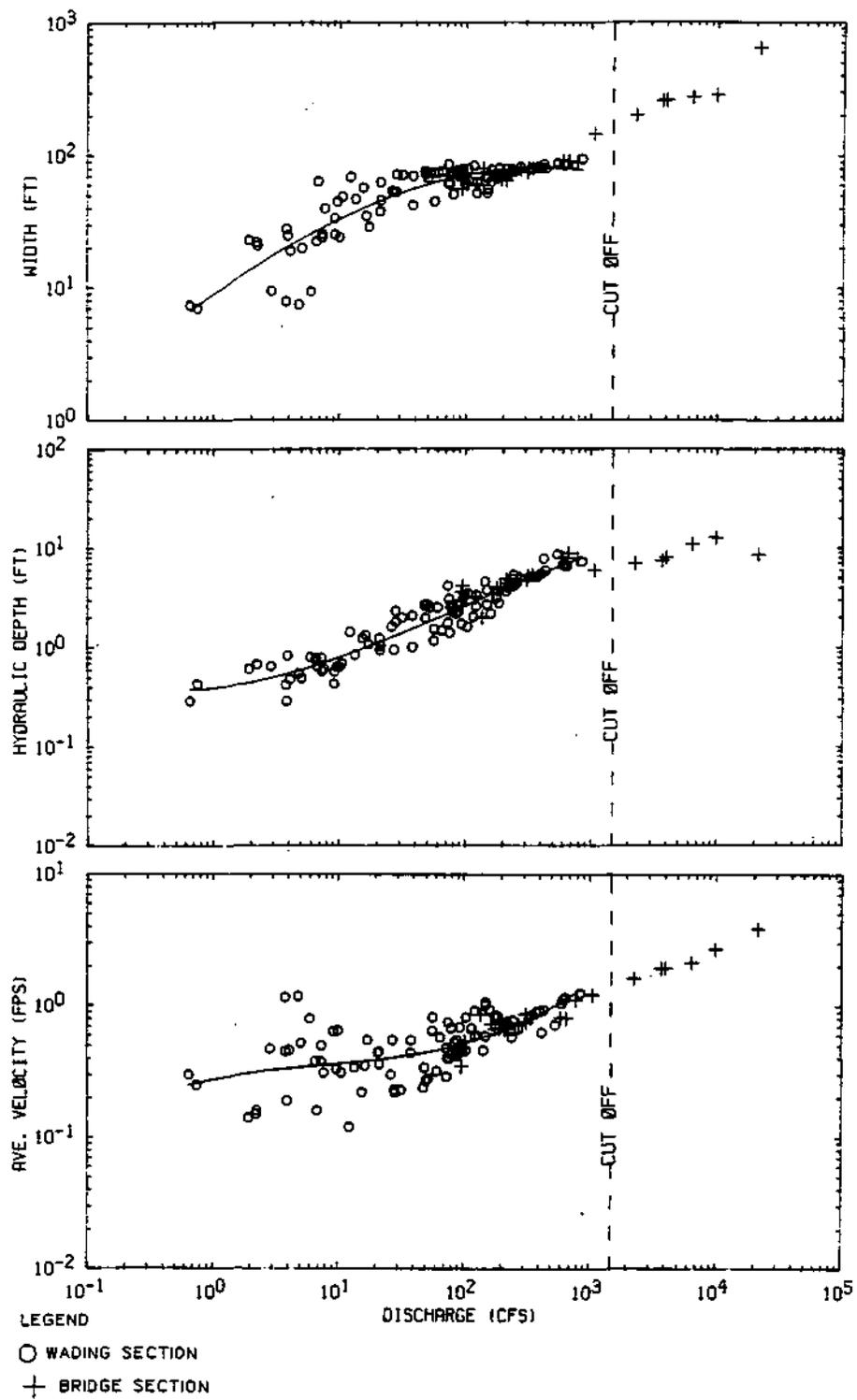


Figure 17. Station hydraulic geometry, South Fork Sangamon at Kincaid

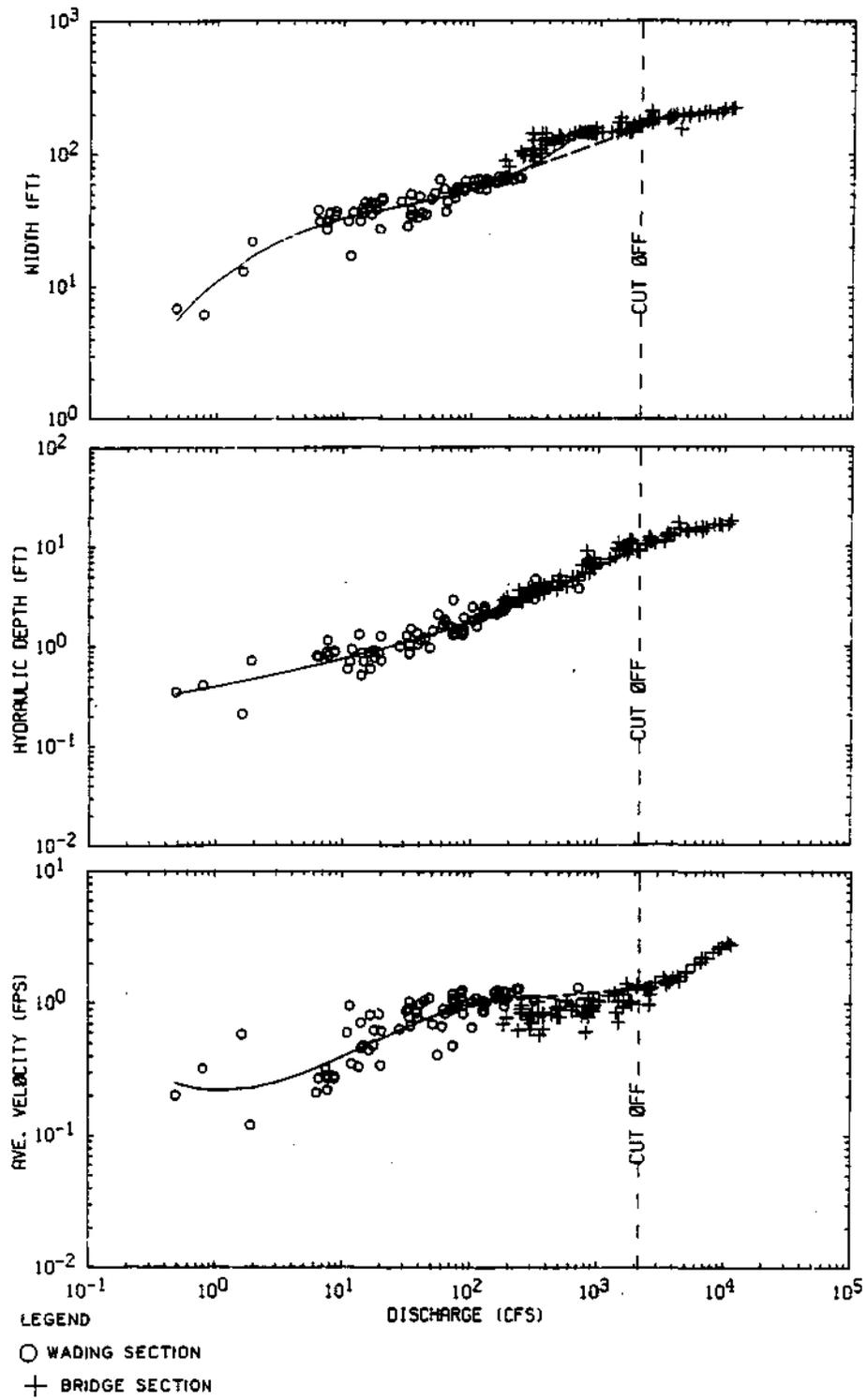


Figure 18. Station hydraulic geometry, South Fork Sangamon near Rochester

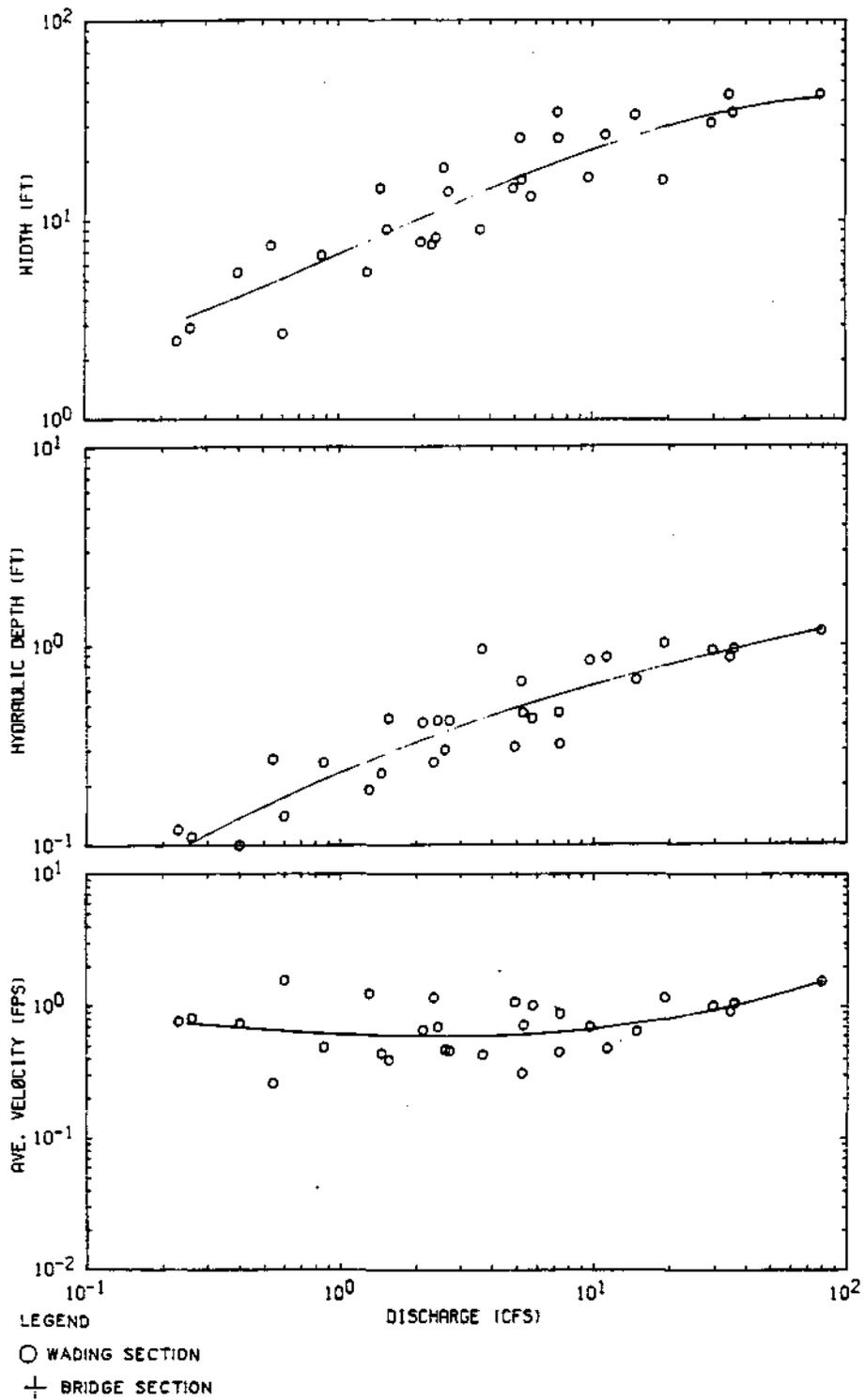


Figure 19. Station hydraulic geometry, Kickapoo Creek near Heyworth

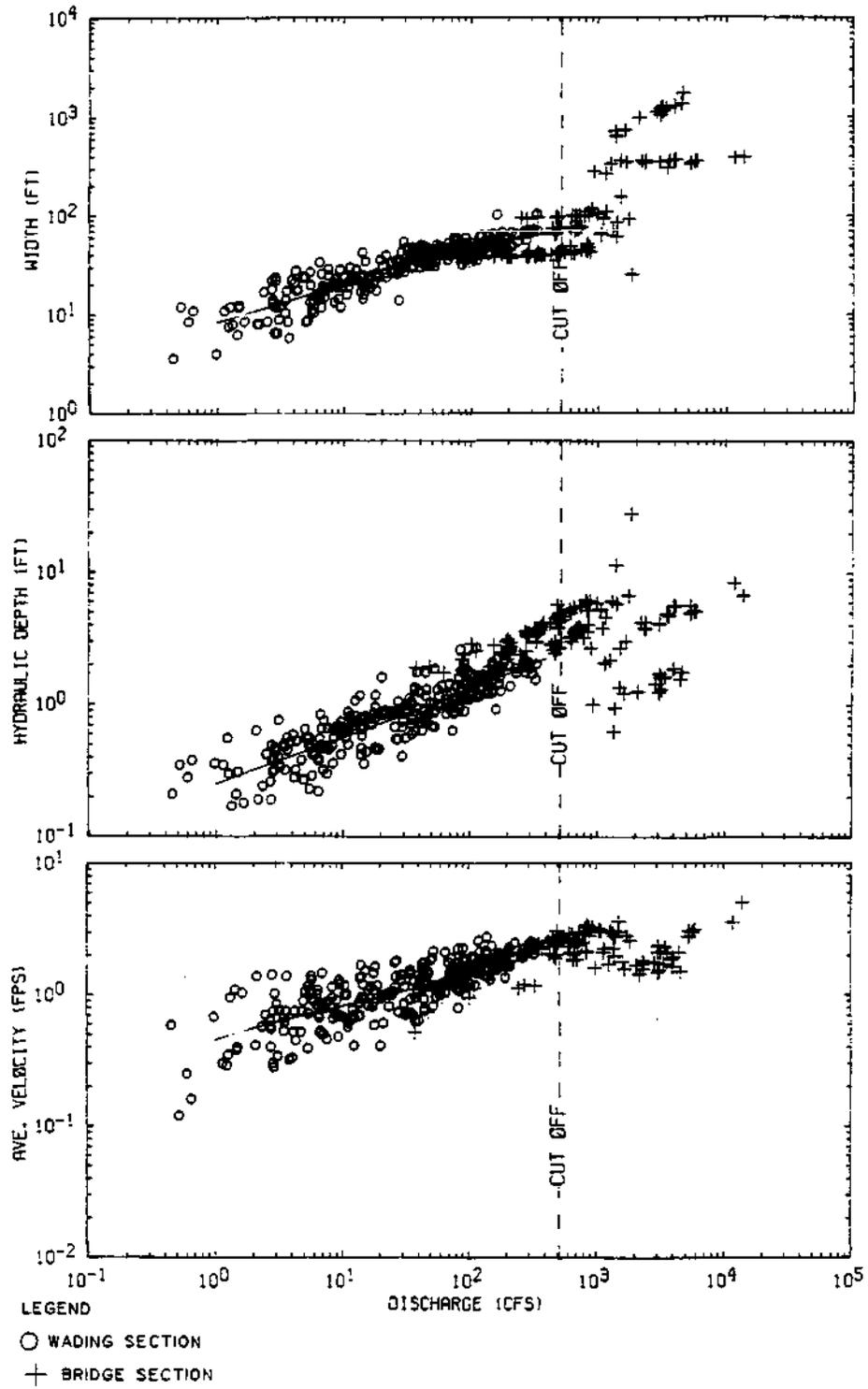


Figure 20. Station hydraulic geometry, Kickapoo Creek at Waynesville

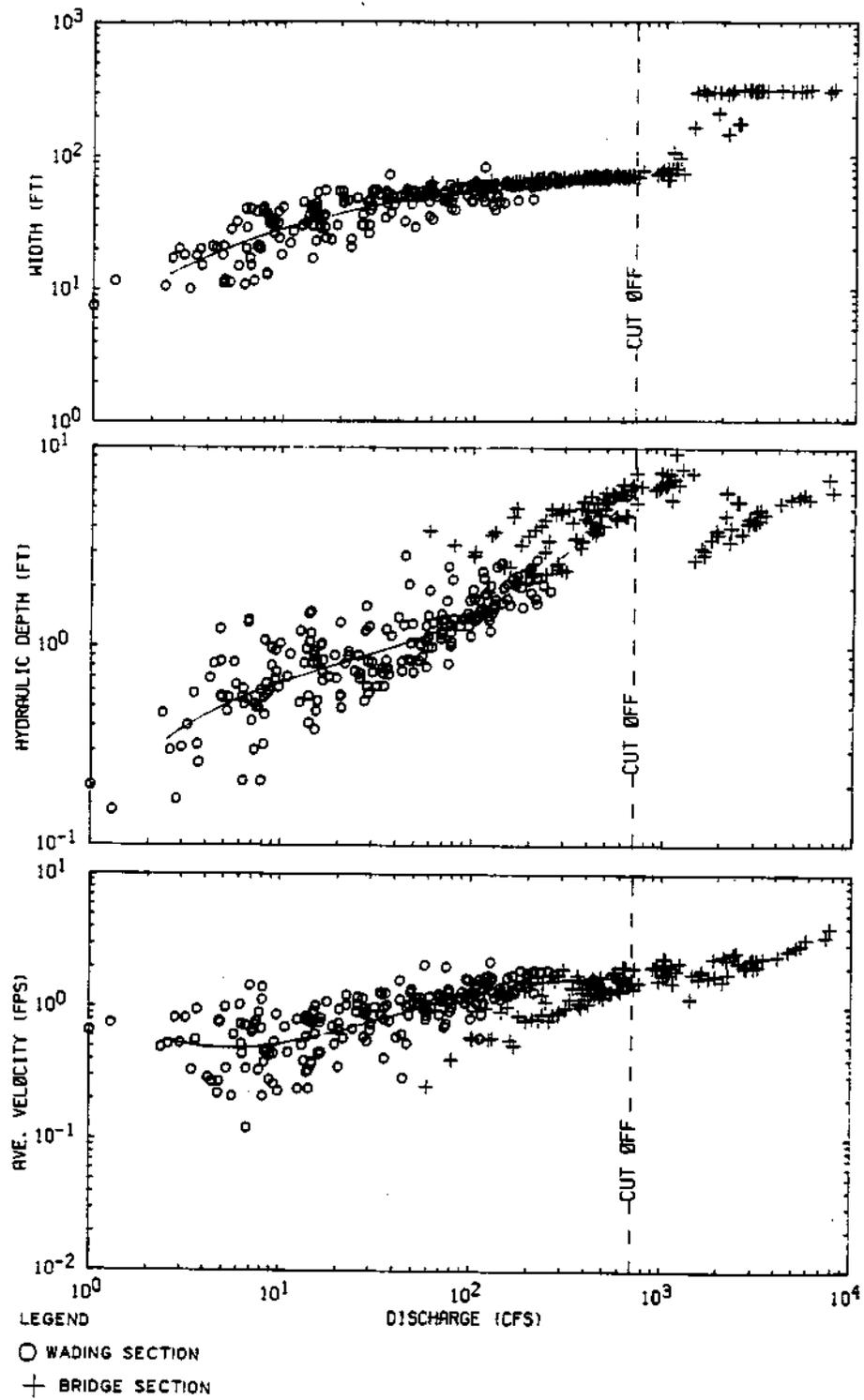


Figure 21. Station hydraulic geometry, Kickapoo Creek near Lincoln

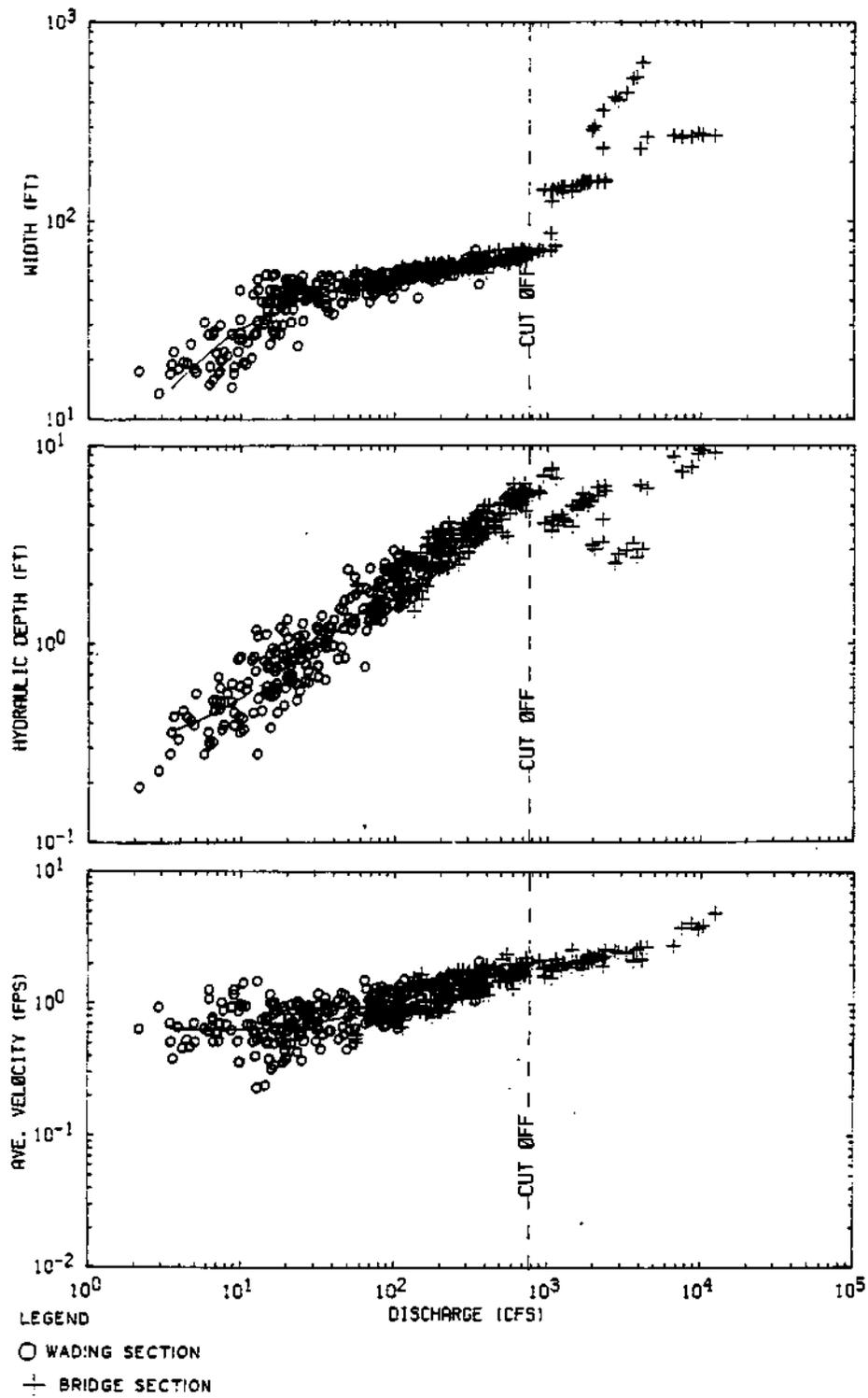


Figure 22. Station hydraulic geometry, Salt Creek near Rowell

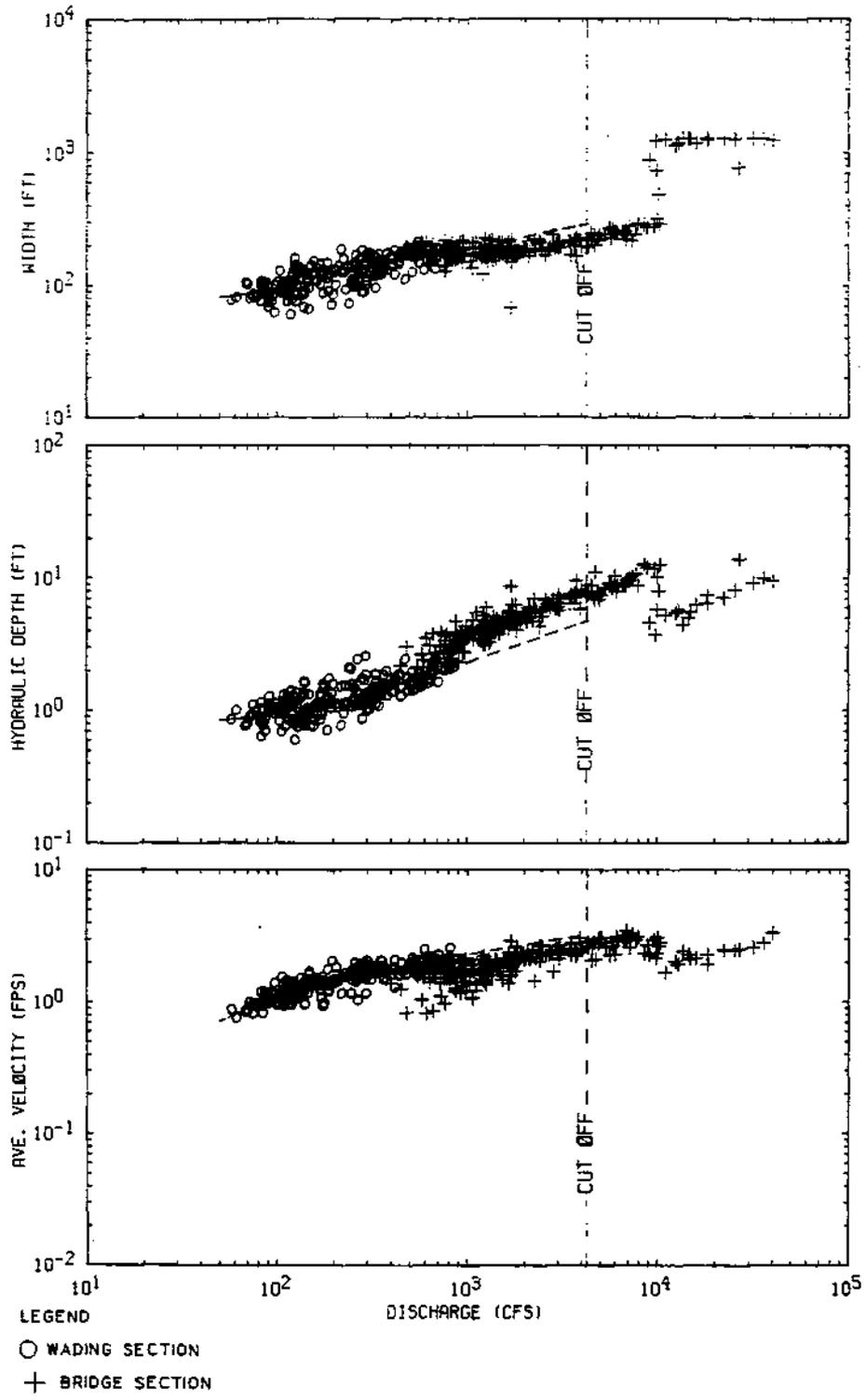


Figure 23. Station hydraulic geometry, Salt Creek near Greenview

sections. Also, there is consistently less scatter in the data collected at bridge sections than at wading sections. The relative differences between trends exhibited by wading and bridge data are site-specific.

Differences in the slope of the W, D, and V versus Q curves fitted to the bridge data and wading data yield different coefficients for the hydraulic geometry equations. The wading sections are clearly more representative of most of the stream length. Therefore, only data collected at wading sections were used in the regression analysis to evaluate the station equations. Station hydraulic geometry plots show the correspondence of flow parameters to discharge at a single cross section. The scatter in the data at lower discharges in Figures 5 through 23 is attributed to the fact that wading measurements are not made at the same place each time (Dunne and Leopold, 1978). This was further confirmed by review of the hydrographer's notes for the gaging stations. The band width of the data is an indication of the variation of depths and velocities which may be observed in a natural channel. It was observed that for the same discharge, measurements made at lesser depths have higher velocities and those at greater depths have lower velocities. Thus, the extremes of the data bands reflect the velocities and depths approaching riffle and pool conditions. Further conclusions cannot be drawn from the gaging station data because the hydrographers' field notes do not specify the location of the measurement relative to the riffle-pool sequence.

Regression Analyses

Computerized regression analyses were performed to determine the best polynomial relation for each flow parameter as a function of Q. The general form of the relation tested is:

$$\log \text{Var} = a_0 + a_1 \log Q + a_2 (\log Q)^2 + a_3 (\log Q)^3 + \dots + a_6 (\log Q)^6 \quad (9)$$

Overall, the third-order polynomial approximation of the station flow parameters had the highest correlation and lowest standard error, S_e , for the wading data. The correlation and standard error of the third-order polynomial approximation was not significantly better than the linear approximation in many cases. However, a comparison of the linear and curvilinear functions plotted with the data indicated that the curvilinear function had a better fit, particularly at the lower discharges. Because

the lower range of discharges was targeted for this study, the third-order polynomial relation was selected for the station hydraulic geometry relations. The station hydraulic geometry equations developed are consistent with the physical law: $Q = V.W.D$.

The coefficients for the station hydraulic geometry equations are listed in Tables 3, 4, and 5 (Sangamon, South Fork Sangamon, and Salt Creek) along with the range of discharges to which they apply, the multiple correlation coefficient, R , and the standard error, S . The equations are plotted in Figures 5-23 with a solid line from the lowest extrapolation limit to the highest extrapolation limit.

The correlation of width and depth with discharge is significant as evidenced by the correlation coefficients shown in Tables 3, 4, and 5. The correlation between velocity and discharge is less than for the other parameters. The values of measured velocity are highly variable; there is considerably more scatter in all station plots of velocity than in plots of the other parameters. This implies that another factor, possibly the position of the measured section relative to the riffle-pool sequence, significantly influences the velocities measured at that section for a given discharge.

The summations of the a_0 , a_2 , and a_3 coefficients for W , D , and V are close to zero and the summations of a_1 are close to 1.0. Thus the product of W , D , and V (determined from the regression equations) practically equals Q .

Approximations for High Flows Not Measured at Wading Sections

Only data collected at wading sections were used in defining the hydraulic geometry relations. Wading measurements are usually not made at depths exceeding 3 feet. As drainage area increases, the flow duration at which the wading depth is exceeded also increases. For example, wading measurements at DeLand, $A_d = 47.3$ sq mi, continue beyond the 10% flow duration discharge; however, wading measurements at Rochester, $A_d = 867$ sq mi, stop at approximately the 50% flow duration discharge. Seven of the stations did not have wading data for high discharges. Relationships developed for the wading data could not be extrapolated through the needed range of discharges for Rochester on the South Fork; for Monticello,

Table 3. Sangamon Basin Station Hydraulic Geometry Equations

$$\log(\text{VAR}) = a_0 + a_1(\log Q) + a_2(\log Q)^2 + a_3(\log Q)^3$$

| <u>Station</u> | <u>VAR</u> | <u>a₀</u> | <u>a₁</u> | <u>a₂</u> | <u>a₃</u> | <u>R</u> | <u>S_e</u> | <u>Range of discharges</u> | | | |
|----------------|------------|----------------------|----------------------|----------------------|----------------------|----------|----------------------|----------------------------|------------------------|-------|--------|
| | | | | | | | | <u>Q_{min}</u> | <u>Q_{max}</u> | | |
| DELAND | W | 0.878 | 0.345 | -0.062 | 0.0097 | 0.928 | 0.070 | 0.38 | 91.4 | | |
| | D | -0.493 | 0.263 | 0.004 | 0.0308 | 0.946 | 0.077 | | | | |
| | V | -0.386 | 0.396 | 0.053 | -0.0390 | 0.913 | 0.106 | | | | |
| ARGENTA | W | 0.827 | 0.508 | -0.022 | -0.0276 | 0.970 | 0.098 | 0.02 | 192.0 | | |
| | D | -0.571 | 0.356 | -0.014 | 0.0172 | 0.956 | 0.117 | | | | |
| | V | -0.262 | 0.137 | 0.042 | 0.0077 | 0.847 | 0.131 | | | | |
| FISHER | W | 0.367 | 2.155 | -1.388 | 0.3175 | 0.844 | 0.111 | 3.78 | 179.0 | | |
| | D | -1.360 | 2.058 | -0.968 | 0.1772 | 0.885 | 0.150 | | | | |
| | V | 0.986 | -3.189 | 2.336 | -0.4900 | 0.729 | 0.157 | | | | |
| MAHOMET | W | 1.085 | 0.408 | -0.120 | 0.0298 | 0.891 | 0.104 | 0.26 | 895.0 | | |
| | D | -0.623 | 0.354 | -0.109 | 0.0514 | 0.912 | 0.131 | | | | |
| | V | -0.465 | 0.246 | 0.224 | -0.0803 | 0.787 | 0.179 | | | | |
| MONTICELLO | W | 0.874 | 0.756 | -0.153 | 0.0103 | 0.888 | 0.091 | 2.41 | 100.0 | | |
| | D | -0.626 | 0.415 | -0.090 | 0.0499 | 0.865 | 0.143 | | | | |
| | V | -0.250 | -0.173 | 0.246 | -0.0608 | 0.347 | 0.162 | | | | |
| | W | 1.260 | 0.300 | | | | | | | 100.0 | 1575.0 |
| | D | -0.901 | 0.570 | | | | | | | | |
| | V | -0.359 | 0.130 | | | | | | | | |
| NIANTIC | W | 3.288 | -3.481 | 2.089 | -0.3574 | 0.930 | 0.070 | 36.8 | 300.0 | | |
| | D | 1.272 | -2.107 | 0.949 | -0.1080 | 0.908 | 0.068 | | | | |
| | V | -4.690 | 6.773 | -3.123 | 0.4782 | 0.370 | 0.120 | | | | |
| | W | 1.123 | 0.370 | | | | | | | 300.0 | 2768.0 |
| | D | -1.093 | 0.540 | | | | | | | | |
| | V | -0.030 | 0.090 | | | | | | | | |
| RIVERTON | W | 3.786 | -3.400 | 1.794 | -0.2864 | 0.660 | 0.103 | 24.0 | 430.0 | | |
| | D | -0.958 | 1.284 | -0.647 | 0.1355 | 0.749 | 0.102 | | | | |
| | V | -2.869 | 3.186 | -1.187 | 0.1581 | 0.819 | 0.091 | | | | |
| | W | 1.517 | 0.200 | | | | | | | 430.0 | 6690.0 |
| | D | -1.220 | 0.620 | | | | | | | | |
| | V | -0.297 | 0.180 | | | | | | | | |

Note: R = multiple correlation coefficient
 S_e = standard error

Table 4. South Fork Sangamon Basin Station Hydraulic Geometry Equations

$$\log(\text{VAR}) = a_0 + a_1(\log Q) + a_2(\log Q)^2 + a_3(\log Q)^3$$

| <u>Station</u> | VAR | <u>a₀</u> | <u>a₁</u> | <u>a₂</u> | <u>a₃</u> | <u>R</u> | <u>S_e</u> | <u>Range of discharges</u> | |
|----------------|-----|----------------------|----------------------|----------------------|----------------------|----------|----------------------|----------------------------|------------------------|
| | | | | | | | | <u>Q_{min}</u> | <u>Q_{max}</u> |
| NOKOMIS | W | 0.698 | 0.424 | 0.043 | 0.0276 | 0.910 | 0.129 | 0.01 | 13.0 |
| | D | -0.525 | 0.474 | 0.006 | -0.0068 | 0.913 | 0.132 | | |
| | V | -0.174 | 0.100 | -0.048 | -0.0164 | 0.332 | 0.191 | | |
| DIVERNON | W | 0.911 | 0.464 | -1.121 | 0.0077 | 0.887 | 0.166 | 0.08 | 69.3 |
| | D | -0.448 | 0.377 | -0.161 | 0.0808 | 0.879 | 0.172 | | |
| | V | -0.463 | 0.162 | 0.280 | -0.0885 | 0.710 | 0.222 | | |
| PAWNEE | W | 0.768 | 0.529 | -0.060 | -0.0257 | 0.921 | 0.161 | 0.05 | 69.9 |
| | D | -0.463 | 0.383 | 0.029 | 0.0071 | 0.906 | 0.163 | | |
| | V | -0.307 | 0.090 | 0.033 | 0.0173 | 0.463 | 0.244 | | |
| SPRINGFIELD | W | 0.866 | 0.384 | -0.040 | 0.0166 | 0.929 | 0.128 | 0.07 | 197.0 |
| | D | -0.393 | 0.402 | 0.003 | 0.0024 | 0.940 | 0.124 | | |
| | V | -0.471 | 0.215 | 0.033 | -0.0172 | 0.627 | 0.209 | | |
| TAYLORVILLE | W | 0.893 | 0.429 | 0.000 | -0.0016 | 0.919 | 0.123 | 0.24 | 440.0 |
| | D | -0.570 | 0.391 | 0.083 | -0.0232 | 0.924 | 0.129 | | |
| | V | -0.324 | 0.180 | -0.082 | 0.0245 | 0.419 | 0.173 | | |
| KINCAID | W | 0.049 | 0.664 | -0.080 | -0.0127 | 0.887 | 0.130 | 0.65 | 853.0 |
| | D | -0.395 | 0.127 | 0.212 | -0.0354 | 0.946 | 0.120 | | |
| | V | -0.553 | 0.204 | -0.129 | 0.0475 | 0.640 | 0.182 | | |
| ROCHESTER | W | 1.039 | 0.793 | -0.415 | 0.0965 | 0.946 | 0.071 | 0.48 | 200.0 |
| | D | -0.387 | 0.243 | 0.018 | 0.0105 | 0.922 | 0.099 | | |
| | V | -0.652 | -0.033 | 0.394 | -0.1064 | 0.851 | 0.126 | | |
| | W | 1.014 | 0.360 | | | | | .200.0 | 2175.0 |
| | D | -0.915 | 0.570 | | | | | | |
| | V | -0.099 | 0.070 | | | | | | |

Note: R = multiple correlation coefficient
 S_e = standard error

Table 5. Salt Creek Basin Station Hydraulic Geometry Equations

$$\log(\text{VAR}) = a_0 + a_1(\log Q) + a_2(\log Q)^2 + a_3(\log Q)^3$$

| Station | VAR | a ₀ | a ₁ | a ₂ | a ₃ | R | S _e | Range of discharges | |
|-------------|-----|----------------|----------------|----------------|----------------|-------|----------------|---------------------|------------------|
| | | | | | | | | Q _{min} | Q _{max} |
| HEYWORTH | W | 0.830 | 0.556 | 0.019 | -0.049 | 0.901 | 0.146 | 9.0 | 107.4 |
| | D | -0.629 | 0.532 | -0.113 | 0.016 | 0.900 | 0.131 | | |
| | V | -0.204 | -0.087 | 0.099 | 0.031 | 0.495 | 0.181 | | |
| WAYNESVILLE | W | 0.923 | 0.347 | 0.082 | -0.032 | 0.905 | 0.109 | 1.0 | 400.0 |
| | D | -0.592 | 0.351 | -0.006 | 0.005 | 0.878 | 0.124 | | |
| | V | -0.333 | 0.305 | -0.079 | 0.028 | 0.776 | 0.136 | | |
| LINCOLN | W | 0.773 | 0.956 | -0.315 | 0.038 | 0.824 | 0.112 | 2.5 | 180.0 |
| | D | -0.807 | 1.064 | -0.578 | 0.144 | 0.819 | 0.141 | | |
| | V | 0.036 | -1.030 | 0.902 | -0.185 | 0.733 | 0.166 | | |
| | W | 1.48 | 0.13 | | | | | 180.0 | 704.8 |
| | D | -0.94 | 0.55 | | | | | | |
| | V | -0.54 | 0.32 | | | | | | |
| ROWELL | W | 0.557 | 1.385 | -0.563 | 0.079 | 0.855 | 0.075 | 3.6 | 200.0 |
| | D | -0.455 | -0.179 | 0.457 | -0.091 | 0.920 | 0.106 | | |
| | V | -0.114 | -0.181 | 0.091 | 0.015 | 0.598 | 0.133 | | |
| | W | 1.31 | 0.18 | | | | | 200.0 | 771.1 |
| | D | -0.82 | 0.55 | | | | | | |
| | V | -0.49 | 0.27 | | | | | | |
| GREENVIEW | W | 2.691 | -1.354 | 0.680 | -0.091 | 0.755 | 0.081 | 50.0 | 750.0 |
| | D | 0.715 | -1.192 | 0.526 | -0.056 | 0.753 | 0.088 | | |
| | V | -3.433 | 3.579 | -1.220 | 0.149 | 0.877 | 0.055 | | |
| | W | 1.45 | 0.28 | | | | | 750.0 | 4266.7 |
| | D | -1.08 | 0.48 | | | | | | |
| | V | -0.37 | 0.24 | | | | | | |

Note: R = multiple correlation coefficient
 S_e = standard error

Niantic, and Riverton on the Sangamon River; and for Lincoln, Rowell, and Greenview in the Salt Creek Basin.

The hydraulic relations for the range of discharges not measured at a wading section were approximated for these stations. A straight line was fitted on the logarithmic plots through the needed range of flows. The line was constructed to follow the trend indicated by the wading data and was guided by the values measured at bridge sections. The coefficients and range of discharges to which these relations apply are listed with the regression coefficients for lower discharges in Tables 3, 4, and 5. The functions are plotted with dashed lines in the station hydraulic geometry plots in Figures 5 through 23.

The data plots in Figures 5-23 illustrate typical hydraulic geometry relations at a station based on available USGS flow measurement data. The solid lines in the plots are the graphical representation of third-order polynomials fit to the data. The dashed lines in some of the figures show approximate linear relations developed in the absence of flow measurements made at representative natural channel cross sections. These relations are used to develop regional hydraulic geometry equations for the three basins.

BASIN HYDRAULIC GEOMETRY RELATIONS

Basin hydraulic geometry relations define the average values of width W , depth D , and velocity V for a given streamflow or for a given flow duration and drainage area. These parameters increase in a consistent manner with drainage area when compared at the same flow duration. Thus, each parameter varies with drainage area and flow duration. Equations expressing the relationship are calibrated for a given stream network by using parameter values calculated from station equations representing a range of drainage areas.

Basin equations were developed for each study basin by using multiple regression analysis. The parameter values used in the analysis were calculated from the equations developed for the stations in each basin at nine different discharges. Discharges for flow durations 10, 20, 30, 40, 50, 60, 70, 80, and 90% were computed by using the flow duration relationships and coefficients in Table 1. The W , D , and V at the computed discharges were then determined for each station.

The degree of association between the dependent variable and multiple independent variables may be expressed by the coefficient of determination, R^2 (Chow, 1964). If the sample size is small, the coefficient is adjusted for the degrees of freedom. The unbiased coefficient, commonly referred to as the adjusted R^2 , is expressed as

$$\text{adj } R^2 = 1 - S^2/s^2 \quad (10)$$

in which s is the unbiased standard deviation of the marginal distribution of the dependent variable, X .

$$s^2 = \frac{\sum_{i=1}^N (X_i - \bar{X})^2}{(N-1)} \quad (11)$$

in which \bar{X} = mean of X values and N is the sample size. S is the unbiased standard deviation of residuals (given value minus the computed value of X), $\sum \Delta^2$ is the sum of squared residuals, and m is the number of variables.

$$S^2 = \frac{\sum \Delta^2}{N-m} \quad (12)$$

Several relationships linking a flow parameter to drainage area, A_d in sq mi, and decimal flow duration, F , were compared on the basis of the adjusted R^2 , the standard error, S , and the confidence interval of the regression equation coefficients. The 95% confidence intervals are evaluated using Student's t test. Higher-order formulations including the terms $(\log A_d)^2$ and F^2 did not have significantly higher correlations or lower standard errors compared to a first-order relationship.

The addition of terms in the regression analysis reduced the degrees of freedom. Due to the limited size of the data set, the significance of the coefficients as measured by the value of Student's t was reduced. The lower value of Student's t is further reflected in an increase in the range of coefficient values estimated to be within the 95% confidence limits. This implies a greater range of values which may be assumed by the coefficients when developed from different data samples and which therefore reduces the reliability of the equations. The coefficients evaluated for a first-order relationship of the form:

$$\log (\text{Var}) = a + bF + c(\log A_d) \quad (13)$$

(where Var = W, D, or V) have less variability. Thus, this expression is most reliably calibrated with the available data. The regression coefficients evaluated for each basin are shown in Table 6 for this equation. The adjusted R^2 and standard error, S_e , of the estimate are listed as well as Student's t for each coefficient and the 95% confidence interval for the coefficient values. The simple correlation coefficients for each variable with F and A_d alone are noted in Table 7.

The Salt Creek Basin gaging stations, located in natural channels, do not represent a wide variety of drainage areas. No data are available for streams with drainage areas between 350 and 1700 sq mi, and only one station is located in a stream with drainage area less than 200 sq mi. Because a full range of drainage areas is not represented, the Salt Creek Basin equations may be less reliable than those developed for the other two basins in this study.

The relationships between flow parameters and drainage area defined by the coefficients listed in Table 6 are graphically illustrated for flow durations 10, 30, 50, 70, and 90% in Figures 24, 25, and 26 for the Sangamon, South Fork Sangamon, and Salt Creek Basins, respectively.

FIELD STUDY

A program of field work was conducted to measure depths and velocities in pools and riffles under a variety of flow conditions. Nine study reaches were selected representing a range of drainage areas. Measurements were made along 13 transects for two different discharges in each reach. Thus 18 sets of field data (for 18 different discharges) were collected. This information was used to investigate the distribution of the local values of depth and velocity through a pool-riffle sequence.

Selection of Study Reaches

Study reaches were selected to provide a representative sample of natural stream conditions throughout a basin. Study reaches are located in both the Sangamon and South Fork Sangamon Basins and represent a variety of drainage areas in each basin. Five reaches are in the Sangamon Basin;

Table 6. Basin Hydraulic Geometry Equations

$$\log(\text{VAR}) = a + bF + c(\log A_d) ; F = \text{decimal flow duration};$$

$$A_d = \text{drainage area (sq mi)}$$

| <u>VAR</u> | <u>a</u> (95% conf. limits) (Student's t) | <u>b</u> (95% conf. limits) (Student's t) | <u>c</u> (95% conf. limits) (Student's t) | Adj R ² | S _e |
|----------------------------|---|---|---|-----------------------|----------------|
| Sangamon | | | | | |
| W | 0.55 (0.43 to 0.67) 9.4 | -0.77 (-0.86 to -0.69) -17.4 | 0.58 (0.54 to 0.63) 28.0 | .95 | .088 |
| D | -0.32 (-0.44 to -0.20) -5.4 | -1.17 (-1.26 to -1.08) -25.8 | 0.41 (0.36 to 0.45) 19.1 | .94 | .089 |
| V | -0.0054 (-0.18 to 0.17) -0.06 | -0.53 (-0.66 to -0.40) -8.2 | 0.13 (0.07 to 0.19) 4.2 | .58 | .128 |
| South Fork Sangamon | | | | | |
| W | 0.68 (0.59 to 0.78) 14.8 | -0.93 (-1.03 to -0.83) -18.7 | 0.55 (0.51 to 0.59) 27.4 | .94 | .091 |
| D | -0.31 (-0.38 to -0.24) -8.9 | -1.22 (-1.30 to -1.15) -32.6 | 0.45 (0.42 to 0.48) 30.3 | .97 | .068 |
| V | -0.025 (-0.12 to 0.07) -0.54 | -0.59 (-0.69 to -0.49) -11.8 | 0.067 (0.03 to 0.11) 3.3 | .71 | .090 |
| Salt Creek | | | | | |
| W | 0.47 (0.32 to 0.61) 6.5 | -0.60 (-0.70 to -0.51) -13.0 | 0.61 (0.56 to 0.67) 23.0 | .94 | .080 |
| D | -0.22 (-0.39 to -0.06) -2.8 | -0.88 (-0.98 to -0.77) -16.9 | 0.30 (0.24 to 0.36) 10.1 | .90 | .090 |
| V | -0.18 (-0.30 to -0.06) -3.1 | -0.61 (-0.68 to -0.53) -15.8 | 0.22 (0.18 to 0.27) 10.1 | .89 | .066 |

Note: Adj R² = unbiased coefficient of determination
S_e = standard error

Table 7. Simple Correlation Coefficients for W, D, and V with A_d and F

| <u>Basin</u> | <u>Var</u> | <u>log A_d</u> <u>r</u> | <u>F</u> <u>r</u> |
|---------------------|------------|---|----------------------|
| Sangamon | W | .82 | -.49 |
| | D | .56 | -.77 |
| | V | .33 | -.68 |
| South Fork Sangamon | W | .77 | -.44 |
| | D | .59 | -.66 |
| | V | .08 | -.81 |
| Salt Creek | W | .84 | -.48 |
| | D | .49 | -.82 |
| | V | .51 | -.80 |

Note: W = width
D = depth
V = velocity
 A_d = drainage area
F = decimal flow duration

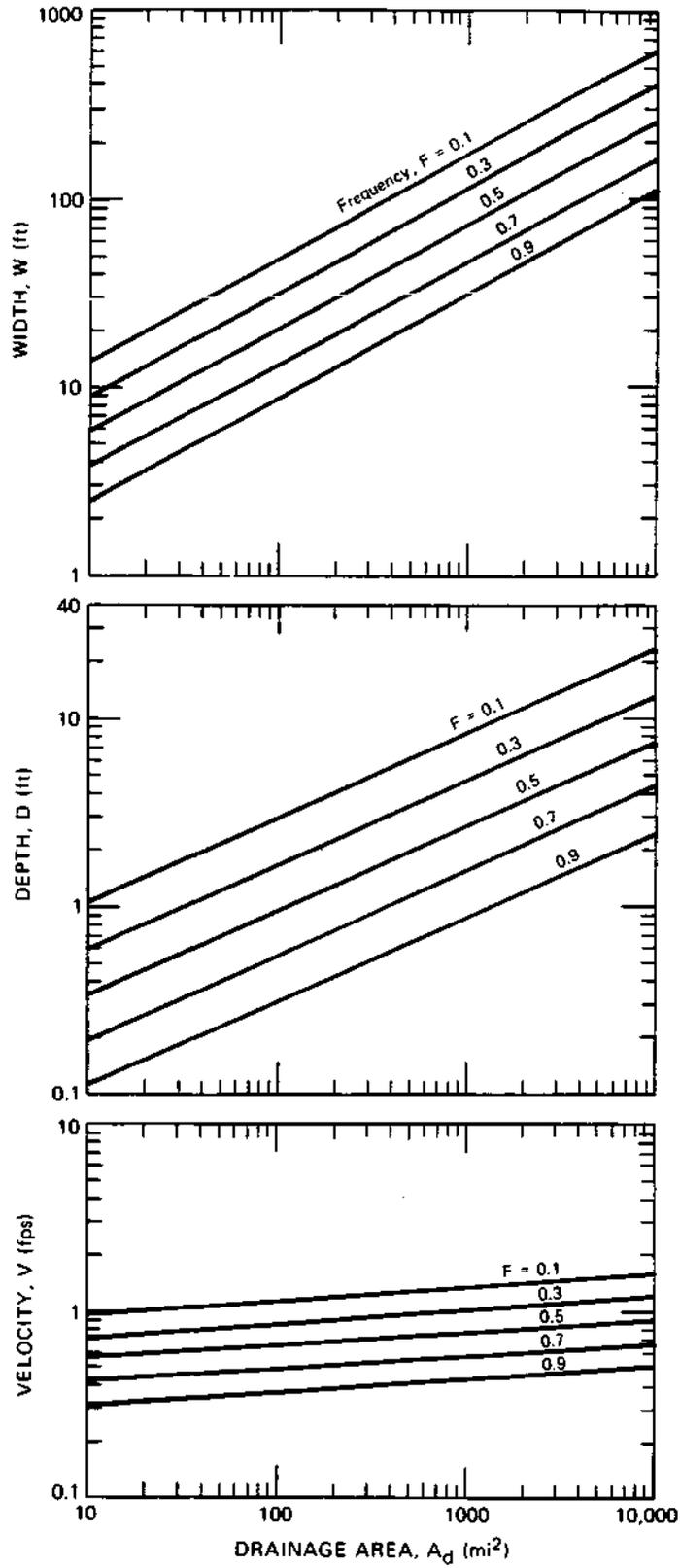


Figure 24. Sangamon Basin hydraulic geometry relations

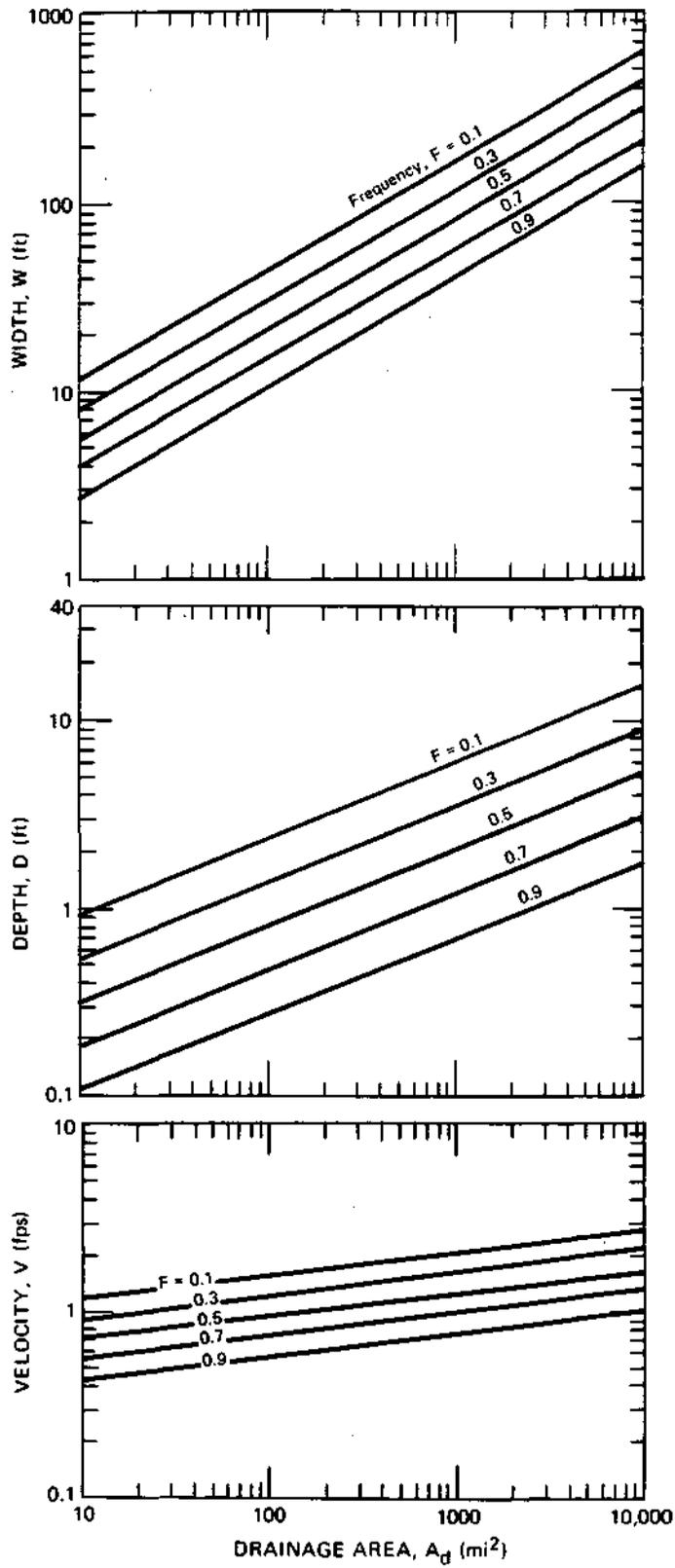


Figure 25. South Fork Sangamon Basin hydraulic geometry relations

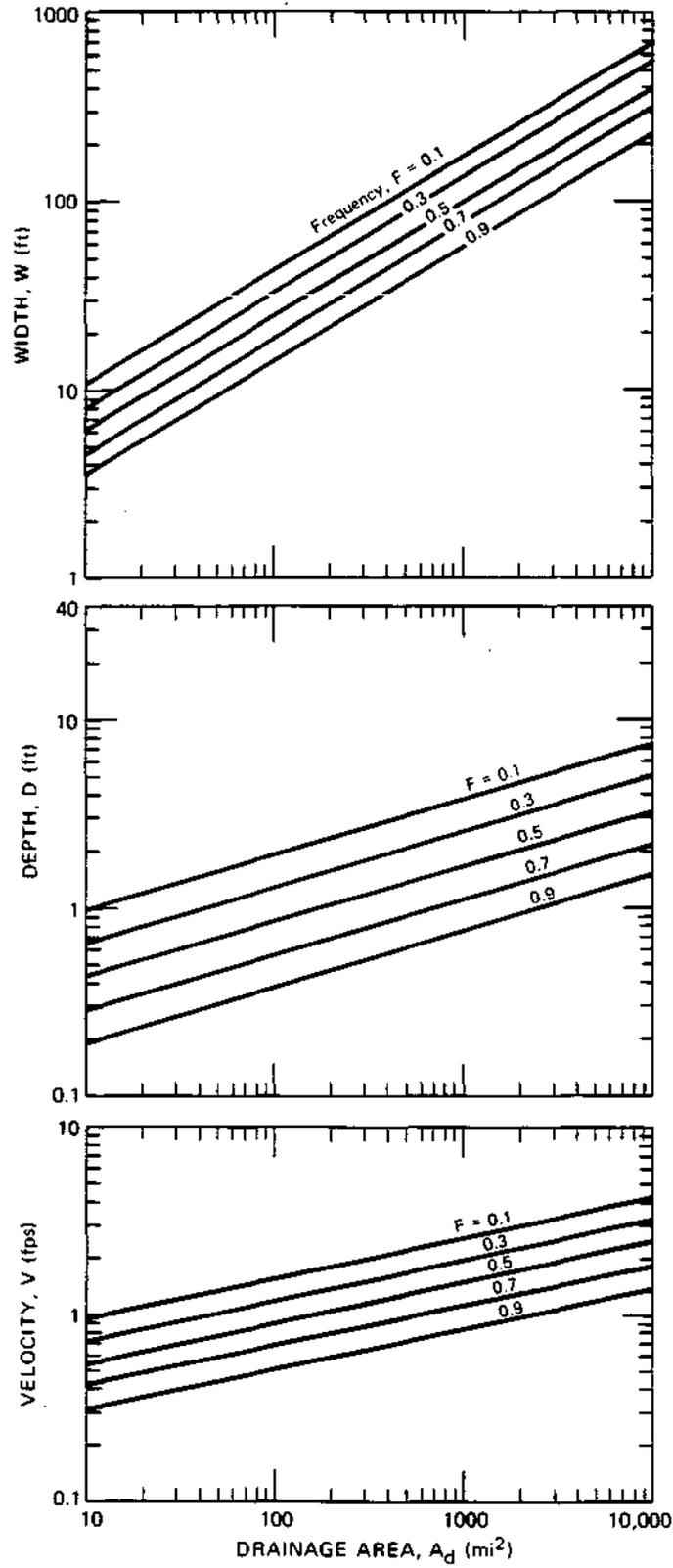


Figure 26. Salt Creek Basin hydraulic geometry relations

drainage areas range from 19.1 to 1439 sq mi. Four reaches are located in the South Fork Sangamon Basin; drainage areas range from 13.4 to 715 sq mi. Reaches are located in sections of streams not affected by backwater from dams or modified by bridge crossings. Reaches are straight or slowly meandering.

Reaches in natural, unaltered streams were selected whenever possible. However, this criterion could not always be met as channel modifications have been performed in many of the streams in the Sangamon River watershed. Sections of streams which have been straightened and have had their banks altered are delineated on the map in Figure 27 as well as the locations of study reaches. The map shown in Figure 27 was prepared for the Illinois Department of Conservation (IDOC) by the Department of Landscape Architecture at the University of Illinois (Riley et al., 1985(a); Riley et al., 1985(b)). The information on channel modifications was compiled from several sources, including IDOC reports, USGS 7-1/2-minute topographic maps, aerial photographs, and some site inspections. Streams identified in the map as "channelized" should include most cases of channel alterations, but some cases involving only bank clearing or channel deepening and widening may not be shown.

Common practice in central Illinois is to dredge natural waterways to improve farmland drainage. The majority of small drainage area streams in the watershed have been altered as shown in Figure 27. Reach 1 is located in a channel which has been dredged. A "natural" channel reach with a drainage area less than 25 sq mi could not be found in the Sangamon Basin. Field conditions suggest that Reach 6, in the South Fork Sangamon Basin, may also have had some modification in the past. However, for the most part the study reaches are located in sections of streams which currently appear to be in a natural state.

Streams which have been straightened, deepened, and/or widened have geometries and flow characteristics which may differ significantly from those in the natural state. Investigation of the hydraulic geometry and flow characteristics of modified streams is suggested for future research.

Each study reach was surveyed to locate three consecutive riffles and two intermediate pools. Streams in the Sangamon and South Fork Sangamon Basins have alluvial channels. Bed materials found in the study reaches ranged from silt to medium-sized pebbles, with the largest pebbles having

an approximate diameter of 1". Bed materials were examined to assist in identifying riffles and pools. Riffles were characterized by sand or by sand and pebbles, and all pools had some silt deposits up to several inches thick as observed at the time of the field work. Only riffles, well defined by lower depths and coarser bed materials, were used to establish the study reaches. Shallow spots with bed materials homogeneous to those of deeper pool sections were considered part of the pool. Additional descriptive information for the reaches is listed in Table 8. The reaches in the Sangamon Basin are numbered 1-5 and those in the South Fork Basin are numbered 6-9.

Field Procedures

A systematic measurement procedure was developed for all streams. Thirteen transects were measured in each reach. One transect was located at each riffle and five transects were located in each pool. Transects were equally spaced between riffles. Six uniformly spaced depth and velocity readings were made across each transect. Thus, there were a total of 78 data points for each discharge measured in a reach. The grid spacing established for the transects and sampling points (point depth and velocity) is in proportion to the stream dimensions: width and riffle-pool spacing. The schematic sketches in Figure 28 show the location of transects and the position of measurements across the stream. Additional velocity and depth measurements were made at one or more transects for accurate computation of discharge.

Velocities and depths were measured for two different discharges in each reach. As only the relative variations in depth and velocity were needed, level surveying to determine water surface slope was not necessary. The procedure that was established requires significantly less field time than data collection requiring level surveying.

Field work was conducted between April and August 1985. Field work was done during relatively dry periods, timed to avoid unsteady flow conditions after rainfall events. An unusually wet June, July, and August 1985 prevented flow from receding to relatively low flow (high value of flow duration). The flow durations of the discharges have the greatest difference that could be achieved during the 5-month field study. Flow durations of measured discharges ranged from 19 to 82% with most of them between 30

Table 8. Study Reaches

| <u>Reach no.</u> | <u>Nearest town</u> | <u>Township Range Section</u> | <u>Stream name</u> | <u>A_d (sq. mi)</u> | <u>Reach length (ft)</u> |
|---------------------|---------------------|-------------------------------|--------------------|-------------------------------|--------------------------|
| SANGAMON | | | | | |
| 1 | Saybrook | T23N R5E S27 | Sangamon | 19.1 | 329.0 |
| 2 | Gibson City | T22N R7E S06 | Sangamon | 55.8 | 166.0 |
| 3 | Fisher | T21N R8E S06 | Sangamon | 240.0 | 860.0 |
| 4 | Allerton Park | T18N R5E S30 | Sangamon | 613.0 | 1200.0 |
| 5 | Riverton | T16N R4W S25 | Sangamon | 1439.0 | 825.0 |
| SOUTH FORK SANGAMON | | | | | |
| 6 | Nokomis | TUN R2W S36 | S.F. Sangamon | 13.4 | 550.0 |
| 7 | Findlay | T13N R2E S22 | Flat Branch | 77.3 | 165.0 |
| 8 | Moweaqua | T14N R1E S34 | Flat Branch | 190.5 | 570.0 |
| 9 | Rochester | T14N R4W S03 | S.F. Sangamon | 715.0 | 1183.0 |

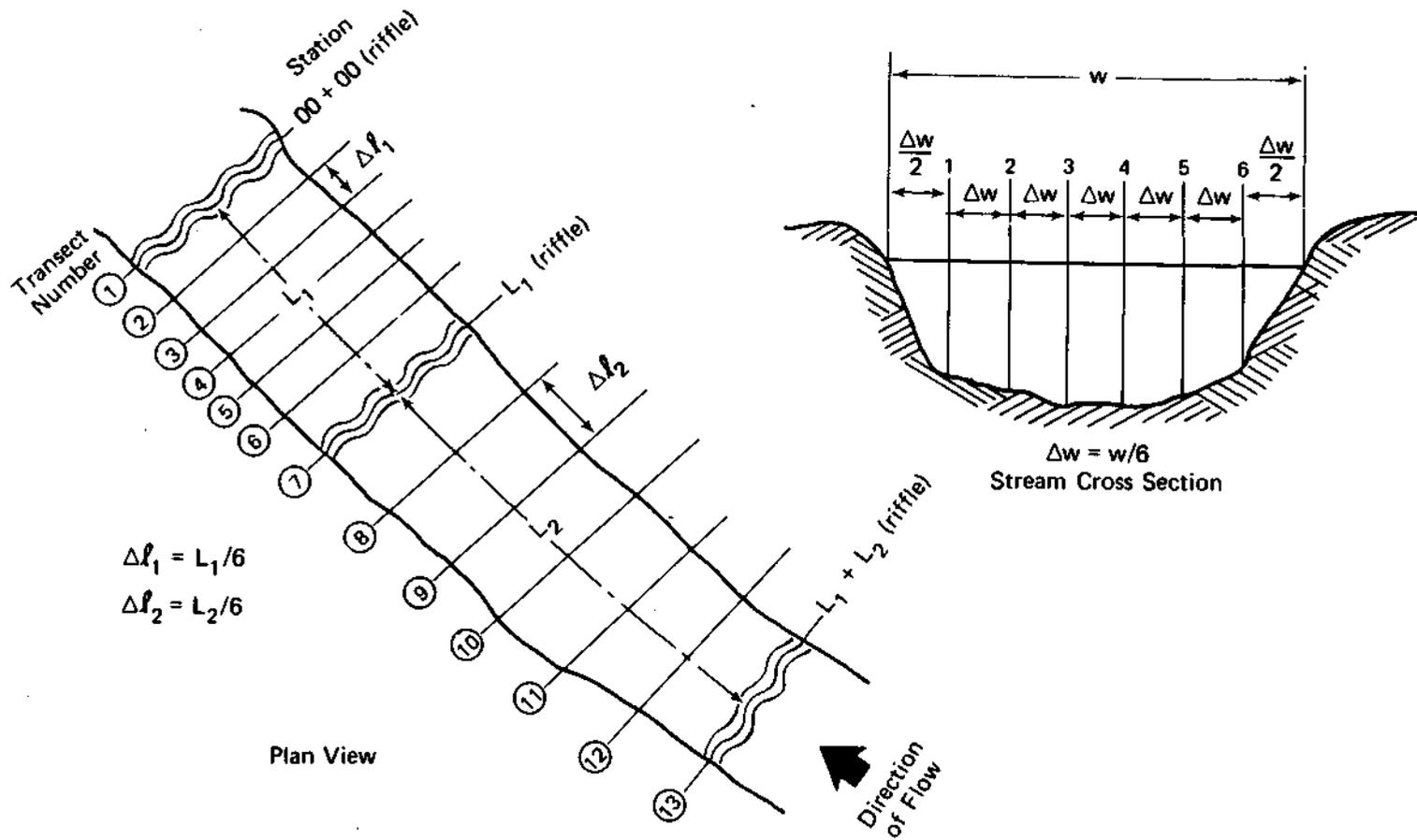


Figure 28. Schematic sketch of transect locations and divisions of channel cross section

and 70%. The flow durations corresponding to the flows observed in the field were computed by interpolating between the computed flows at various flow durations with the regression equations previously presented in Table 1.

Analysis of Field Data

Field data were analyzed by using computer programs developed specifically for the study, augmented by statistical analysis procedures available in the SPSS (Statistical Package for the Social Services) computer software package. Field data were entered and stored on the Illinois State Water Survey VAX computer. Recorded information includes the reach drainage area, discharge, flow duration, stationing of transects, cross-sectional area of flow, top water width at each transect, and the 78 velocity and depth measurements. Transect average depths and velocities and flow cross-sectional area were computed. Discharge, flow duration, beginning date of field work, and reach average parameter values are listed in Table 9. The two discharges measured at each reach are designated a and b. Due to the hydrologic and geomorphologic differences between the Sangamon and South Fork Sangamon, the data collected were analyzed independently for each basin.

Each depth and velocity sampled is assumed to represent flow conditions in a portion of the reach designated by a quadrilateral flow surface area, a_k . The bounds of the quadrilateral are defined by the mid-point distance between measurements. A weighting factor, W_k , proportional to the ratio between this quadrilateral stream surface area and the total surface area of the pool riffle sequence was computed for each data point. A riffle-pool sequence was defined as the section of the reach from riffle center to riffle center, e.g., the reach section between transect 1 and transect 7 and between transect 7 and transect 13. The flow surface area, A_{RP} , of the riffle-pool sequence was computed. The percent of the riffle-pool sequence represented by a quadrilateral component was then calculated by dividing a_k by the A_{RP} of the sequence. The weighting factor, W_k , was determined by dividing this quotient by the number of riffle pool sequences in the reach, i.e., 2. W_k is the proportion of the total reach area represented by a_k , as follows:

Table 9. Discharge and Average Values of W, D, V, and A Measured at Study Reaches

| Station No. | Q No. | Start date | Q (cfs) | Flow duration | Average values | | | |
|----------------------------|-------|------------|---------|---------------|----------------|--------|------------|----------------------|
| | | | | | W (ft) | D (ft) | V (ft/sec) | A (ft ²) |
| Sangamon | | | | | | | | |
| 1 | a | 06-05-85 | 4.7 | 46 | 21.4 | 0.43 | 0.60 | 9.0 |
| | b | 07-11-85 | 4.0 | 48 | 21.4 | 0.42 | 0.57 | 9.0 |
| 2 | a | 06-03-85 | 14.8 | 46 | 26.4 | 1.08 | 0.69 | 28.7 |
| | b | 08-13-85 | 8.3 | 56 | 20.3 | 0.96 | 0.50 | 18.7 |
| 3 | a | 06-10-85 | 58.0 | 49 | 49.7 | 2.05 | 0.59 | 102.2 |
| | b | 08-14-85 | 23.3 | 64 | 45.7 | 1.72 | 0.32 | 78.7 |
| 4 | a | 06-18-85 | 383.0 | 29 | 84.8 | 4.34 | 1.07 | 370.0 |
| | a | 06-19-85 | 317.0 | 33 | 81.2 | 3.79 | 0.96 | 307.2 |
| | b | 07-26-85 | 137.0 | 52 | 72.9 | 2.49 | 0.77 | 181.6 |
| 5 | a | 07-17-85 | 683.0 | 36 | 114.8 | 4.17 | 1.44 | 475.5 |
| | b | 08-09-85 | 398.0 | 49 | 106.6 | 2.54 | 1.33 | 267.3 |
| South Fork Sangamon | | | | | | | | |
| 6 | a | 07-03-85 | 10.6 | 19 | 17.8 | 1.04 | 0.57 | 18.2 |
| | b | 06-20-85 | 2.8 | 43 | 16.9 | 0.72 | 0.30 | 11.9 |
| 7 | a | 07-08-85 | 8.7 | 56 | 15.5 | 0.75 | 0.68 | 11.6 |
| | b | 07-23-85 | 0.9 | 82 | 9.7 | 0.57 | 0.25 | 5.9 |
| 8 | a | 07-10-85 | 16.0 | 61 | 28.5 | 1.59 | 0.37 | 44.5 |
| | b | 07-19-85 | 4.3 | 78 | 27.2 | 1.26 | 0.19 | 33.7 |
| 9 | a | 06-26-85 | 182.0 | 43 | 63.5 | 3.42 | 0.82 | 217.8 |
| | b | 07-18-85 | 35.1 | 72 | 55.3 | 2.27 | 0.27 | 126.5 |

$$W_k = (a_k/A_{RP})/2.0 \quad (14)$$

where $\sum_{k=1}^N W_k = 1.0$ and $N =$ number of data points, 78

Thus the data collected in each riffle-pool sequence is equally weighted even if the areal extent of the riffle-pool sequences in the reach differ. The weights are equal if stream width is constant and the transects are equally spaced. The weights were used in all statistical calculations. The average and standard deviation of all measured depths and velocities were computed for each observed discharge at each of the nine reaches. For purposes of discussion, these values will be referred to as averages and standard deviations for each reach.

Riffles and Pools

Riffle-to-riffle spacing in each reach was compared to results reported in the literature. Along the stream length, average riffle-to-riffle spacing typically reported is 5 to 7 times the channel width (Leopold and Maddock, 1953; Harvey, 1975). Channel width increases with drainage area. Thus the distance between riffles increases as drainage area increases. The spacing between riffles has been shown to correlate closely with average flow widths calculated from hydraulic geometry relations for the 20% flow duration discharge (Harvey, 1975). The relationship between logarithms of riffle spacing and width is linear.

A logarithmic plot of riffle spacing for the study reaches versus width (width, W_{20} , corresponds to 20% flow duration) was developed by using the combined data from both the basins and is shown in Figure 29. The relationship appears to be the same for both basins. Two points are plotted for each reach, representing the spacing between transects located at the three riffles identified by field personnel. The reach number appears adjacent to the plotted point in the figure. A straight line was fit by eye to the data and is shown in the figure.

The points for the intermediate drainage-area reaches show a linear trend. The smallest drainage area reaches, 1 and 6, had more erratic riffle spacing, and the plotted points for those reaches do not fall on the line. This may be attributable to dredging activities in these reaches.

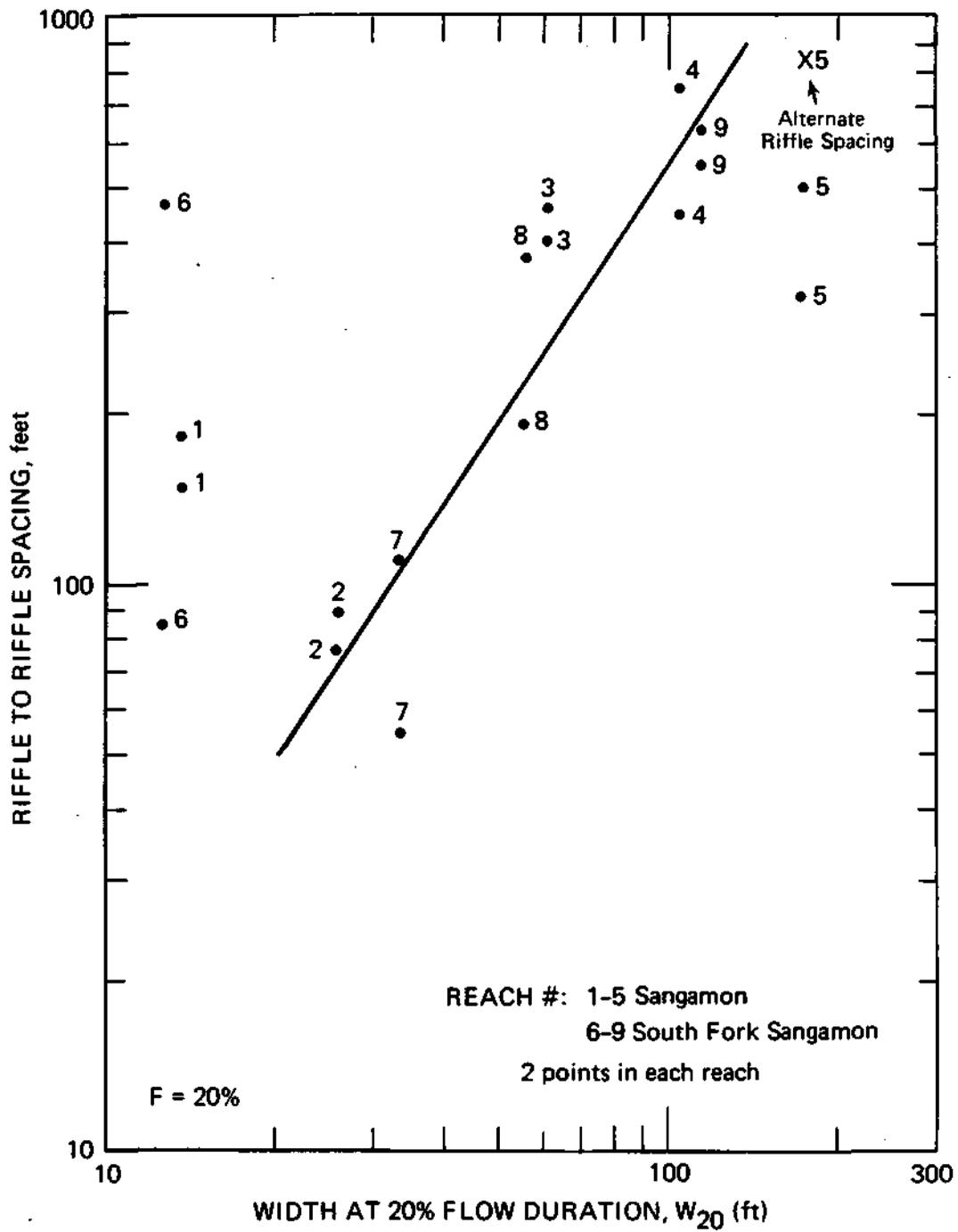


Figure 29. Study-reach riffle spacing versus W_{20}

The apparent riffle-pool sequences differ with discharge at reach 5. This may be the result of an unobserved obstruction downstream, but the plotting position of riffle spacing, based on transect location, suggests that reach 5 may comprise only one riffle-pool sequence. Alternatively, a point representing the full reach length versus W_{20} is also plotted. This point plots near the line indicated by the other data.

The average riffle spacing for the Sangamon and South Fork Sangamon for all the reaches was 7 times the width (calculated for 20% flow duration). Excluding the relatively long spacing found at the smallest drainage area reaches, the average spacing is 4.5 times the width. When the alternate value of riffle spacing for reach 5 is substituted, the average is 5.0.

The terms riffle and pool refer to relative differences in flow conditions and bed materials, and are not precisely defined in terms of hydraulics. The transition zone between a riffle and a pool, and vice versa, has by definition intermediate flow conditions. An attempt was made to develop a means of estimating relative lengths of pools and riffles in a reach without direct field observation. However, the relatively low depths and high velocities found at the silted, shallow sections of pools hampered efforts to define flow conditions unique to riffles and to pools. There is also an apparent dependence of riffle lengths (and pool lengths) on flow duration, which adds another dimension to the problem of subdividing Sangamon and South Fork Sangamon streams into riffle sections with characteristic flow condition, spacing, and length, and pool sections with unique flow conditions, spacing, and length. The variation of depth and velocity through the riffle and pool sequence in the study reaches is better described as a continuum of values rather than discrete sections of a reach with characteristic depth and velocity. The continuum conceptual model was adopted in developing the flow model for depth and velocity.

Depth Distribution

The distribution of depths in a reach was investigated by plotting the depths measured at a single discharge on normal probability paper. The depths measured were ranked from low to high. The cumulative non-exceedance probability, p , was computed by using the weighting scheme

described earlier and the plotting position formula (N = total number of points):

$$P_i = m_i / (N+1) \tag{15}$$

where $m_i = \sum_{k=1}^i w_k$ and $w_k = W_k \times N$ so that $\sum_{i=1}^N w_k = N$

For each flow, the plotted points fall on an approximately straight line between the 10% and 90% non-exceedance probability levels. The slope of the lines varies with discharge and drainage area. The reach average depth plots at approximately the 50% non-exceedance probability for each case. The reach average depth, D, computed for each discharge ranged from 0.4 ft to 4.3 ft and from 0.6 ft to 3.4 ft in the Sangamon and South Fork Sangamon, respectively.

The standard deviation of a variable with normal distribution is a measure of the spread of values about the mean. The variation of depth in a channel is predominantly influenced by pool and riffle formation; thus, the standard deviation is a measure of the difference between pool and riffle depths. The difference between pool and riffle depths increases with an increase in drainage area. Consistent with this observation, the standard deviation of field measured depths, S_d , is typically greater for a larger drainage area reach than for a smaller drainage-area reach.

Plots of S_d versus drainage area are drawn in Figures 30a and b for each basin. A straight line (shown dashed) was fit by eye to the data. The slope of the line is similar for the two basins. The corresponding flow duration is noted above each data point. A comparison of S_d for the two discharges measured in each reach shows that in most cases S_d is larger at the smaller flow duration. This corresponds to greater variability in depths for low discharges. However, the difference is small. The relationship between S_d and flow duration cannot be defined without conducting field measurement over a broader range of flow durations. The simple linear relation shown in the plots is the best estimate with the available data. The relationship for the South Fork Basin data is fairly well approximated by a straight line. The relatively greater data scatter for the Sangamon Basin reaches may be attributable in part to conditions unique to the reaches measured or to field conditions at the time the measurements were made.

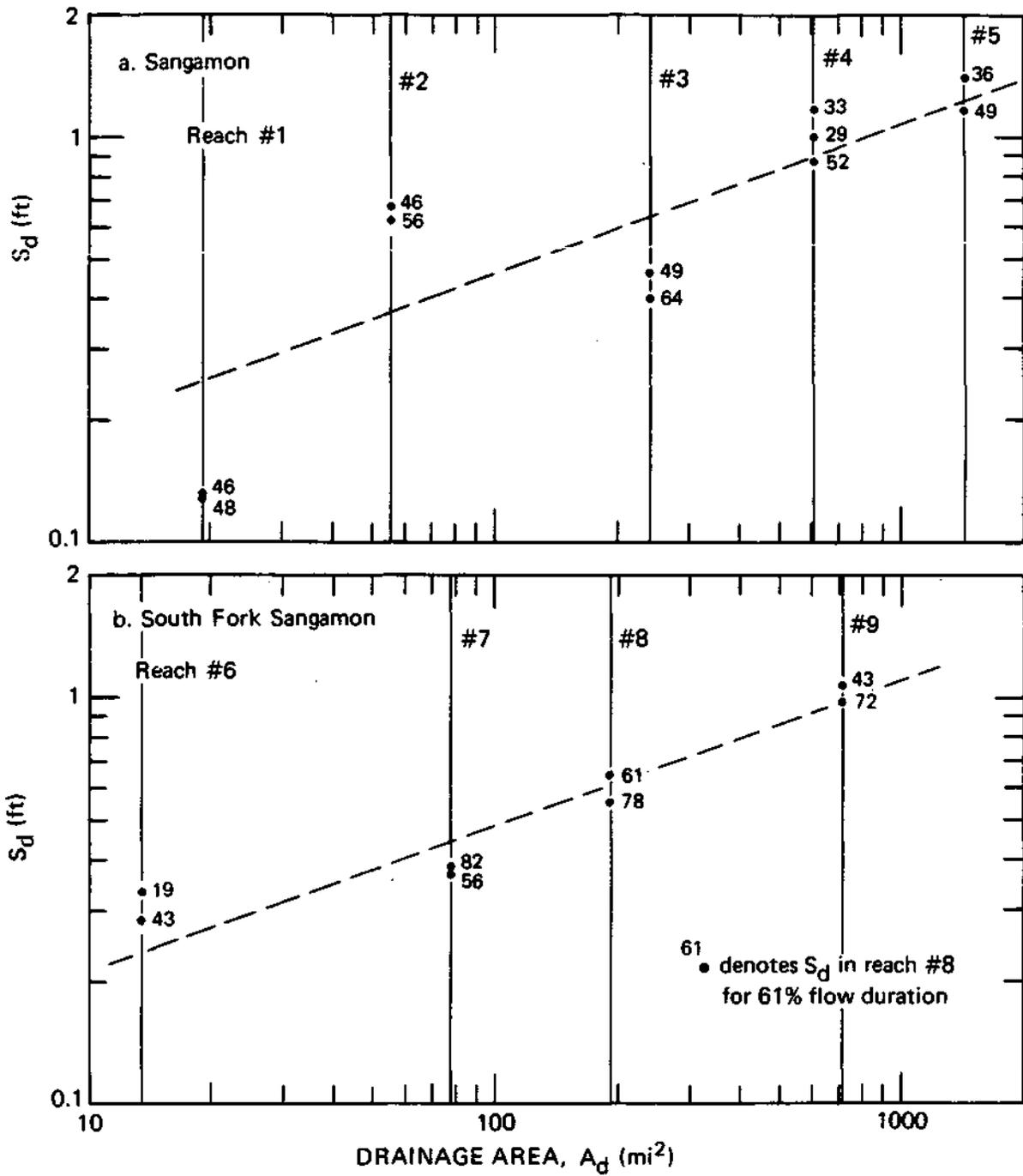


Figure 30. Standard deviation of depth, S_d , versus drainage area, A_d ,

Reach 1 is located in a channel which has been dredged periodically. Local residents report that the latest dredging occurred in 1983. Dredging would smooth out channel variations and result in a lower standard deviation of depths than might be found in a natural channel with the same drainage area. The apparently low values of computed standard deviation indicate that the stream may not yet have returned to its natural regime.

One measurement at reach 4 was conducted while the discharge was decreasing. Timing and weather did not permit another measurement at the site. The standard deviation of depths may be high due to the unsteady flow. The flow duration was approximately 29% for one riffle-pool sequence measured and 33% for the riffle-pool sequence measured the following day. These were taken into consideration when fitting the lines shown in Figure 30.

The relationship between the standard deviation of depth, S_d , and drainage area of the reach links the distribution of depths (through the riffle-pool sequence) in reaches throughout a basin. The average value of depth is related to drainage area and flow duration through hydraulic geometry. Figure 31 illustrates the non-dimensional depth distribution developed.

The variety of local depths expected within a reach for a given flow duration can be determined from the combined results of hydraulic geometry relations and relations developed from field data defining the distribution of depth. The average or mean depth, D , is calculated from the basin hydraulic geometry equation for depth. The distribution of normalized depths, Z , in a reach can be obtained from the normal cumulative probability distribution:

$$P(Z) = \frac{1}{\sqrt{2\pi}} \int_{-\infty}^Z \exp(-z^2/2) dz \quad (16)$$

where P is the non-exceedance probability, $Z = (d - D)/S_d$, and d is the actual depth for which P is calculated.

The value of Z is computed for a level of non-exceedance probability using a numerical solution of the inverse standard normal probability distribution function. The standard deviation of depth is a function of the drainage area of the reach; its value is obtained from the relationship shown in Figure 30a or b. Substituting the appropriate values of D , S_d ,

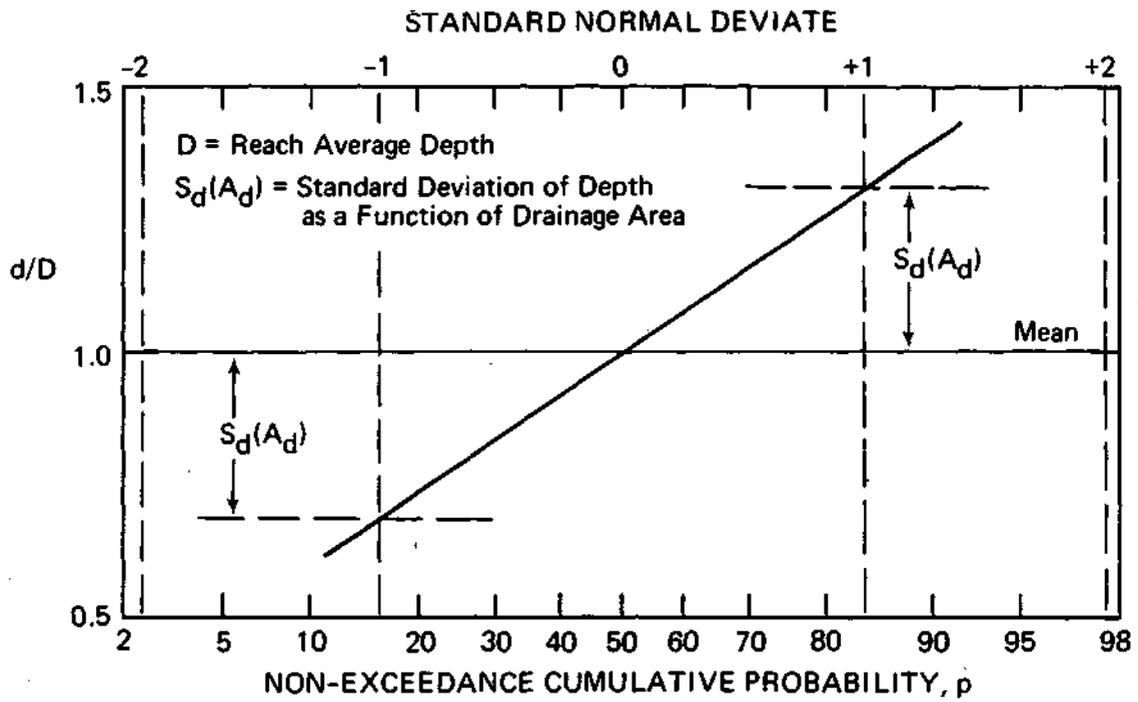


Figure 31. Non-dimensional depth distribution

and Z, the depth d for a given non-exceedance probability level, i, can be evaluated by solving for d_i , as

$$d_i = Z_i(s_d) + D \tag{17}$$

For example, 30% of the depths measured in a reach will be less than or equal to the depth, d_{30} , calculated from the value of Z at $P(Z) = 0.30$. The frequency of occurrence for each calculated depth is equal to the difference between successive non-exceedance probabilities; e.g., 10% of the depths in a reach will range between d_{20} and d_{30} , and the average depth in that range will be about d_{25} .

By following this methodology, the hydraulic geometry and depth distribution relationships developed for the basin can be used to compute the expected values of local depths in a reach for any drainage area, over a full range of flow durations.

Velocity Distribution

The distribution of local velocity values in a reach was first investigated independently of the depths. There is a large degree of variation in local velocity values. This is reflected in the standard deviation of velocity, S_v , which ranged between 40 and 95% of the reach average velocity. The reach average velocity, V, computed for each measured discharge ranged from 0.32 feet per second (fps) to 1.44 fps for the Sangamon Basin reaches and from 0.19 to 0.81 fps for measurements made in the South Fork Sangamon Basin. The standard deviation increased in value as the reach average velocity increased. There is a strong linear correlation between S_v and V. The simple correlation coefficient, r, computed from the field data is tabulated below as well as the linear functions relating S_v and V for each basin and for all the data combined.

| <u>Basin</u> | | <u>n*</u> | <u>r</u> |
|--------------|----------------------------|-----------|----------|
| Sangamon | $S_v = 0.12 + 0.38V$ | 10 | 0.97 |
| South Fork | $S_v = 0.091 + 0.43V$ | 8 | 0.97 |
| All data | $S_v = 0.10 + 0.40V$ | 18 | 0.98 |
| | or $S_v/V = 0.10/V + 0.40$ | | |

*n = sample size

Figure 32 shows a plot of S_v versus V for the 18 discharge measurements. The number appearing by each point is the reach number. The value

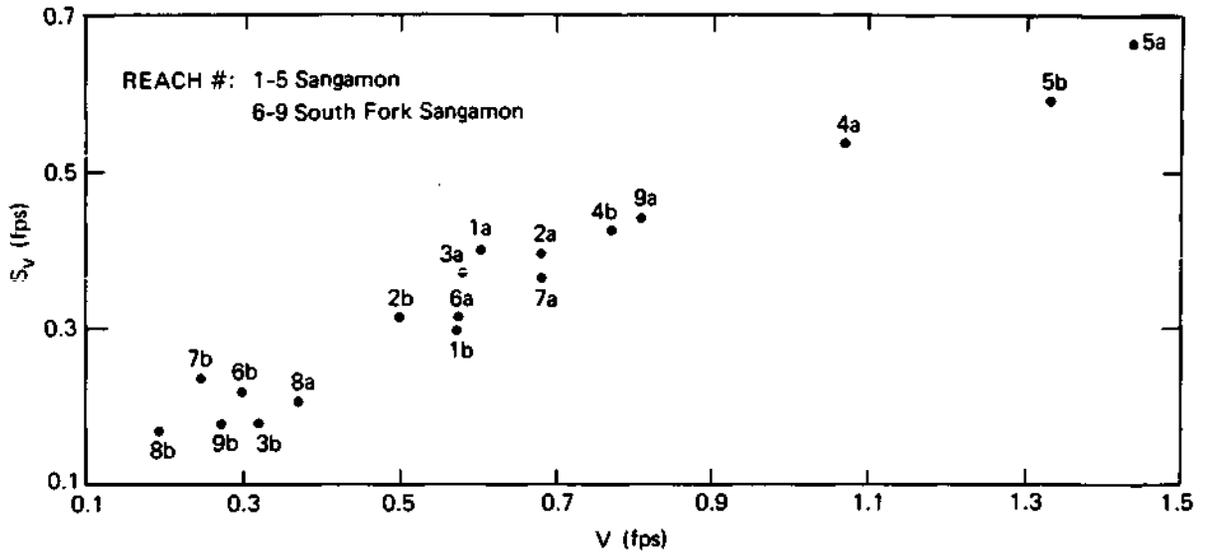


Figure 32. Standard deviation of velocity, S_v , versus reach average velocity, V

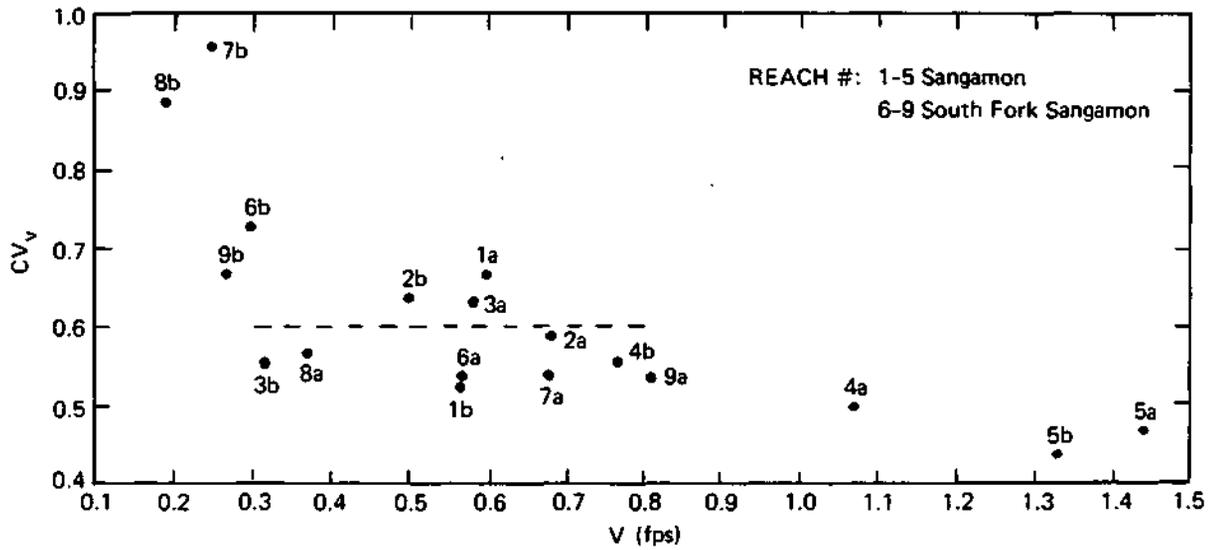


Figure 33. Coefficient of variation of velocity, CV_v , versus reach average velocity, V

of the standard deviation of velocity appears to be predominantly related to the magnitude of velocity and to be independent of drainage area. There is some scatter in the plot of S_v versus V and there does not appear to be any ordering or segregation of data by drainage area (as indicated by the reach numbers).

The coefficient of variation for the velocities, $CV_v = S_v/V$, was plotted with respect to V , as shown in Figure 33. There is an apparent trend of decreasing CV_v with increasing V ; i.e., the standard deviation becomes a larger percent of the average velocity as the average velocity decreases. The trend flattens for V between about 0.3 fps and 0.8 fps, and the approximate average value of CV_v is about 0.6 in this range. In a single reach CV_v will increase with flow duration as velocity decreases. This generality can be observed in the hydraulic geometry station plots where there is greater scatter in the data at low discharges than at high discharges. The exact nature of the relationship cannot be determined from limited flow measurements.

Joint Distribution of Depth and Velocity

The joint distribution of depths and velocities was investigated by grouping velocities according to the cumulative probability of the simultaneously measured depth. Ten divisions of cumulative probability of depth between 0 and 1.0 were delineated, each corresponding to a probability interval of 0.1. The velocities measured concurrently with a depth having a non-exceedance probability between 0 and 0.1 form a group, velocities associated with depths having a non-exceedance probability between 0.1 and 0.2 form a group, and so on. For each flow measured in a reach there are between 7 and 9 velocity and depth measurements within each incremental range of depth cumulative probability. Point velocities were normalized by dividing by the reach average velocity, V . Plots of normalized velocity versus coincident depth non-exceedance probability were developed for each discharge. The variation of normalized measured velocities within each depth probability group was then considered.

Velocities in each depth probability interval typically varied between 0.2 and 2.0 times V for groups with small to greater than average depths (cumulative probability under 0.8), and between 0.2 and 1.8 times V for groups with greater depths (cumulative probability above 0.8). Eighty-

six percent of all measured velocities were between 0.2 and 2.0 times V. The ratio computed for the minimum velocity in each probability group was on the order of 0.2 times V with little variation between groups or from discharge to discharge. There were some extreme velocities such as 4 to 6 times V; however, they were only isolated values.

The average velocities associated with lesser depths, those depths having non-exceedance probability less than about 0.2, were, on the average, less than the reach average velocity. The combination of relatively low velocity and depth reflects conditions which are sometimes encountered near stream banks where depth is less and velocity is reduced by side friction. The velocities measured with these lesser depths lower the overall average velocity for this depth probability group. The majority of depths in this probability range were measured at the first position from the bank in the transect, i.e., closest to the bank. However, not all measurements made at the ends of a transect fall within this depth probability range.

Velocities measured with depths having non-exceedance probabilities between about 0.4 and 0.7 on the average are greater than the reach average velocity. This seems to correspond to riffle-like flow conditions. Velocities with depths having higher non-exceedance probabilities averaged near the reach average velocity.

These trends can be seen in a tabulation of the joint frequency distribution of depth probability and normalized velocity developed from the combined data shown in Table 10. The columns show the depth probability range, and the rows show the normalized velocity range. The numbers in the table show the percentage of all measurements (depth and velocity pairs) within the depth probability and normalized velocity ranges indicated. The underlined numbers denote the maximum frequency of occurrence for the column (depth probability range). The column of numbers to the right of the table are the row totals or percentage of velocities in each row range. It can be seen from Table 10 that normalized velocities between 0.2 and 2.0 times V are fairly widely distributed. The frequency of occurrence (for normalized velocity 2.0) ranges between a minimum of 0.2 percent and a maximum of 2.0 percent with the majority between 0.7 and 1.2 percent.

Table 10. Joint Frequency of Occurrence in Percent with
Depth Probability and Normalized Velocity

| Normalized velocity range | <u>Depth cumulative non-exceedance probability range</u> | | | | | | | | | | Row Total |
|---------------------------------|--|---------------------------|---------------------------|---------------------------|---------------------------|---------------------------|---------------------------|---------------------------|---------------------------|--------------------------|--------------|
| | 0.0 to <u>0.10</u> | 0.11 to <u>0.20</u> | 0.21 to <u>0.30</u> | 0.31 to <u>0.40</u> | 0.41 to <u>0.50</u> | 0.51 to <u>0.60</u> | 0.61 to <u>0.70</u> | 0.71 to <u>0.80</u> | 0.81 to <u>0.90</u> | 0.91 to <u>1.0</u> | |
| 0 to 0.20 | 1.3 | 0.7 | 0.8 | 0.8 | 0.4 | 0.5 | 1.1 | 0.2 | 0.5 | 0.3 | 6.6 |
| 0.21 to 0.40 | <u>2.0</u> | 1.4 | 1.2 | 1.1 | 0.7 | 0.9 | 0.7 | 0.9 | 1.1 | 1.0 | 11.0 |
| 0.41 to 0.60 | 1.4 | <u>1.7</u> | 1.1 | 1.0 | 1.1 | 0.8 | 0.7 | 0.6 | 0.7 | 0.9 | 10.0 |
| 0.61 to 0.80 | 0.8 | 1.1 | <u>1.4</u> | 1.0 | 1.1 | 0.7 | 1.1 | 0.8 | 1.1 | <u>1.4</u> | 10.5 |
| 0.81 to 1.00 | 0.8 | 1.4 | 1.2 | <u>1.4</u> | 1.4 | 0.9 | 0.6 | 1.4 | 1.3 | 1.0 | 11.4 |
| 1.01 to 1.20 | 0.7 | 0.7 | 0.8 | 1.0 | <u>1.6</u> | 1.1 | <u>1.5</u> | <u>2.0</u> | <u>1.4</u> | 1.3 | 12.1 |
| 1.21 to 1.40 | 1.2 | 1.1 | 1.3 | 0.8 | 0.9 | 1.4 | 1.4 | 1.4 | 1.2 | 1.0 | 11.7 |
| 1.41 to 1.60 | 0.7 | 0.6 | 1.0 | 0.7 | 0.7 | <u>1.6</u> | 1.1 | 1.1 | 1.1 | 0.9 | 9.5 |
| 1.61 to 1.80 | 0.2 | 0.7 | 0.4 | 0.5 | 0.8 | 0.6 | 0.6 | 0.9 | 1.1 | 0.4 | 6.2 |
| 1.81 to 2.00 | 0.6 | 0.2 | 0.2 | 0.4 | 0.7 | 0.5 | 0.5 | 0.3 | 0.3 | 0.3 | 4.0 |
| >2.0 | 1.1 | 0.7 | 1.0 | 1.0 | 1.0 | 0.8 | 0.5 | 0.6 | 0.2 | 0.1 | 7.0 |

Though the composite joint distribution of depths and velocities suggests these general observations, local non-uniformities in flow conditions may result in a fairly wide range of velocities which may occur over any limited range of depth values in any given reach. The relationship between the standard deviation of local velocity and average velocity indicates that the velocity distribution will also vary with the bulk flow velocity.

A velocity distribution was constructed from the general observations drawn from the composite joint frequency distribution, an examination of individual plots of velocity versus coincident depth probability for each discharge, and the relationship between reach average velocity and its standard deviation. The velocities in the proposed distribution range between a minimum of 0.2 times V to a maximum of 2.0 times V . The velocity distribution is shown in Figure 34. The solid line drawn in the figure represents the approximate average velocity for each probability level. Ten velocities are plotted for each probability level, and the points are distributed so that their average equals the average shown by the solid line for that probability range. The average of all the velocities is 1.

In a population sample, if the variates are defined by forming ratios to the mean, the coefficient of variation equals the standard deviation because the mean is then unity. Thus, the standard deviation of the normalized velocities defining the distribution in Figure 34 is equivalent to the coefficient of velocity variation for the reach. The distribution of normalized velocities illustrated has a standard deviation of 0.6, compatible with the average coefficient of variation for velocities between 0.3 and 0.8 ft/sec (see Figure 33).

The distribution may be used for velocities in the range of 0.3 to 0.8 with relatively small error; the error becomes greater as V deviates significantly from this range. This can be seen in Figure 33, where the departure of the data values from the straight line (constant coefficient of variation representing the proposed velocity distribution) becomes greater the farther V is from this range. The velocity distribution shown may not predict the full range of velocities throughout a reach if the average velocity is very small. Local velocity values may cluster more about the mean for high average velocity. The joint distribution illustrated is approximate and is a composite of the observed variation of

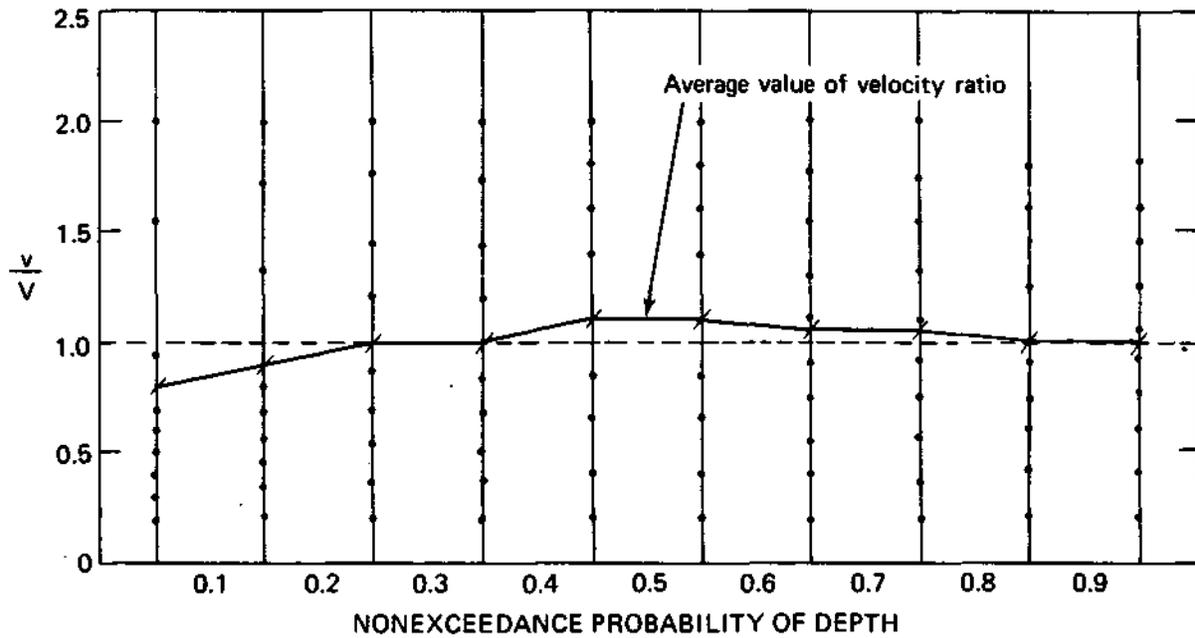


Figure 34. Non-dimensional velocity distribution with $CV = 0.6$

velocities with depths as measured in the field. Other velocity distributions corresponding to different ranges of average velocity can be developed with additional data. The complex interaction of velocity magnitude, channel area, and local variations in channel shape creates a multitude of velocity patterns which may be observed simultaneously with depths having a limited range of values. On the assumption that the field measured velocities represent typical flow conditions for the Sangamon and South Fork Sangamon, the distribution developed will approximate the average distribution of velocities found over a sufficiently long reach in either basin.

The range of 10 expected velocities for any depth probability can be determined from the distribution. The reach average velocity is computed from hydraulic geometry equations. Each of the 10 normalized, equally weighted velocities identified for the depth probability is multiplied by the reach average velocity. Selecting 10 depths having probabilities of 5, 15, 25...95%, ten velocities can be computed for each depth, generating 100 depth and velocity pairs defining the expected variation of depth and velocity in a reach.

COMPARISON OF FIELD DATA AND RESULTS OF HYDRAULIC GEOMETRY EQUATIONS

The average values of width (W), depth (D), and velocity (V) were computed from the field data for each discharge measured in a stream reach. These average values were compared to the W, D, and V calculated from basin hydraulic geometry equations for the respective reach drainage areas and the flow durations of the measured discharges. There are considerable differences between calculated values and those computed from the field data. These differences are not random, but have a systematic pattern. Depths and widths predicted by the basin equations were in nearly all cases lower than the average of measured values for each of the reaches in both basins. Velocities computed from the equations were higher than the reach average velocities computed from the field data. The magnitude of the difference between hydraulic geometry values and field measured values varies with flow duration.

The basin hydraulic geometry values for D and V are typically closer to the transect average depth and velocity measured at or near the riffles in the study reaches. The hydraulic geometry equations better estimate

riffle conditions than reach average conditions. The implication is that the USGS flow measurement data used to develop the station equations and ultimately the basin equations were obtained near riffles and relatively shallow portions of the pools, whereas the average depths and velocities computed from the field data represent a sampling from a range of flow conditions throughout riffles and pools.

The object of the flow measurements made by USGS personnel is to accurately determine the discharge. Wading measurements are made at sections where depths do not exceed 3 ft, flows are least turbulent, and velocities are sufficiently high to produce an adequate number of current-meter revolutions in a reasonable time. Although not an established practice, it would be expected that in the interest of expediency narrow flow sections would be preferred for routine measurements. In general, these criteria systematically exclude the deeper portion of pools with low velocities. The data used to develop hydraulic geometry relations have a strong potential for bias. The predicted flow parameter values need to be adjusted to reflect average conditions as indicated by field measurements.

The ratios of field data values for W , D , and V to the values calculated from basin hydraulic geometry equations were computed for each of the two discharges measured in each of the nine reaches. Plots of these ratios versus flow duration (F) are shown in Figures 35,a,b,and c. Departure of these ratios from 1.0 increases with increasing flow duration (decreasing discharge). The reach number is noted next to each plotted point. For each reach (except reach 5) the difference between calculated parameter values and field values is greater at the higher flow duration (lower flow) than at the lower flow duration (higher flow). Overall, for high discharges (flow durations less than about 40%) calculated values are a good approximation of reach average values; as discharge decreases (higher flow durations) the calculated depths become progressively smaller than the field values, and calculated velocities become progressively greater than the field values.

During low flows, bed forms dominate flow dynamics. As a result, velocities and depths in pools and riffles vary greatly. As discharge increases, these local variations in channel geometry become less significant and are effectively "drowned out" at high discharges. There is less variation in flow conditions throughout a stream reach at high discharges

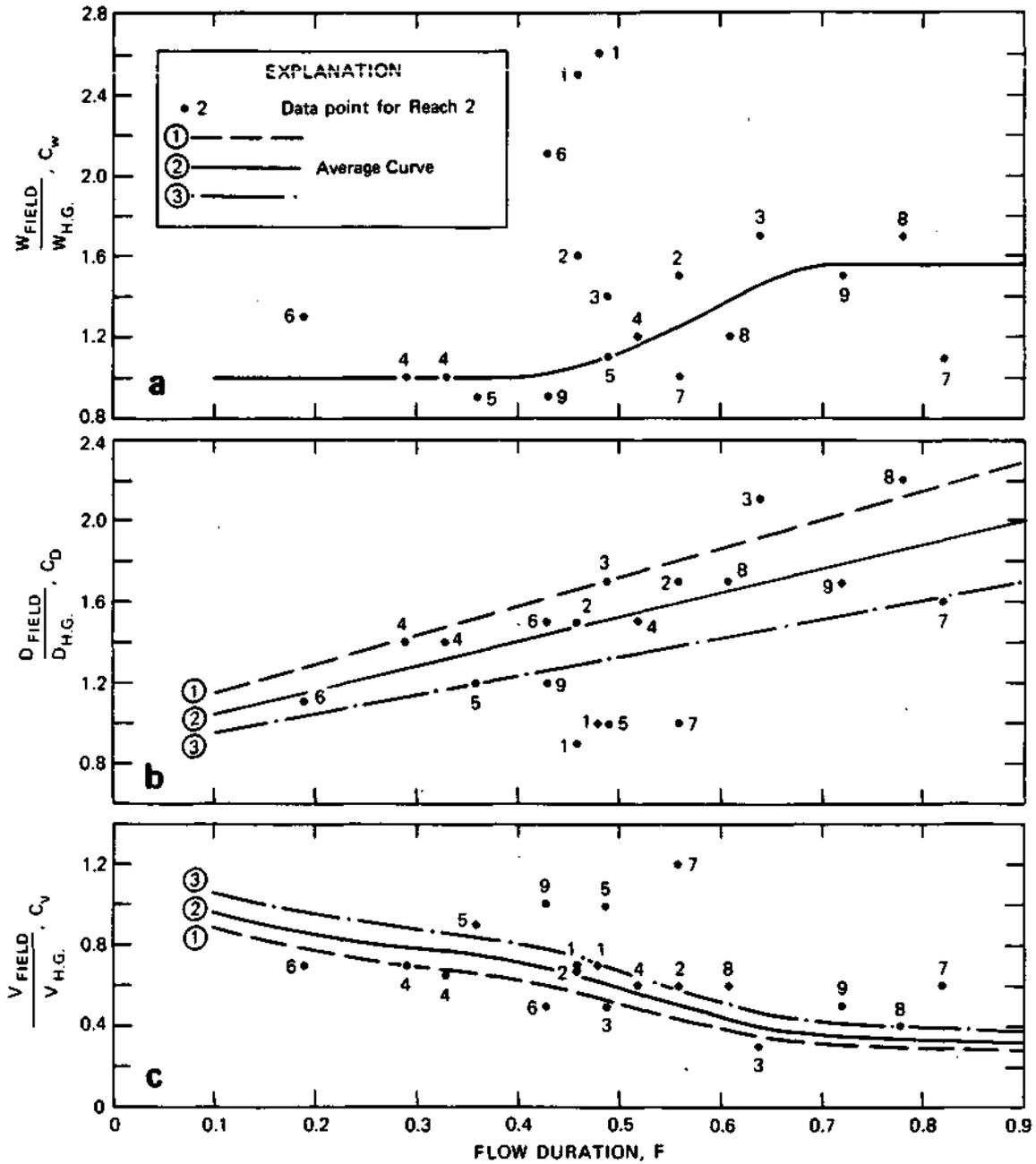


Figure 35. Hydraulic geometry correction factors for W, D, and V versus flow duration

than at low discharges. The trend of increasing disparity between calculated and measured values with decreasing discharge and the evidence of hydraulic geometry equations (developed from USGS data) reflecting near-riffle conditions are consistent with the above observations. At high discharges there is little significant variation in flow conditions throughout a reach, and parameter values typical of riffles are a sufficiently good approximation of average conditions. At low discharges pool conditions vary greatly from riffle conditions, and consequently reach average values vary considerably from the average flow parameter values at riffles.

There is no clear relationship between the computed values of the ratios and drainage area. For the plots shown in Figure 35, there is no apparent ordering in the magnitude of the ratio with respect to drainage area. The two width ratios computed for reach 1 and one ratio computed for reach 6 deviate from the trend indicated by the other data points; this is probably attributable to the channel dredging activity in those reaches. The configuration of the two riffle-pool sequences measured at reach 6 were different. The distance between the upstream riffle and the middle riffle is 85 ft, whereas the next riffle does not appear until another 465 ft downstream. This particular pool-riffle sequence may be in a period of transition.

Channel geometry and flow characteristics may vary significantly along a stream reach. The data scatter seen in the station hydraulic geometry plots (Figures 5 through 23) shows how transect average flow parameter values may differ in a stream at any given discharge. With the basin hydraulic geometry equation results used as a datum, the scatter seen in the plots of Figure 35 shows the possible variations in reach average parameter values which may occur throughout a basin.

Through a determination of correction factors, parameter values calculated from the hydraulic geometry equations may be adjusted to better reflect reach average values measured in the field for all flow durations. The solid lines plotted in Figures 35a, b, and c represent the "best fit" average ratio. The dashed lines in Figures 35b and c, above and below the solid lines, represent the approximate range of ratio values for depth and velocity. These relations may be used to define correction factors as

functions of flow duration. The correction factor (C_{var}) for each parameter may be expressed as:

$$C_{Var} = \frac{Var_{field}}{Var_{hy. geo.}} \quad (18)$$

where Var = W, D, or V.

The parameter value calculated from hydraulic geometry is multiplied by the correction factor, C_{var} , to obtain the adjusted reach average parameter value for a given flow duration. By using each of the three values of the correction coefficient for depth and velocity (the average, upper, and lower bounds), the range of possible average values can be determined.

The correction factors for velocity and depth are paired in Figure 35; the upper dashed line labeled 1 for the depth correction factor corresponds to the lower dashed line for the velocity correction factor, also labeled 1, and so forth. The product of $C_w \cdot C_d \cdot C_v = 1$ at all points satisfying continuity. A single value of C_w is defined as there is somewhat less scatter in the data. The relationship for width differs from the trends seen in the velocity and depth plots. The greater data scatter in the plot of width ratios seems to occur near the mid-flow range, indicating that other undetermined factors influence width.

There are insufficient data to conclusively define the relationship between the correction factors and flow duration. Flow measurements over a broader range of discharges in a number of reaches are needed to determine the exact form of the relationship. The relationships shown in Figure 35a, b, and c are the best approximations that can be derived from the available data.

DEVELOPMENT OF THE FLOW MODEL FOR BASINWIDE ASSESSMENT OF WEIGHTED USABLE AREA

The basin flow model simulates the needed hydraulic information to evaluate the WUA (Weighted Usable Area) for streams throughout a basin. The model predicts the local depths and coincident velocities throughout a stream reach as well as the proportion of the reach characterized by each depth and velocity pair for any desired discharge. The basin flow model

combines hydraulic geometry equations, correction factors, and the relations derived from field data defining depth and velocity distributions in a riffle-pool sequence. Specifically the adjusted average depth, the relation between S_d and A_d , and the normal probability distribution function are used to evaluate a range of depths for a given drainage area and flow duration. Coincident velocities are calculated by multiplying the non-dimensional velocities defined in the joint distribution (Figure 34) by the adjusted average velocity for the given drainage area and flow duration. The flow surface area of a reach is the product of the adjusted average width and the selected stream length. Typically a stream length of 1000 ft is used and WUA per 1000 ft of stream length is calculated.

Using the IFG flow models for calculating the WUA, a stream reach is conceptually segmented into cells having a measured surface area, and each cell is hydraulically represented by measured or interpolated depth and velocity. The probabilistic approach to flow modeling developed in this study does not provide depth and velocity information for a specific cell in a known reach. Rather, pursuing the statistical approach, depth and velocity are estimated for a given frequency of occurrence in the riffle-pool sequence.

The depth distribution defines the cumulative non-exceedance probability of a given depth. The velocity distribution provides information on the various velocities expected to occur for each depth representing an interval of the cumulative depth probability function. Depths calculated at successive cumulative probabilities have a frequency of occurrence equal to the difference between the current and the previous cumulative probability. Evaluating depth and velocity at uniformly incremented cumulative probability levels yields an equal frequency of occurrence for each depth-velocity pair.

The data collection and analysis conducted in this study were structured such that the probability of occurrence for the depth-velocity pair is related to a percentage of a riffle-pool sequence surface area. For illustrative purposes, consider 10 depths evaluated at the 5%, 15%, 25%, and so on up to the 95% cumulative probability level for a given drainage area and flow duration. Each calculated depth has an equal frequency of occurrence from riffle center to riffle center (i.e., one riffle-pool sequence). Ten percent of the stream (as measured by flow surface area)

will be represented by the 5% cumulative probability depth, d_{05} ; 10% by the 15% cumulative probability level depth, d_{15} ; and so on. Ten velocities having an equal frequency of occurrence, may be calculated for each depth from the applicable velocity distribution. Each depth-velocity pair, therefore, represents 1/100 of the stream flow surface area. The reach may be any length provided the drainage area remains approximately the same and the reach extends through at least one riffle-pool sequence, beginning and ending at the same location relative to the riffle-pool sequence (e.g., riffle to riffle).

Once the flow model relations have been calibrated for a given basin, depths and velocities may be simulated for any flow duration (discharge) given the drainage area of the stream. The flow model is readily interfaced with the IFG habitat suitability preference functions for depth and velocity, $S(d)$ and $S(v)$, for any fish species and life stage, to evaluate WUA, thus forming a basinwide habitat model. The flow model and WUA calculations proceed in a stepwise fashion as illustrated by the following example.

Example Calculation

The system input for this example is as follows:

Basin: Sangamon

Stream drainage area: 250 mi²

Flow duration: 50%

Target fish species and life stage: Bluegill, juvenile

I. Basin Flow Model Calculations

A. Calculate average W , D , and V from basin hydraulic geometry relations.

$$\log W = 0.55 - 0.77 (0.50) + 0.58 (\log 250); W = 35.96 \text{ ft}$$

$$\log D = -0.32 - 1.17 (0.50) + 0.41 (\log 250); D = 1.20 \text{ ft}$$

$$\log V = -0.005 - 0.53 (0.50) + 0.13 (\log 250); V = 1.10 \text{ ft/sec}$$

B. Adjust results of hydraulic geometry equations.

For this example use correction factor values for 50% flow duration from Figure 35.

| | <u>1</u> | <u>2</u> | <u>3</u> |
|-------|----------|----------|----------|
| C_w | 1.13 | 1.13 | 1.13 |
| C_d | 1.72 | 1.52 | 1.32 |
| C_v | .51 | 0.58 | 0.67 |

The adjusted values W' , D' , and V are calculated by multiplying W , D , and V by appropriate correction factors. Only the detailed calculations for condition 2 (or the average) are given below.

$$W' = C_w \cdot W = 40.6$$

$$D' = C_d \cdot D = 1.82$$

$$V' = C_v \cdot V = 0.64$$

C. Determine the distribution of depths in the reach by computing 10 depths with equal frequency of occurrence.

1. Obtain the estimate of standard deviation of depth for a 250-sq-mi drainage area reach from Figure 30a; $S_d = 0.64$.
2. Compute the normalized variable Z , representing 10 equal intervals of cumulative probability between 0 and 1.0. The 10 cumulative probabilities and values of Z_i (i corresponds to percent probability of 05 to 95) are listed in Table 11.
3. Substituting the adjusted reach average depth D' and the standard deviation of depth, solve for depth at each selected cumulative probability as:

$$d_i = (Z_i)(S_d) + D', \quad i = 5, 15, 25 \dots 95$$

The difference between successive probabilities is 10%; thus each computed depth has a 10% frequency of occurrence, e.g., represents 10% of the riffle-pool sequence area.

The computed depths are:

$$d_{05} = 0.77 \quad d_{15} = 1.16 \quad d_{25} = 1.39 \quad d_{35} = 1.57 \quad d_{45} = 1.74$$

$$d_{55} = 1.90 \quad d_{65} = 2.07 \quad d_{75} = 2.25 \quad d_{85} = 2.48 \quad d_{95} = 2.87$$

D. Compute 10 velocities associated with each depth. The reach average velocity is in the range of 0.3 to 0.8, thus figure 34 provides the ratios of local velocity to reach average velocity

$$\left(\frac{v}{V}\right)_{i,j} \quad \text{for each depth } (i = 5, 15, \dots, 95, \text{ corresponding to the}$$

percent cumulative probability of the depth, $j = 1, 10$). Computed velocities $v_{i,j}$ are similarly double-subscripted. The first subscript i identifies the depth cumulative probability; the

Table 11. Selected Values of the Inverse Normal (0,1) Probability
 Distribution Function from the International
 Math and Science Library Routine MDNRIS

| <u>Cumulative probability</u> <u>$P_i(x)$</u> | <u>$Z_i = (d-D')/S_d$</u> |
|---|--------------------------------------|
| 0.05 | -1.645 |
| 0.15 | -1.036 |
| 0.25 | -0.674 |
| 0.35 | -0.385 |
| 0.45 | -0.126 |
| 0.55 | 0.126 |
| 0.65 | 0.385 |
| 0.75 | 0.674 |
| 0.85 | 1.036 |
| 0.95 | 1.645 |

second, j ranges from 1 to 10 for each of 10 velocity ratios obtained from the distribution. The velocities are computed as:

$$v_{i,j} = \left(\frac{v}{V}\right)_{i,j} \times v'$$

The following tabular joint frequency distribution of depths and velocities is developed. Each depth velocity pair $(d_i, v_{i,j})$ represents 1/100 of the surface area of the stream reach.

Values of $v_{i,j}$, fps, for j equal to:

| i | d_i (ft) | Values of $v_{i,j}$, fps, for j equal to: | | | | | | | | | |
|----|---------------|--|------|------|------|------|------|------|------|------|------|
| | | 1 | 2 | 3 | 4 | 5 | 6 | 7 | 8 | 9 | 10 |
| 05 | 0.77 | 0.13 | 0.19 | 0.26 | 0.32 | 0.38 | 0.45 | 0.51 | 0.61 | 0.99 | 1.28 |
| 15 | 1.16 | 0.13 | 0.21 | 0.29 | 0.36 | 0.43 | 0.51 | 0.59 | 0.85 | 1.10 | 1.28 |
| 25 | 1.39 | 0.13 | 0.23 | 0.33 | 0.43 | 0.54 | 0.64 | 0.77 | 0.92 | 1.12 | 1.28 |
| 35 | 1.57 | 0.13 | 0.23 | 0.33 | 0.43 | 0.54 | 0.64 | 0.77 | 0.92 | 1.12 | 1.28 |
| 45 | 1.74 | 0.13 | 0.26 | 0.41 | 0.54 | 0.64 | 0.70 | 0.89 | 1.02 | 1.15 | 1.28 |
| 55 | 1.90 | 0.13 | 0.26 | 0.41 | 0.54 | 0.64 | 0.70 | 0.89 | 1.02 | 1.15 | 1.28 |
| 65 | 2.07 | 0.13 | 0.24 | 0.35 | 0.47 | 0.59 | 0.70 | 0.84 | 0.98 | 1.12 | 1.28 |
| 75 | 2.25 | 0.13 | 0.24 | 0.35 | 0.47 | 0.59 | 0.70 | 0.84 | 0.98 | 1.12 | 1.28 |
| 85 | 2.48 | 0.13 | 0.26 | 0.38 | 0.48 | 0.57 | 0.67 | 0.80 | 0.92 | 1.02 | 1.15 |
| 95 | 2.87 | 0.13 | 0.26 | 0.38 | 0.48 | 0.57 | 0.67 | 0.80 | 0.92 | 1.02 | 1.15 |

E. The total flow surface area of the reach (A_R) is the product of the reach length and the average flow width, W' , per 1000 ft of stream length, $A_R = 40.6 \times 1000 = 40,600$ sq ft flow surface area. Each cell represented by $(d_i, v_{i,j})$ has a flow surface area, $a_{i,j} = 1/100 \cdot A_R$. It follows that:

$$A_R = \sum_{i=1}^{10} \sum_{j=1}^{10} a_{i,j}$$

II. WUA Calculations

The WUA is computed from a modified form of equation 1.

$$WUA = \sum_{i=1}^{10} \sum_{j=1}^{10} S(d_i) \cdot S(v_{i,j}) \cdot a_{i,j} \quad (18)$$

where $S(d)$ and $S(v)$ are the fish preference indexes defined earlier.

Taking $a_{i,j}$ - out of the summation, the resulting equation is

$$WUA = \frac{A_R}{100} \sum_{i=1}^{10} \sum_{j=1}^{10} S(d_i) \cdot S(v_{i,j}) \quad (19)$$

A tabular index of fish preference functions is used to determine the values of $S(d)$ and $S(v)$ for the desired fish species and life stage (Singh and Ramamurthy, 1981). The value of $S(d)$ and $S(v)$ for each depth and velocity in the joint distribution is thus determined. The 100 products of the depth and velocity preference indexes are summed, and for the juvenile bluegill:

$$\sum_{i=1}^{10} \sum_{j=1}^{10} S(d_i) \cdot S(v_{i,j}) = 8.16$$

Substituting this sum and the value of A_n into equation 19, the WUA for the juvenile bluegill for the example drainage area and flow duration is:

$$WUA = \frac{40,600 \text{ ft}^2}{100} \cdot 8.16 = 3313 \text{ ft}^2$$

This procedure is repeated for conditions 1 and 3. The results are shown below.

| <u>Condition</u> | <u>WUA/1000 ft</u> |
|------------------|--------------------|
| 1 | 4572 |
| 2 | 3313 |
| 3 | <u>2160</u> |
| Average | 3348 |

The average WUA is the most representative for the stream reach.

This procedure can be followed for calculating average WUA at any flow duration. The relationship between discharge and WUA may be determined by computing the discharge for the corresponding flow duration from equation 7 and Table 1.

The hydraulic geometry equations and the velocity and depth distribution relations developed were incorporated in a computer program which performs the calculation illustrated in the preceding example. The computer model simulates depths and velocities using each combination of hydraulic geometry correction factors for any given drainage area and flow duration. Digitized preference functions, $S(d)$ and $S(v)$, for selected fish species

are included in the computer model and are used to calculate the WUAs. Preference functions for bluegill and catfish, juvenile and adult life stages, were used to illustrate the model performance for this study. The basinwide flow and aquatic habitat model thus developed calculates the WUA for a given fish species for any stream in a basin as a function of drainage area and flow duration.

BASIN WUA RELATIONS

Habitat response functions (WUA versus discharge or flow duration) may be readily developed for any stream in a basin by using the proposed computer model. Table 12 shows the average WUAs calculated for bluegill adults in the Sangamon, South Fork Sangamon, and Salt Creek Basins. Plots of WUA versus flow duration for bluegill and catfish, juveniles and adults, at three drainage areas in the Sangamon Basin are shown in Figures 36 and 37. The three curves plotted for each drainage area represent the WUAs calculated by using each of the three hydraulic geometry correction factor pairs for depth and velocity at each flow duration. Most of the variation in WUA may be within the range typified by the upper and lower curves.

WUA versus discharge relations can be readily developed by using the flow duration functions from Table 1 to calculate discharge corresponding to the drainage area and flow duration. Gaging station daily flow data may be converted to equivalent flow duration by interpolation, using the flow duration equations. Daily WUAs may then be calculated for a station. Flow duration for a flow corresponding to a duration derived from the flows for a particular month can easily be obtained and WUAs calculated using the model.

Comparison of Computational Techniques for WUA

The IFG methodology provides a means of investigating the micro-habitat structure of a stream, i.e., the suitability of the habitat of incremented portions of the stream or cells. The habitat suitability of each stream cell is a function of the depth and velocity (substrate, etc.) for the given discharge. The method used to determine the combined suitability of flow conditions in the cell greatly affects the WUA calculated for a reach.

Table 12. Average WUA/1000 ft Stream Length
 Fish Species: Bluegill Life Stage: Adult

| Drainage area (sq mi) | % Flow duration | | | | | | | | | | | | | | | | | |
|----------------------------------|-----------------|-------|-------|-------|-------|-------|-------|-------|-------|---|---|---|---|---|---|---|---|---|
| | 1 | 0 | 2 | 0 | 3 | 0 | 4 | 0 | 5 | 0 | 6 | 0 | 7 | 0 | 8 | 0 | 9 | 0 |
| Sangamon Basin | | | | | | | | | | | | | | | | | | |
| 25 | 227 | 141 | 77 | 38 | 21 | 11 | 5 | 1 | 0 | | | | | | | | | |
| 50 | 845 | 570 | 347 | 204 | 137 | 93 | 54 | 23 | 9 | | | | | | | | | |
| 100 | 2943 | 2107 | 1320 | 811 | 604 | 472 | 317 | 163 | 81 | | | | | | | | | |
| 200 | 6844 | 6115 | 4509 | 3004 | 2336 | 1888 | 1365 | 768 | 421 | | | | | | | | | |
| 300 | 8947 | 9272 | 7796 | 5764 | 4897 | 4162 | 3075 | 1746 | 942 | | | | | | | | | |
| 400 | 9801 | 11427 | 10562 | 8440 | 7720 | 6989 | 5415 | 3114 | 1742 | | | | | | | | | |
| 600 | 9449 | 13426 | 14468 | 12989 | 13118 | 13063 | 11101 | 6816 | 3946 | | | | | | | | | |
| 800 | 8042 | 13550 | 16586 | 16367 | 17816 | 18977 | 17052 | 11138 | 6807 | | | | | | | | | |
| 1000 | 6433 | 12700 | 17587 | 18716 | 21678 | 24447 | 22903 | 15506 | 9928 | | | | | | | | | |
| 1200 | 4998 | 11484 | 17652 | 20361 | 24836 | 29264 | 28557 | 19915 | 13064 | | | | | | | | | |
| South Fork Sangamon Basin | | | | | | | | | | | | | | | | | | |
| 25 | 622 | 374 | 197 | 95 | 50 | 25 | 10 | 3 | 0 | | | | | | | | | |
| 50 | 2615 | 1610 | 914 | 494 | 307 | 186 | 94 | 38 | 15 | | | | | | | | | |
| 100 | 8493 | 6220 | 3836 | 2139 | 1390 | 922 | 530 | 246 | 111 | | | | | | | | | |
| 200 | 15402 | 15036 | 11950 | 8043 | 5789 | 4005 | 2348 | 1137 | 551 | | | | | | | | | |
| 300 | 16552 | 19670 | 18486 | 14352 | 11664 | 8916 | 5502 | 2686 | 1295 | | | | | | | | | |
| 400 | 14855 | 21075 | 22759 | 19722 | 17590 | 14539 | 9642 | 4882 | 2363 | | | | | | | | | |
| 600 | 9214 | 18708 | 25983 | 27027 | 27795 | 25877 | 18986 | 10455 | 5388 | | | | | | | | | |
| 800 | 4777 | 14185 | 24962 | 30526 | 35172 | 36053 | 28540 | 16565 | 9074 | | | | | | | | | |
| 1000 | 2270 | 9959 | 22104 | 31261 | 40220 | 44415 | 37646 | 22798 | 12885 | | | | | | | | | |
| 1200 | 997 | 6706 | 18671 | 30475 | 43156 | 51048 | 45777 | 28919 | 16870 | | | | | | | | | |
| Salt Creek Basin | | | | | | | | | | | | | | | | | | |
| 25 | 207 | 174 | 131 | 92 | 73 | 55 | 33 | 16 | 7 | | | | | | | | | |
| 50 | 573 | 511 | 413 | 322 | 286 | 255 | 186 | 105 | 55 | | | | | | | | | |
| 100 | 1527 | 1403 | 1166 | 944 | 903 | 887 | 742 | 433 | 1061 | | | | | | | | | |
| 200 | 3562 | 3578 | 3159 | 2657 | 2672 | 2757 | 2458 | 1660 | 1061 | | | | | | | | | |
| 300 | 5068 | 5523 | 5188 | 4584 | 4853 | 5244 | 4859 | 3349 | 2203 | | | | | | | | | |
| 400 | 6145 | 7096 | 6982 | 6419 | 7096 | 8008 | 7751 | 5498 | 3657 | | | | | | | | | |
| 600 | 6145 | 9328 | 9868 | 9592 | 11189 | 13521 | 14060 | 10592 | 7420 | | | | | | | | | |
| 800 | 8177 | 10697 | 11992 | 12144 | 14699 | 18552 | 20067 | 15822 | 11612 | | | | | | | | | |
| 1000 | 8495 | 11553 | 13537 | 14215 | 17731 | 23148 | 25856 | 20894 | 15889 | | | | | | | | | |
| 1200 | 8589 | 12044 | 14699 | 15868 | 20301 | 27201 | 31126 | 25793 | 19977 | | | | | | | | | |

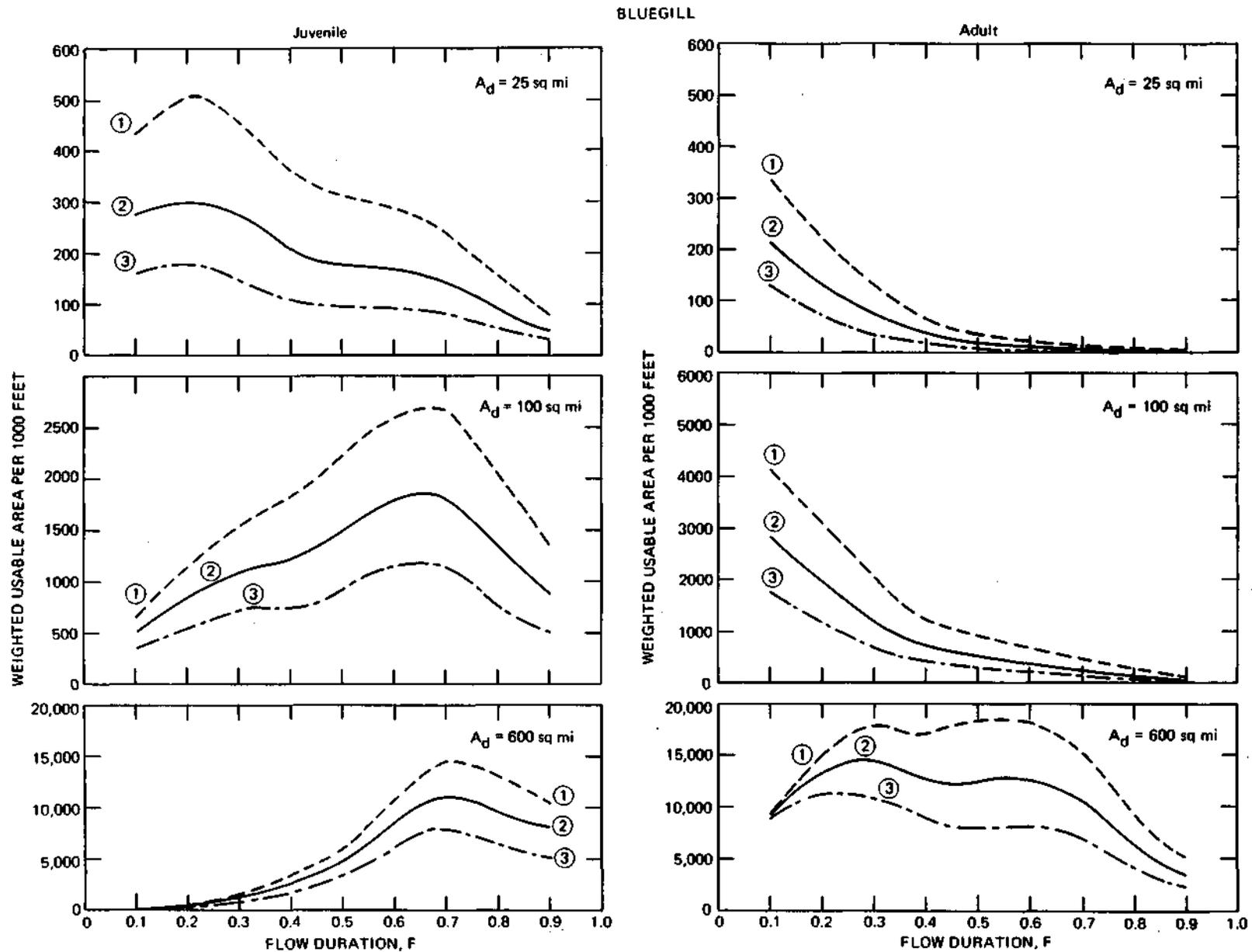


Figure 36. WUA versus flow duration for Bluegill in the Sangamon Basin

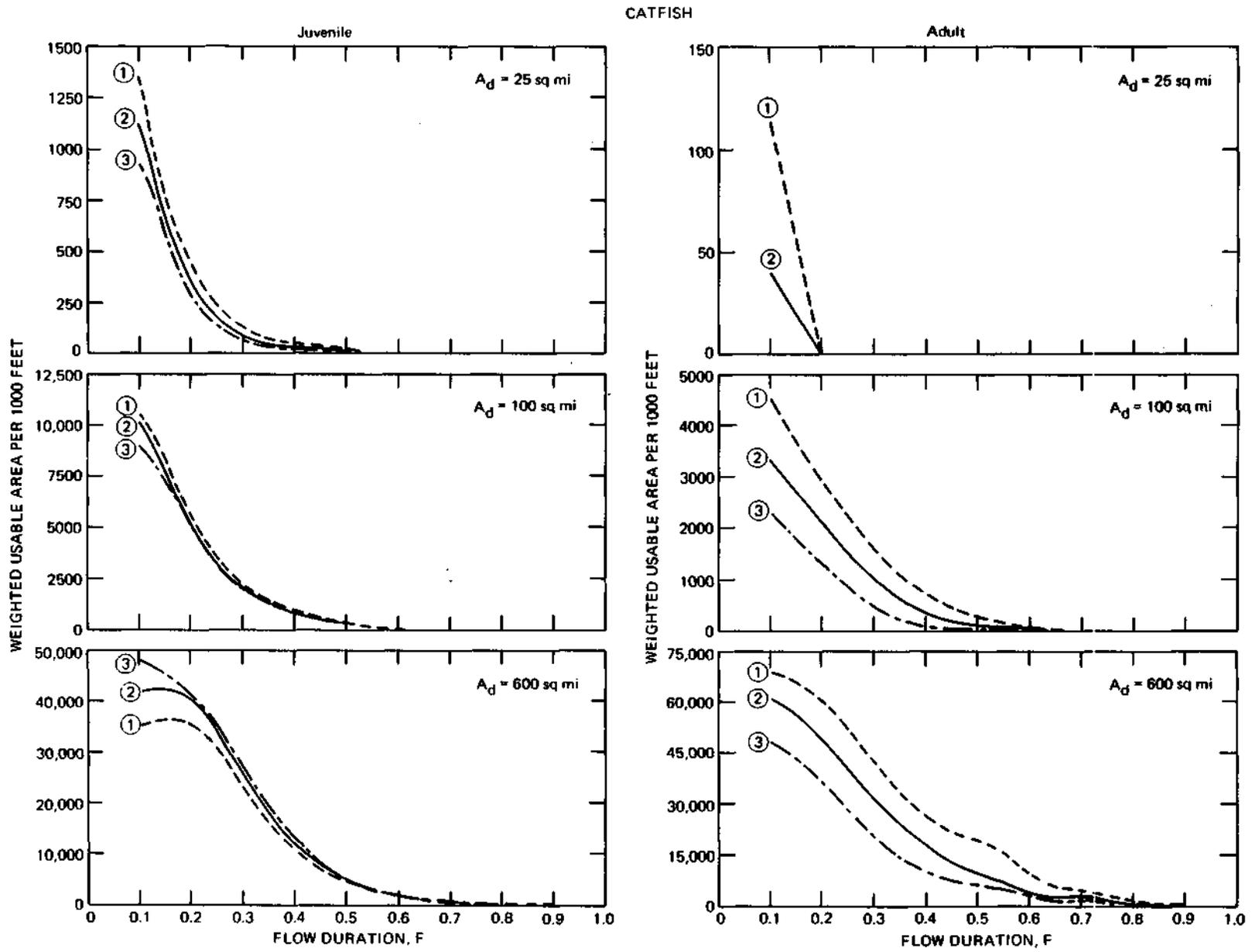


Figure 37. WUA versus flow duration for Catfish in the Sangamon Basin

Preference curves developed by the IFG, for various fish species and life stages, functionally define the relationship between cell flow parameters and the probability of their use. A low preference or low probability of use for a parameter value means that the fish type is less likely to frequent areas of a stream with that condition, or that a cell with such a condition may be inhabited (by the particular fish species) only after more suitable areas are fully used (Bovee, 1982).

One method of evaluating the combined effects of velocity and depth is the use of joint frequency preference functions. This approach is being explored (Bovee, 1982; Voos, 1981). Originally, the IFG developed independent functions for depth and velocity. These are available for a greater variety of fish species and are typically used. Several different approaches may be used to evaluate the combined preference function (probability of use) from the independent functions.

The joint preference or combined probability of use of a cell may be calculated as the product of the depth and velocity preference values, the geometric mean of the preference values, or the minimum preference value (equations 1, 2, and 3, respectively). Each of these three methods yields significantly different values. Taking the product of the preferences produces very low estimates of use, the geometric mean has a higher value, and using the minimum yields a preference value between the two. For example, if the depth and velocity have preference values of 0.3 and 0.5 respectively, the product is 0.15, the geometric mean is 0.38, and the minimum is 0.30. The flow surface area of a cell is multiplied by the joint preference value, reducing the total surface area to an equivalent area of preferred habitat. Thus, the value of the joint preference equals the percent of each cell area summed to compute the WUA of a stream. The magnitude of the difference in the various mathematical combinations can be seen in Table 13, which shows the three possible values of the combined preferences for bluegill adults for different drainage areas in the Sangamon Basin.

Table 13. Joint Preference Values from Alternative Computational Techniques, Sangamon Basin

% of Total Area = Area of Preferred Habitat for Bluegill Adults

| A_d (sq mi) | F (%) | $\sum_{i=1}^{10} \sum_{j=1}^{10} S(d_i) \cdot S(v_{i,j})$ | | $\sum_{i=1}^{10} \sum_{j=1}^{10} \sqrt{S(d_i) \cdot S(v_{i,j})}$ | | $\sum_{i=1}^{10} \sum_{j=1}^{10} \min[S(d_i), S(v_{i,j})]$ | |
|------------------|----------|---|--|--|--|--|--|
| | | (%) | | (%) | | (%) | |
| 25 | 90 | 0 | | 0 | | 0 | |
| | 70 | 0.04 | | 0.68 | | 0.05 | |
| | 50 | 0.18 | | 2.21 | | 0.32 | |
| | 30 | 0.52 | | 4.79 | | 1.47 | |
| | 10 | 1.13 | | 6.79 | | 3.11 | |
| 100 | 90 | 0.48 | | 3.34 | | 0.50 | |
| | 70 | 1.30 | | 7.08 | | 1.58 | |
| | 50 | 2.36 | | 11.35 | | 4.85 | |
| | 30 | 4.06 | | 14.35 | | 8.04 | |
| | 10 | 6.65 | | 15.41 | | 10.02 | |
| 600 | 90 | 8.24 | | 19.37 | | 9.41 | |
| | 70 | 16.39 | | 31.45 | | 20.31 | |
| | 50 | 18.96 | | 35.37 | | 23.00 | |
| | 30 | 17.14 | | 28.65 | | 18.87 | |
| | 10 | 8.07 | | 15.55 | | 9.57 | |
| 1000 | 90 | 15.64 | | 27.76 | | 17.51 | |
| | 70 | 25.50 | | 41.10 | | 29.70 | |
| | 50 | 23.65 | | 39.74 | | 26.61 | |
| | 30 | 15.86 | | 26.98 | | 17.62 | |
| | 10 | 4.11 | | 9.95 | | 6.14 | |

SUMMARY

The stream aquatic habitat assessment methodology developed by the IFG is a useful tool for evaluating instream flow needs. The inadequacy of currently available hydraulic models has severely impaired the utility of the IFG methodology for broad-based applications. The methodology for basin flow modeling developed in this study broadens the scope of applications of the IFG methodology. Basinwide evaluation of fishery habitat flow requirements for instream flow needs assessment will greatly assist in the formulation of water allocation policies which protect, or minimize adverse affects on, stream aquatic environments.

The hydraulic geometry relations which form the basis of the flow model are an effective tool for predicting average flow parameter values for unmeasured streams. The data scatter in station plots of W , D , and V versus Q , measured by wading, is largely attributable to the practice of not performing discharge measurements at the same stream transect each time. The variation in transect average values of W , D , and V for the same discharge in the plots increases as discharge decreases. The range of transect average values at the same discharge is an indication of the variability of flow conditions throughout a reach. Reach average values may likewise be quite diverse for different segments or sub-reaches of a stream.

Hydraulic geometry equations developed from the USGS flow measurement data model average riffle conditions more closely than reach average values. Correction factors may be developed to adjust results to reflect reach average values. The correction factors vary with flow duration. A range of correction factor values may be used, particularly for low discharge flow durations, when reach average values may differ significantly between sub-reaches of the stream. The correction factors adjust average parameter values for bias in USGS flow measurement data and account for average flow parameter variability in a reach.

The relationships between flow parameters (W , D , V , and Q) at natural stream cross sections differ from the corresponding relationships for these parameters at stream cross sections modified by bridge piers and abutments. Only data collected at natural stream sections should be used to calibrate

hydraulic geometry equations. Channels which have had extensive modification such as widening, deepening, or bank alterations have hydraulic characteristics which also differ from the natural state. Flow parameter relationships (similar to those developed from natural channels in this study) need to be developed to model flows in modified reaches.

The depth and velocity distribution models developed from the field data provide the necessary information on local variations in depth and velocity to evaluate the suitability of the stream habitat. The relationship between S_d and A_d links the normal distribution of depth observed in the study reaches. Furthermore, the relationship permits extrapolation of field observations to unmeasured reaches. The increase in S_d with increase in A_d is consistent with recognized, systematic patterns of channel formation in the stream network. The influence of flow duration on the relationship requires further investigation. The variation of velocity throughout a reach is principally related to the magnitude of the bulk velocity of the flow. The greater the reach average velocity, the greater the standard deviation of local velocities in a reach. The normalized velocity distribution developed illustrates the broad range of velocities which may occur concurrently over a limited range of flow depth.

The methodology developed is applicable to hydrologically homogeneous basins with reliable relationships between discharge and flow duration. Geologic differences between watersheds can significantly alter the low flow hydrology of a drainage system. Low flows are critical periods for stream ecologies, and accurate prediction of low flow relationships is necessary for reliable evaluation of instream flow needs.

The probabilistic flow model provides the necessary hydraulic information to evaluate stream aquatic habitat using the IFG Weighted Usable Area (WUA) model. In this capacity the probabilistic flow model has two distinct advantages over conventional hydraulic functional models. First, hydraulic geometry relations combined with relationships defining the distribution of depth and velocity in a reach provide a valuable link relating flow conditions throughout a basin. On the other hand, models based on equations such as Manning's must be calibrated by direct field measurements for each reach.

Secondly, for low discharges flow models based on Manning's equation or other uniform flow equations are subject to gross inaccuracies due to

the non-uniformity of the flow in riffles and pools. The calibration of such models for low flows quite often yields physically unrealistic values for the friction factor. The probabilistic flow model is not based on the assumption of uniform flow, but on a general relationship derived directly from field data. The variability of local depths and velocities is directly addressed in the probabilistic model by determination of the standard deviation of those parameters. The basinwide probabilistic flow model, interfaced with the IFG methodology, may be used to evaluate the stream network aquatic habitat for any discharge scenario. This flexibility enhances the utility of applying the IFG methodology to quantify instream flow needs for water allocation planning.

Recommendations for Future Research

The reliability of the relationships developed from field data may be improved by providing a broader data base. Field data collection should be expanded to include measurement of 5 or more discharges in each study reach. Study reaches should include 3 or more riffle-pool sequences. Measurement of flow parameters over a broader range of discharges will provide a better definition of the relationship between hydraulic geometry correction factors and flow duration. The extent of variation in average parameter values along a reach may be better examined by increasing the length or the number of the study reaches. The dependence of local depths and velocity distribution parameter values on flow duration can be investigated by making 5 or more discharge measurements in each reach. Joint distribution of depth and velocity may be developed for different ranges of velocity.

For basins where numerous streams have been modified by channel alterations, relationships similar to those developed for natural channels should be developed for the modified streams. Comparisons of WUA functions for natural streams and modified streams would assist in the evaluation of the impact of completed or proposed channel modifications. The benefit of planned channel restoration projects can be evaluated in terms of improved aquatic habitat.

Substrate and dissolved oxygen content are two important aspects of the aquatic environment. Substrate varies along the length of a stream, typically decreasing in coarseness as drainage area increases. Basin

relations between substrate distribution and drainage area can be developed and incorporated in the basinwide habitat assessment model, improving the stream habitat evaluations. Study of the variations in dissolved oxygen content through riffles and pools and along the stream length will contribute to the understanding of stream reaeration under various flow conditions.

REFERENCES

- Bovee, K.D., and R.T. Milhous, 1978. Hydraulic Simulation in Instream Flow Studies: Theory and Techniques. Cooperative Instream Flow Services Group, Instream Flow Information Paper No. 5, U.S. Fish and Wildlife Service, FWS/OBS-78/33, 130 p.
- Bovee, K.D., 1982. A Guide to Stream Habitat Analysis Using the Instream Flow Incremental Methodology. Cooperative Instream Flow Service Group, Instream Flow Information Paper No. 12, U.S. Fish and Wildlife Service, FWS/OBS-82/26, 248 p.
- Chow, Ven Te (Ed.), 1964. Handbook of Applied Hydrology. McGraw-Hill, New York.
- Chow, Ven Te, 1959. Open Channel Hydraulics. McGraw-Hill, New York.
- Dunne, T., and L.B. Leopold, 1978. Water in Environmental Planning. W.H. Freeman and Co., San Francisco, CA.
- Elser, A.A., 1976. Use and Reliability of Water Surface Profile Program Data on a Montana Prairie Stream. In: J.F. Orsborn and C.H. Allman (Ed.), Instream Flow Needs. Proc. American Fishery Society. Vol. II. pp. 496-504.
- Fehrenbacher, J.B., J.D. Alexander, I.J. Jansen, R.G. Darmody, R.A. Pope, M.A. Flock, E.E. Voss, J.W. Scott, W.F. Andrews, and L.J. Bushue, 1984. Soils of Illinois. University of Illinois Agricultural Experiment Station, Bulletin 778, 85 p.
- Harvey, A.M., 1975. Some Aspects of the Relations Between Channel Characteristics and Riffle Spacing in Meandering Streams. American Journal of Science, Vol. 275, April, pp. 470-478.
- Illinois State Water Plan Task Force, 1984. Illinois State Water Plan. Springfield, Illinois, 75 p.
- Leighton, M.M., G.E. Ekblaw, and L. Horberg, 1948. Physiographic Divisions of Illinois. Illinois State Geological Survey Report of Investigation 129, 19 p.
- Leopold, L.B., and M.G. Wolman, 1957. River Channel Patterns: Braided, Meandering, and Straight. U.S. Geological Survey Professional Paper 282-B, 85 p.
- Leopold, L.B., and T. Maddock, 1953. The Hydraulic Geometry of Stream Channels and Some Physiographic Implications. U.S. Geological Survey Professional Paper 252, 57 p.
- Loar, J.M., and M.J. Sale, 1981. Analysis of Environmental Issues Related to Small-Scale Hydroelectric Development. V. Instream Flow Needs for Fishery Resources. Oak Ridge National Laboratory Publication 1829, 123 p.

- Milhous, R.T., and W.J. Grenney, 1980. The Quantification and Reservation of Instream Flows. Water and Science Technology, Vol. 13, No. 3, pp. 129-154.
- Milhous, R.T., D.L. Wegner, and T. Waddle, 1984. User's Guide to the Physical Habitat Simulation System (PHABSIM). Instream Flow Information Paper 11, FWS/OBS-81/43, Revised January 1984, U.S. Fish and Wildlife Service, Ft. Collins, CO, 475 pp.
- Miller, B.A., and H.G. Wenzel, 1984. Low Flow Hydraulics in Alluvial Channels. University of Illinois Water Resources Center, Research Report 192, 49 p.
- Nunnally, N.R., and E. Keller, 1979. Use of Fluvial Processes to Minimize Adverse Effects of Stream Channelization. Water Resources Research Institute of the University of North Carolina, Research Report 144, 115 p.
- Riley, R.B., et al., 1985(a). ISIS: An Introduction. Illinois Streams Information System, Department of Conservation State of Illinois, 30 p.
- Riley R.B., et al., 1985(b). ISIS Data Descriptions Manual. Illinois Streams Information System, Department of Conservation State of Illinois, 116 p.
- Rzhanitsyn, N.A., 1960. Morphology and Hydraulic Regularities of the Structure of the River Net, translated by D.B. Krimgold, for Soil and Water Conservation Research Division and USGS Water Resources Division, originally published by Gidrometeoizdat, Leningrad, U.S.S.R.
- Singh, K.P., 1971. Model Flow Duration and Streamflow Variability. Water Resources Research, Vol. 7(4): 1031-1036.
- Singh, K.P., and J.B. Stall, 1971. Derivation of Base Flow Recession Curves and Parameters. Water Resources Research, Vol. 7(2): 292-303.
- Singh, K.P., and J.B. Stall, 1973. The 7-Day 10-Year Low Flows of Illinois Streams. Illinois State Water Survey Bulletin 57, 24 p and 11 maps.
- Singh, K.P., 1981. Evaluation of Hydraulic Geometry Parameters for Various Low Flow Releases Downstream of Dams on Illinois Streams. Illinois State Water Survey Contract Report 251, 42 p.
- Singh, K.P. and G.S. Ramamurthy, 1981. Desirable Low Flow Releases from Impounding Reservoirs: Fish Habitat and Reservoir Cost. Illinois State Water Survey Contract Report 273, Vol I, 150 p.
- Stall, J.B., and Y.S. Fok, 1968. Hydraulic Geometry of Illinois Streams. University of Illinois Water Resources Center, Research Report 15, 47 p.

- Stall, J.B., and C.T. Yang, 1970. Hydraulic Geometry of 12 Selected Stream Systems of the United States. University of Illinois Water Resources Center, Research Report 32, 73 p.
- Stalnaker, C.B., 1979. The Use of Habitat Structure Preferenda for Establishing Flow Regulation Necessary for Maintenance of Fish Habitat. In "Ecology of Regulated Streams," by J.V. Ward and J.A. Stanford (Editors), Plenum Press, New York, pp. 321-337.
- Voos, K.A., 1981. Simulated Use of the Exponential Polynomial/Maximum Likelihood Technique in Developing Suitability of Use Functions for Fish Habitat. Ph.D. dissertation, Utah State University, Logan, UT. 85 p.